High Temperature Creep of Platinum and Its Alloys

Tokio HAMADA

OSAKA UNIVERSITY
Graduate School of Engineering Science
Department of Physical Science
Division of Materials Physics
Toyonaka Osaka

January 1998

abstract

Platinum and its alloys are widely used in the glass-melting industry because of their high melting point, high resistance to oxidation and inertness with molten glass. Since they are usually used above 1273K, creep phenomena are observed even if at very low stresses. However, the detailed behavior and the mechanism of high-temperature creep of platinum and its alloys is not yet clear.

In this study, high temperature creep behaviors of the pure platinum, the platinum-rhodium alloys and the Sm_2O_3 added platinum alloy have been investigated. Following results are obtained.

1. **Pure Platinum**

   (a) In the present experimental conditions, platinum shows the power-law creep and the stress exponent n to be 5 for the steady-state creep rate with a few exceptions. The result suggests that the dislocation climb controls the steady-state creep rate in the whole experimental conditions.

   (b) Platinum shows the transgranular creep rupture with the void-coalescence at grain boundaries in fine grained specimens. The rupture mode is similar to that of other metals.

   (c) Platinum shows the transgranular creep rupture with the necking or sharing-off with clear slip bands in coarse grained specimens. The rupture mechanism is different from that of other metals, on the view points of the grain size. In other metals, the recrystallized fine grains are usually observed by the dynamic recrystallization.

   (d) A strain-burst (a sudden increase in the strain) has been detected on the creep curves in some specimens. This is the newly found phenomenon in platinum.

   (e) Strong grain-size dependence of the steady-state creep rate is also the newly found phenomenon, which suggests that the conventional common sense of the creep study might be amended.

2. **Platinum-Rhodium alloy**

   (a) Platinum-rhodium alloys also obey the power-law creep with the stress exponent n to be 3 in whole experimental conditions. The result suggests that the glide movement of dislocations dragging solute atom controls the creep process.

   (b) Platinum-rhodium alloys shows the transgranular creep rupture with the void-coalescence at grain boundaries in whole experimental conditions. The rupture mode is similar to that of other metals and alloys.

(c) All creep curves have the three stages, *e.g.*, the primary, steady and accelerating stages. This is a newly found result comparing with the old report in which only accelerating stage was observed at high stress conditions.

3. **Sm_2O_3 added Platinum**

(a) Sm_2O_3 added Platinum is also obey the power-law creep. At low temperatures (below 1473K), the stress exponent n is around 10, which is similar to other *Oxide Dispersion Strengthened* (O.D.S.) alloys. But with increasing temperature, the stress exponent n approaches to that of the pure platinum value 5.

(b) The creep mechanism seems to be different from that of other O.D.S. alloys at high temperatures (above 1573K). The threshold stress haven't observed in present whole experimental conditions. Sm_2O_3 added platinum is not strengthened by the oxide particles but by its microstructure with a large aspect ratio. The creep strength is influenced by the growth of voids located at grain boundaries.

Contents

List of Figures

List of Tables

Chapter 1

General Introduction

There might be a prejudice that platinum and its alloys are only for jewels because they are the precious metals. However, they are widely used in industry because of their **high melting point, high resistance to oxidation and inertness**. For example, platinum crucibles for glass melting industry, bushing for glass fiber spinning, platinum thermocouples, platinum resistance thermometer, spinneret for chemical fiber spinning, crucibles for chemical analysis, catalyst and so on.

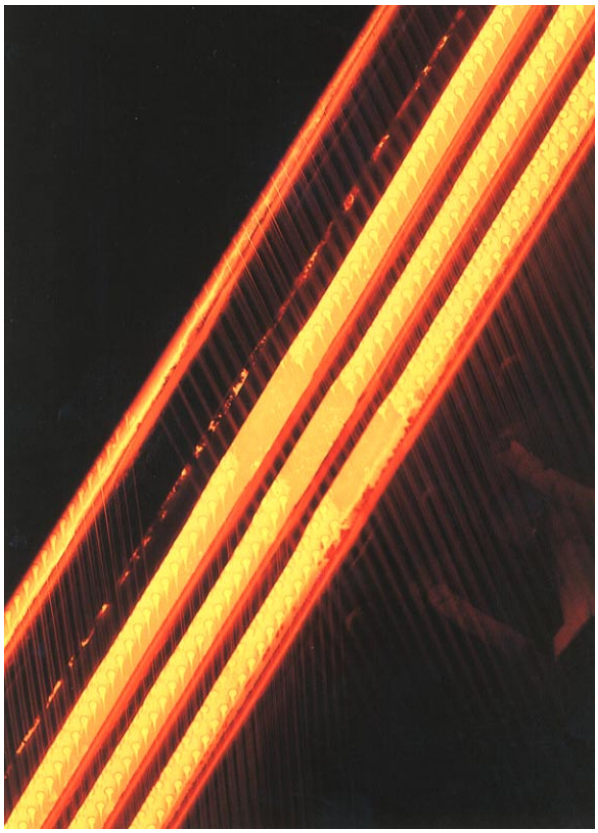

Figure 1.1: Bushing for glass fiber spinning.

Especially, it is little known that the platinum and its alloys are used in high quality glass melting such as the production of cathode ray tube, glass fiber spinning, optical glass (lens, prism *etc.*), cover glass of liquid crystal and so on. The contamination should be avoided in these glass melting because the impurities solved in the glass as ions and as colloid reduce the transparency of the glass and/or cause the unintentional coloring of the glass. Flouting hyperfine solids in melting glass should be also avoided. The refractories used at high temperatures is usually made from oxide such as Al_2O_3, ZrO_2, SiO_2, CaO *etc.*, *i.e.*, the component of the refractories are similar to the glass itself[1], so that they have a tendency to contaminate the glass. Platinum is a metal not an oxide, so that it is basically inert with both glass and refractories. That the reason why platinum is used in the glass melting industry in order to avoid the contamination. Platinum is essentially important to support the high quality glass production which is used in the recent, so called, *high-tech* product.

Since they are usually used above 1273K[2] under the constant load, so that it is essen-

[1] Usually glass is also consisted of some oxides.

[2] Often used at 1500K∼1600K, sometimes just below the melting points.

tially important to understand the high temperature creep behavior not only in order to understand the practical running glass melting plant but also as the basic knowledge to improve the high temperature creep properties.

Figure 1.1[(1)] is an example of the glass melting device made of platinum-rhodium alloys. Glass fibers are spinning. The device is called the bushing. Shining with orange color is the bushing and molten glass has been supplying over it. Glass fibers are coming though the holes[3] of the bushing baseplate[4]. The bending stress has been applied during the glass fiber spinning by the pressure of the molten glass over it and drawing force of the glass fiber spinning. These pressure and the drawing force at high temperature cause real **high temperature creep** of the platinum-rhodium alloy.

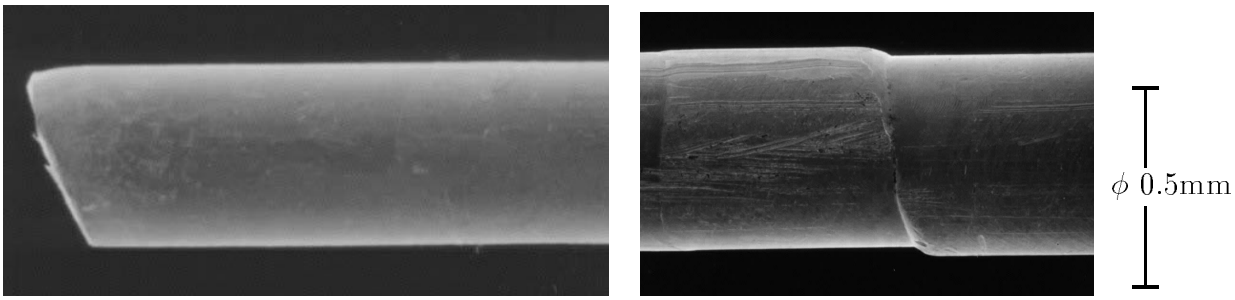

Figure 1.2: Bamboo-structure of used R thermocouple (negative branch).

Another example of platinum and its alloy use is the platinum thermocouples. Figure 1.2 shows an example of the broken type R[5] thermocouples. The photographs shows the broken area and a little far from the broken point. Platinum thermocouple is sometimes broken and usually at the negative branch (pure platinum branch) as same as the present case. This one had been used at around 1400K and the grain growth (or recrystallization) occurred to form the bamboo-structure. It was broken at a grain boundary of the bamboo-structure.

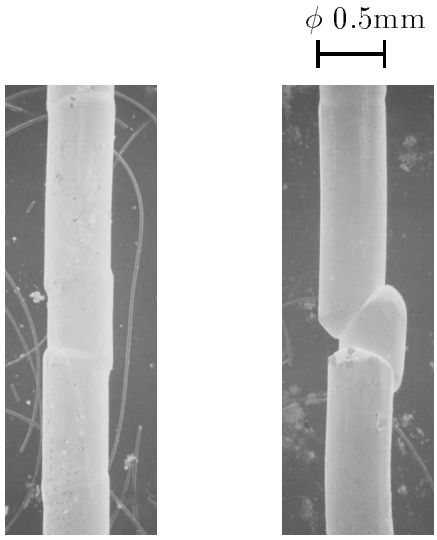

Figure 1.3: Examples of bamboo-structure.

Figure 1.3 also shows the surface morphology of the negative branch of type R thermocouples after exposed at 1973K for 2057 hours. Similar phenomenon with Fig. 1.2 is reproduced in a laboratory. As the experiments were mainly performed to examine the

[3] Max. 6 000 holes bushing is manufactured.

[4] The area of the bushing is called baseplate.

[5] Type R thermocouple is based on the JIS (Japanese Industrial Standard) C 1602^{-1995}. The negative branch is made of high purity platinum and the positive branch is made of platinum-13%rhodium alloy. The most common platinum thermocouple in Japan. Type R thermocouple is a little different from old PR type thermocouples (in JIS C 1602^{-1974}) whose negative branch is made of high purity platinum and the positive branch is made of platinum-12.8%rhodium alloy.

drift of the thermo-electro motive force[2], the similar bamboo-structure was observed after the exposure. The platinum material for the thermocouple has higher purity in order to fit the international standard[3] than that for other glass melting devices. High purity platinum such as negative branch of type R thermocouples has a tendency to form the bamboo-structure than industrial grade platinum. As already shown as the example, the bamboo-structure often observed in thermocouples. And it often occurs at higher temperatures under higher stresses, so that the phenomenon might have a dependence on the temperature and stress. However the details are unclear. In the case of Fig. 1.3, the thermocouple was exposed under the stress by the weight of the thermocouple itself and its insulator-tube, so that the stress may affect the formation of the bamboo-structure. In the condition, the stress was not tensile but compress, so that the clear grain boundaries with the angle of about 45° to the stress axis were observed.

The conditions, which show the tendency of the formation of the bamboo-structure, are as follows.

1. In the industrial grade platinum (99.95mass% up), it is rare. It often appears in the high purity platinum such as negative branch of type R thermocouples.

2. It often appears at higher temperatures.

3. It often appears under the stress.

According to the above experienced facts, the formation of the bamboo-structure might be a dynamic recrystallization which were reported in other f.c.c. metals and alloys[4,5]. However, the condition of the appearance of it depends on the purity, production process, temperature, stress and so on, so that the detailed origin is still unclear.

Some examples of practical platinum uses and observed phenomena of platinum have been mentioned above. Platinum and its alloys are usually used at much higher temperatures[6] than other heat resistant alloys. For example, the heat resistant steels, which are used for the steam turbine in therm-power-plant, are useable up to 923K at best[6]. Even if the nickel based supper alloys, which will be used for the turbine blade of the aircraft engine over 1273K, are still under research and development[7-9].

If the temperature ratio (T/T_m) is same, the absolute thermodynamic temperature is higher in the platinum use, so that the theory or explanation in other f.c.c. metals and alloys is not always available to the platinum and its alloys.

It is essentially important to understand the high temperature creep behavior of platinum and its alloys not only in order to understand the phenomena in practical use but also as the basic knowledge to improve the high temperature creep properties.

However, very few were reported on the high temperature creep behavior of the platinum and its alloys. The purpose of this study is to clear the following items by using the **pure platinum**, **platinum-rhodium alloys**[7] and **Sm_2O_3 added platinum**[8].

1. To examine the high temperature creep behavior of high purity platinum, industrial grade platinum, platinum-rhodium alloys and Sm_2O_3 added platinum and to clarify the difference from other pure metals, solid solution alloys and oxide dispersion strengthened alloys.

[6] It means the thermodynamic temperature is high. Not relative temperature such as T/T_m

[7] In the glass melting industry, platinum-rhodium alloy is popularly used.

[8] Recently, the O.D.S. technology has applied in platinum alloys.

2. To clarify the application limit of conventional theories to the platinum creep and to suggest the new theory to the unexplained phenomena with the conventional theory.

Chapter 2

Experimental Procedure

2.1 Specimens

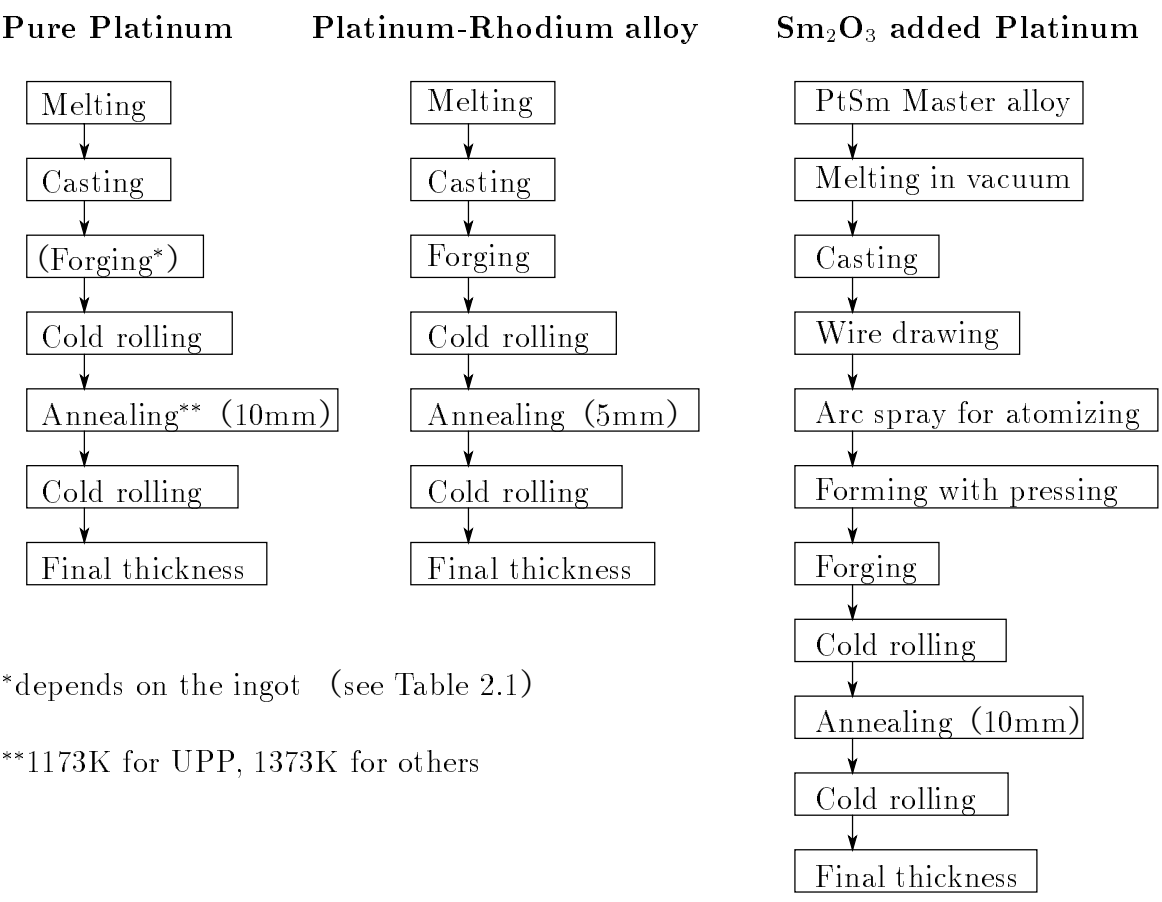

*depends on the ingot (see Table 2.1)

**1173K for UPP, 1373K for others

Figure 2.1: Preparation process of the Platinum specimens.

Figure 2.1 shows the production process of pure platinum, platinum-10% and 20%rhodium alloys and Sm_2O_3 added platinum. The detailed production process and the final thickness of the specimens depend on the ingots, so that the difference is summarized in Table 2.1. The final thickness of the platinum specimens were between 0.5mm through 1.5mm except

Table 2.1: Summary of the Platinum specimens.

Ingot No.	Weight	Forging	R.R.R.	Thickness (final reduction)
UPP-2	2Kg	×	—	1.0mm(90%)
UPP-3	2Kg	×	—	0.5mm(95%), 1.5mm(85%)
UPP-4	5Kg*	×	1200	1.0mm(90%)
UPP-5	5Kg*	○	1200	1.0mm(90%)
UPP-6	5Kg	×	—	1.0mm(90%)
UPP-8	2Kg	×	—	1.0mm(90%)
UPP-9	2Kg	×	—	1.0mm(90%), 5.0mm(75%)
IND	10Kg	○	—	1.0mm(90%)

*Same ingot

for the 5mm thick specimens obtained from a part of UPP-9.

Specimens for chemical analysis and microstructure observations before the creep tests were taken from near the rest sheet after punched out of the creep specimens, so that the impurity analysis results and the microstructures before the creep tests will be assumed that they are equal to the crept specimens themselves.

Platinum and platinum-rhodium alloys were made from chemically refined powder. They were melt in an induction furnace with high purity alumina crucible and cast into a copper mold in the air. Samaria (Sm_2O_3) added platinum ingots were melt as platinum samarium solid solution alloy. After wire drawing, it was atomized into the water. The platinum samarium (partly samaria) powder was formed by cold pressing. After that, hot forging and cold rolling process were applied. The samarium added first as a metal turns to samaria (Sm_2O_3) during atomizing and hot forging, and the samaria particles disperse into the platinum matrix[10].

Platinum specimens for the creep tests were prepared from eight batches of chemically refined platinum powder. Seven (UPP-2, 3, 4, 5, 6, 8, 9) of them are of high purity and one (IND) is of an industrial grade. **To study the high temperature creep properties of the platinum itself** is one of the most important purpose of this study, so that high purity platinum was mainly used. Industrial grade platinum is only compared the difference with the high purity one. High purity ingots weigh 2Kg or 5Kg each, and the industrial grade one 10Kg.

The final heat-treatment will be refereed to the pre-annealing, *i.e.*, annealing prior to the creep test. The grain size[1] is almost same when the high purity platinum is pre-annealed for an hour below 1673K. In the case of the experiment of the grain size dependence of the steady-state creep rate, per-annealing was performed at 1673K and 1973K. In other cases pre-annealing was performed at the same temperature with the creep tests.

The similar pre-annealing was applied for the platinum-rhodium alloy specimens. When the grain size dependence of the steady-state creep rate was examined, the pre-annealing temperature was usually higher than creep temperature. In other cases, when the steady-state creep rate and/or creep rupture time dependence of the temperature and stress are examined, the pre-annealing temperature was same as the creep temperature. In Sm_2O_3 added platinum experiment, the pre-annealing temperature was same as the creep temper-

[1] In this paper, **grain size** means the **average grain cut-off length** $\bar{l}$[11].

ature because the examination of the grain size dependence of the steady-state creep rate had not performed and the form of the grains were usually similar after the pre-annealing from about 1000K[2] to 1973K.

No cross rolling was applied for all specimens, those are pure platinum, platinum-rhodium alloys and Sm_2O_3 added platinum. As shown in chapter 5 (page 55), Sm_2O_3 added platinum showed the strong dependence on the cold rolling direction. However, no dependence on the cold rolling direction was observed in pure platinum and platinum-rhodium alloys.

2.2 Creep tests

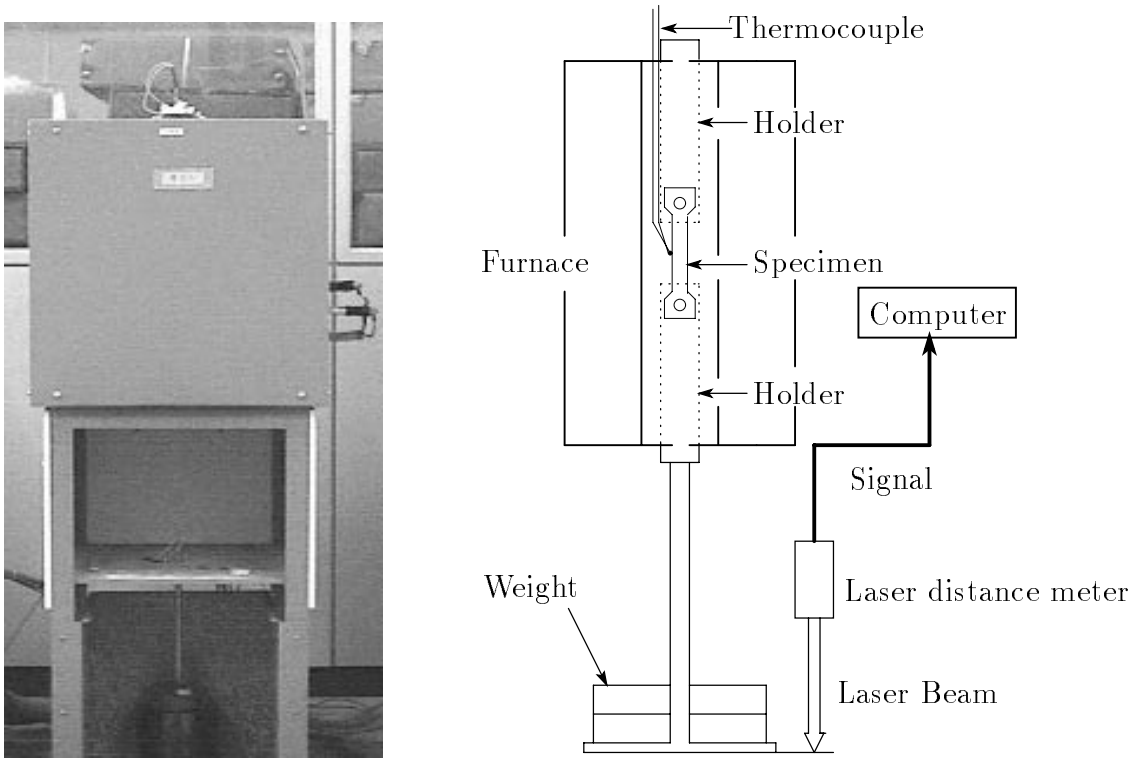

Figure 2.2: Outline of the creep furnace and creep testing system.

[2] It is the recrystalline temperature of the Sm_2O_3 added platinum.

Figure 2.2 shows the overview of a creep furnace and the outline of the creep system. As mentioned about an use of platinum in the glass melting industry in chapter 1, one of the most important information of the creep test is creep rupture time in general[3].

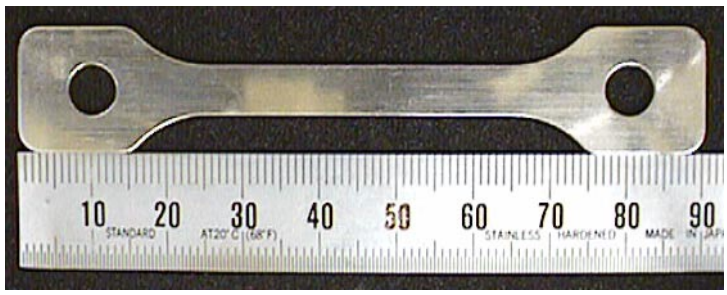

Figure 2.3: Initial shape of the creep specimen.

It was impossible to measure the elongation during the creep by using an old style creep furnace[4]. Minimum necessary information would be obtained with the use of the old style creep furnace, however, it will be not enough to discuss the creep deformation mechanism. So that, the new creep furnace and system, by which the measurement of the specimen during the creep is possible, was designed and manufactured for the present experiment. Two furnaces were manufactured first. Then more four were manufactured with some improvement. Total six furnaces were applied for the present experiment.

The production process of the test sheets has already shown in Fig. 2.1. 5mm specimens taken from UPP-9 were cut off by electric discharge machine and others were punched out from the die of the press machine. A punched out specimen is shown in Fig. 2.3. As the final thickness depends on the each specimen (see Table 2.1), other gauge dimensions were same, those are 6.3mm wide, 38mm long and 15mm R from the gauge to chucking area. The specification of the specimen follows to the No.7 specimen in **JIS Z 2201**[5]. The 5mm specimens have also similar dimensions except for the chamfering R of the corners (see Fig. 3.17). In **JIS Z 2271 and 2272**, creep test and creep rupture test are regulated. However, these JIS standards were regulated mainly for the heat resistant steels. So that, it is not good to apply the standards for the platinum creep, such as dimensions and temperatures[6]. These are reasons why the specimens were manufactured following to the JIS Z 2201. The detailed creep test processes

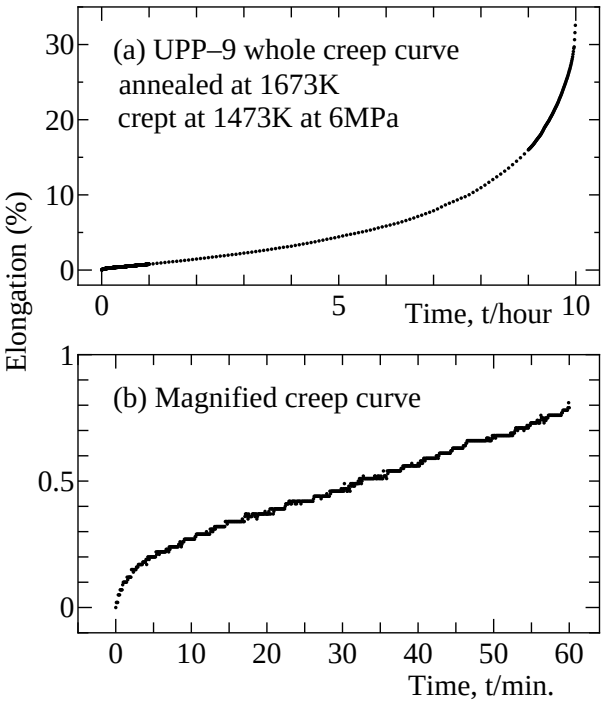

Figure 2.4: An example of the creep curve.

[3] Actually, many creep data sheets of heat resistant steels at various temperatures and stresses, which are applied such as the turbine of the therm-power-plant, have been publishing by National Research Institute for Metals of the Science and Technology Agency.

[4] The rupture time and the rupture elongation obtained by direct measurement of the crept specimens after the creep rupture were the only information in the old style creep test.

[5] Japanese Industrial Standard.

[6] It is impossible to produce the huge creep specimens for the financial reason and the temperature is limited up to 1273K which is too low for the platinum creep test.

are as follows.

1. Set and keep the creep furnace temperature before the creep test.
2. Put the specimen with the holders into the furnace[7].
3. Wait for an hour to be homogeneous temperature of the specimen.
4. Put the weights for loading.
5. Start the elongation measurement.
6. Take off the specimen from the furnace after the specimen ruptured with a few exceptions.

As the elongation measurements were started just after the loading, so that the instantaneous plastic deformation of the specimen and the elastic deformation of the specimen was not recorded. These factors are important for the tensile tests but not always necessary for the creep tests lasted for at least several hours to at longest over a thousand hours. When the specimen is loaded, the specimen holders and other parts of the equipment (see Fig.2.2) are also deformed. Especially, the holders, which hold a specimen in the furnace, are exposed at the almost same temperatures with the specimen and loaded with the same weights. So that, the holders should be made of more heat resistant and more rigid material, ideally. Unfortunately, there seems to be no material for the holders[8]. Sm_2O_3 added platinum, whose details were examined in chapter 5 (page 55) was applied for the folders and their cross-sectional area was several times larger than the specimen cross-section even if the case of 5mm specimens, so that they are regarded as rigid bodies.

As details have been described, all creep tests were performed with a **constant load** in the present experiment. It is, however, regarded as a **constant stress** test. The reason is as follows. Figure 2.4 (a) is an example of the creep curve obtained from the present experiment. The whole creep curve seems to be occupied by the accelerating stage without primary and steady-state stages, however, as shown in Fig. 2.4 (b), which is magnified the short period just after the creep started, shows the clear primary and steady-state stage[9].

In the case of Fig. 2.4 (b), the steady-state creep begins 10 minutes later after the loading with about 0.3% elongation. The time and strain of the appearance of the steady-state creep depend on the detailed experimental conditions. It appeared within several percent strain in all present experimental conditions[10]. The steady-state creep rate were determined in a range of small strains, so that, the test is of a constant load, but regarded as a constant stress test because the reduction of cross-section is small. The difference was considered in the uncertainty budget in section 2.3. In this report, stress and strain are nominal ones not true ones.

It is possible to obtain maximum 149880 points[11] in a creep curve with this creep measuring system. This number is equal to the maximum storage of the media; the data are

[7] Of course after set the specimen to the holders.

[8] I tried to use high density ceramics holders, but they were broken with the thermal shock when the specimen was ruptured.

[9] The reason why the magnified plots seems to be steps due to the resolution(0.01mm$\approx$0.026%) of the laser distance meter.

[10] *e.g.* in Fig. 3.14(page 30), the steady-state creep appeared with several percent strain.

[11] A point is a pear of time and strain.

stored in a diskette. It means that it is possible to store the date in a creep curve for 999 minutes with a second interval both after the loading and before the rupture and 2500 hours with 5 minutes interval. However, it is not necessary to measure such detailed conditions, so that usually the measurements were performed for an hour with a second interval after loading and before rupture and 5 minute interval after an hour passed. When the detailed curve should be obtained, the measurement conditions were changed flexibly.

As a lot of creep curves are shown in this report, it is not always necessary to display all the points of each creep curve to understand the creep phenomena. So that, the creep curves were displayed with the thinned-out points, *e.g.*, each 6 second point (a part of six) were used in Fig. 2.4 (b).

2.3 Uncertainty of the measurement

It is very important to evaluate the reliance of the results. There is a few in which the **uncertainty** of the measurement is evaluated by themselves. I'm also study the temperature measurement and thermometer calibration[12,13], so that, according to the guide published by International Organization[14], the uncertainty of the present experiment was evaluated. Elements of the uncertainty in the present experiment are as follows.

1. Temperature
   (a) Temperature distribution in the creep furnace.
   (b) Temperature stability of the creep furnace.
   (c) Uncertainty of the measuring system.
   (d) Calibration uncertainty of the thermocouples.
   (e) Traceability of ITS-90[15] to the thermodynamic temperature.
2. Time
   (a) Uncertainty of the clock in the computer.
3. Distance
   (a) Accuracy of the laser distance meter.
   (b) Influence of the elongation of the parts of the equipment except for the specimen.
   (c) Vibration from the environment.
4. Stress
   (a) Gravity at the place.
   (b) Mass measurement of weights and holders.
   (c) Stress change due to the elongation of the specimen (the reduction of the cross-section).

Among these elements which will affect the uncertainty of the measurement, 1e, 2a, 3b, 3c, 4a and 4b are obviously negligibly small. In other elements, 1a and 1b were measured by using a calibrated thermocouple. 1c and 1d were obtained by comparison with a higher standard, 3a was estimated by direct measurement of the ruptured specimens and 4c was calculated with the assumption of homogeneous elongation of the gauge length.

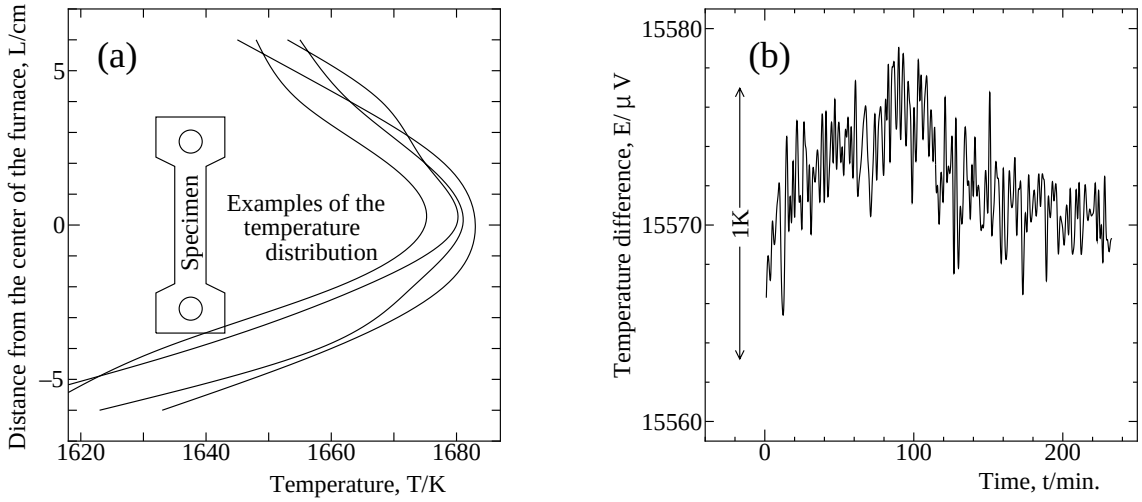

Figure 2.5: Temperature stability and its distribution in the creep furnace.

Figure 2.5 shows the examples of the temperature measurements for the uncertainty estimation. The measurements were performed for the temperature of the furnace, which was determined by the output of the thermocouple nearby the creep specimen[12]. Output of the thermocouple was set at the intended temperature ±10K.

Figure 2.5 (a) shows examples of the temperature distribution of the furnaces at around 1673K. It was measured parallel to the tensile direction of the specimen. The position of the specimen in the furnace is illustrated in the figure. There is about 10K difference (distribution) in the gage length. The temperature distribution in a plane vertical to the tensile direction is negligibly small because of the cross-section size (small enough) of the specimen and the symmetry of the furnace. Figure 2.5 (b) is an example of an output (μV) of the type R thermocouple nearby the specimen. Usually, the temperature is recorded with 10K resolution, however, it was magnified to detect smaller change. According to the measurement, the temperature change during the creep is small enough comparing with the temperature distribution. Including these results, an example of the uncertainty budget is shown in Table 2.2.

The combined uncertainty is calculated by root sum square (equation 2.1) with the assumption that each source of uncertainty is independent.

$$\begin{aligned}&\sqrt{0.69^2+0.17^2+0.35^2+0.30^2+0.21^2+0.12^2+0.01^2}\\&\overline{+0.26^2+0.01^2+0.50^2+0.05^2+0.10^2+2.75^2}=3.02.\end{aligned}\qquad(2.1)$$

[12] Thermocouple in Fig. 2.2

Table 2.2: Uncertainty budget of creep test.

Source of Uncertainty	Value	Distribution	Divisor	σ
Temperature distribution of the furnace	20K	rectangular($\sqrt{3}\sigma$)	0.06%/1K	0.69%
Temperature stability of the furnace	5K	rectangular($\sqrt{3}\sigma$)	0.06%/1K	0.17%
Temperature difference between furnace	10K	rectangular($\sqrt{3}\sigma$)	0.06%/1K	0.35%
Uncertainty of the measuring system	5K	normal(σ)	0.06%/1K	0.30%
Uncertainty of the thermocouple	3.5K	normal(σ)	0.06%/1K	0.21%
Traceability to ITS-90	<2K	normal(σ)	0.06%/1K	<0.12%
Uncertainty of the clock in PC	<1min./1week	normal(σ)	—	<0.01%
Uncertainty of the laser distance meter	0.1mm	normal(σ)	2.63%/mm	0.26%
Deformation except for the specimen	2mm/year	normal(σ)	—	<0.01%
Vibration disturbance	—	rectangular($\sqrt{3}\sigma$)	From the curve	<0.50%
Gravity at the place	0.05MPa	rectangular($\sqrt{3}\sigma$)	1.00%/1MPa	0.05%
Mass measurement of weights and holders	<0.1%	rectangular($\sqrt{3}\sigma$)	—	0.10%
Stress change due to the elongation	Max.4.76%(assumption)	rectangular($\sqrt{3}\sigma$)	—	2.75%
Combined uncertainty(1σ)	—	normal(σ)	—	3.02%

It was impossible to obtain the similar reproductivity $(\dot{\varepsilon}, t_r)$ in the creep test. However, the inconsistency between uncertainty estimation and experimental results is not due to the estimation of uncertainty but due to the creep specimen itself which means that the creep phenomenon itself depends on the each specimen. It is the most important thing to describe the details of the experiment.

The uncertainty budget of Table 2.2 is for the absolute value of the measurement. Apart from the absolute value of the thermodynamic temperature, the temperature dependence of the elastic moduli is negligibly small when the activation energy of the steady-state creep is calculated. So that, the activation energy of the creep will be obtained with relatively small uncertainty when the interval of the two temperatures are measured with relatively small uncertainty even if the absolute value of the thermodynamic temperature is obtained with relatively large uncertainty such as several Kelvin. Of course, in the case of it, propagation of errors should be estimated with the relationship as a function of measured parameter and calculated value. Anyway, this is not the main purpose of the present investigation, so it is not discussed further. The most important things in present investigation are to describe the detailed experimental conditions.

2.4 Analysis

Table 2.3: Impurity concentrations (mass ppm).

Ingot No.	Au	Ag	Pd	Rh	Al	B	Bi	Ca	Cr	Cu	Fe	Mg	Ni	Pb	Si	Zn
UPP-2	4	0.2	<1	2	ND	ND	ND	ND	ND	0.9	<1	0.2	ND	ND	<0.1	ND
UPP-3	4	1	1	<1	ND	ND	ND	ND	ND	1	<1	0.1	ND	ND	<0.1	ND
UPP-4	0.4	0.6	2	<1	ND	ND	ND	<0.1	<1	2	<1	0.5	ND	ND	3	ND
UPP-5	0.2	0.9	2	<1	ND	ND	ND	<0.1	<1	1	<1	0.5	ND	ND	3	ND
UPP-6	<0.1	0.4	<1	<1	ND	ND	<1	<0.1	<1	0.6	<1	0.1	ND	<1	<0.1	ND
UPP-8	2	0.8	2	<1	ND	ND	ND	0.1	ND	0.6	<1	0.5	ND	ND	2	ND
UPP-9	<1	0.4	<1	2	ND	ND	ND	<0.1	ND	0.6	<1	0.1	ND	ND	0.5	ND
IND-1	52	30	32	60	3	10	<10	15	<1	<1	<1	<1	2	11	26	4

ND : less than level of detection Ir, Ru, Os, As, Co, Mn, Sb, Sn, Ti, W, Zr and Mo are less than level of detection

Impurity concentrations of cold-rolled sheets were spectroscopically analyzed and results obtained are shown in Table 2.3. The specimens for the analysis were taken from the part nearby the creep specimens, so that the analysis results are same as those of crept specimens.

The original ingot of UPP-4 and UPP-5 were same. They were divided into two pieces after the melting in order to examine the influence of the production process, so that hot-forging was applied only for the UPP-5. Wire specimens were made from these two ingots to measure the residual resistance ratio (R.R.R.)[13] whose the temperatures of the measurement were 4.2K (boiling point of liquid helium at 0.1013MPa) and 273.16K (triple point of water). As shown the results ($R_{273K}/R_{4.2K}$) in Table 2.1, the values were 1 200. It is still unclear the relationship between the R.R.R. value and high temperature creep properties, although there is a report of the relationship between R.R.R. value and impurities(16).

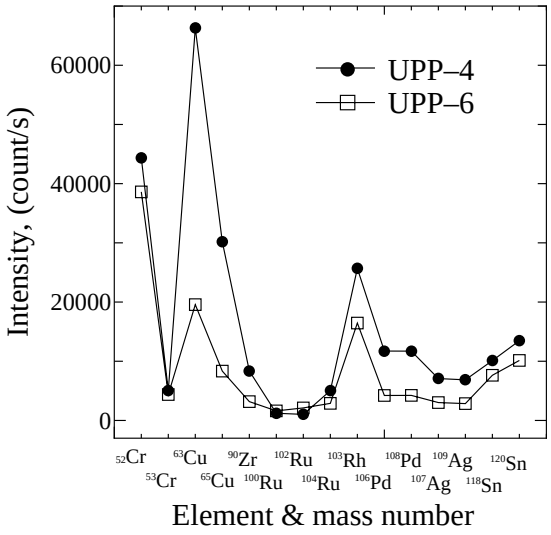

Figure 2.6: Results from ICP-mass spectrometry.

It is essentially important to understand the impurity concentration when a specific properties of the pure metal is studied. Generally, the instrumental analysis like spectroscopic analysis, atomic absorption, inductive coupled plasma and so on are applied. However, possible identification elements, identification limit of each element and uncertainty of the analysis *etc.* are not always clarified in the report except for the case that analysis itself is a main purpose of the study. The identification limit of each element strongly depends on the element in the spectroscopic analysis applied in the present experiment, *i.e.*, as seen in Fig. 2.3, Au, Ca and Si were identified less than 0.1ppm but the identification limit of Ir is over 100ppm. It is not enough to describe the nominal purity but analytical method and/or possible identification elements should be described in the report when a specific property of the pure metal is studied.

[13] In order to estimate the purity of the pure metal, R.R.R. is sometimes used as a scale.

It is ideal to use the material with the highest purity obtained for the study of a specific property of pure metal. Of course, there is a sensitive specific property such as temperature co-efficient of resistivity at low temperatures and an insensitive specific property such as tensile strength at room temperature. The UPP platinum used in this experiment has similar purity to the material for platinum resistance thermometer and/or platinum thermocouples, for which the highest purity material has been applied historically. And also this is the highest purity platinum as a commercial product except for the small amount[14] experimental product. So that, the results in this report will be regarded as the **High Temperature Creep Propertied of Platinum** at the present time.

Anyway, IND is the industrial grade platinum whose nominal purity is better than 99.95mass%.

Apart from the spectroscopic analysis, inductive coupled plasma mass spectrometry[15] was applied for the UPP-4 and UPP-6 whose creep properties were different to each other. The analyzed elements and mass numbers are ^{7}Li, ^{9}Be, ^{23}Na, ^{24}Mg, ^{27}Al, ^{44}Ca, ^{45}Sc, ^{47}Ti, ^{51}V, ^{52}Cr, ^{53}Cr, ^{55}Mn, ^{56}Fe, ^{58}Ni, ^{59}Co, ^{60}Ni, ^{63}Cu, ^{64}Zn, ^{65}Cu, ^{66}Zn, ^{69}Ga, ^{73}Ge, ^{75}As, ^{82}Se, ^{85}Rb, ^{88}Sr, ^{89}Y, ^{90}Zr, ^{93}Nb, ^{95}Mo, ^{100}Ru, ^{102}Ru, ^{103}Rh, ^{104}Ru, ^{106}Pd, ^{107}Ag, ^{108}Pd, ^{109}Ag, ^{111}Cd, ^{114}Cd, ^{115}In, ^{118}Sn, ^{120}Sn, ^{121}Sb, ^{126}Te, ^{133}Cs, ^{137}Ba, ^{138}Ba, ^{139}La, ^{140}Ce, ^{141}Pr, ^{146}Nd, ^{147}Sm, ^{151}Eu, ^{157}Gd, ^{159}Tb, ^{162}Dy, ^{165}Ho, ^{166}Er, ^{169}Tm, ^{174}Yb, ^{175}Lu, ^{177}Hf, ^{178}Hf, ^{181}Ta, ^{182}W, ^{184}W, ^{185}Re, ^{191}Ir, ^{193}Ir, ^{197}Au, ^{202}Hg, ^{205}Tl, ^{207}Pb, ^{209}Bi, ^{232}Th and ^{238}U; 63 elements, 77 nuclide.

In order to determine the quantity of each impurity, reference standard is required. Unfortunately, as there is no reference standard for the analysis now, two specimens were compared if there were some difference of the impurity by only comparing the counts. The one is UPP-4, which showed clear strain-burst[16] and the other is UPP-6, which showed no strain-burst.

Among these elements, the difference are summarized in Fig. 2.6. The vertical axis is the count of the nuclide and the horizontal axis is the element and nuclide. There is no meaning of the lines connected between each points, just for guide.

The results from each analysis are compared with Table 2.3 and Fig. 2.6. The copper is the most different element between UPP-4 and UPP-6 in Fig. 2.6; the both counts of ^{63}Cu and ^{65}Cu of UPP-4 are about three times larger than those of UPP-6. In the quantity analysis of copper in Table 2.3, UPP-4 contains 2ppm and UPP-6 contains 0.6ppm. These results are consistent. Palladium and silver also show consistent result between ICP-mass and spectroscopic analysis. As long as considering these analysis, UPP-4 is a little lower purity ingot than others. However, unfortunately, it is impossible to control the impurities with parts per million level and prepare the sheets and creep specimens. In order to discuss the influence of the trace impurities to the platinum creep behavior, over-all technical level including refining and analysis should be improved.

[14] Several grams to several hundred grams.

[15] Generally called ICP-mass

[16] Details are mentioned in section 3.3.1(page 20), strain-burst is a sudden increase of the creep rate during the creep.

Chapter 3

High Temperature Creep of Pure Platinum

3.1 The purpose of the study in this chapter

In this chapter, results and some problems reported by the previous study of the platinum creep will be described in section 3.2.1 and the grain-size dependence of the steady-state creep rate will be discussed in section 3.2.2. On the bases of the previous study, the creep behavior of high purity platinum (UPP) and industrial grade platinum (IND) at relatively high temperatures (1373K to 1773K, T/T_m=0.67 to 0.87) has been investigated in this chapter to establish the basic knowledge for the further development of the material for high temperature use. Details are as follows.

1. To clarify the creep behavior of the platinum comparing with that of other f.c.c. metals.

2. To mention the creep deformation mechanism and creep rupture mode of platinum relating with the phenomena in item 1.

3. To calculate the activation energy of the steady-state creep rate of the platinum again using a same method by Dushman *et al* in 1944.

3.2 Previous works

3.2.1 Study of the platinum

As long as the author knows, the oldest report of the high temperature creep study of the platinum was done by S. Dushman, L.W. Dumbar and H. Huthsteiner[17] in 1944. In this study, they crept the platinum from 1000K through 1200K to obtain the steady-state creep rate. According to the steady-state creep rate, they calculated the activation energy of the platinum creep. The value (2.3×10^5J/mol) is smaller than the activation energy of the self-diffusion (2.8×10^5J/mol).

After the report by Dushman *et al.*, there is no report concerning the activation energy of the steady-state creep rate of the platinum. So that the value 2.3×10^5J/mol have been quoted for a half century[18-22]. In 1950, Carreker[23] reported the platinum creep behavior

from 77K through 1550K. This report was worth to read considering the experimental equipment at that time. But the study reported by Dushman *et al.* and Carreker contain some problems on the standpoint of recent use of the platinum. Such as,

1. Impurities in the specimens were not declared (report[17,23]).
2. Test temperature range is not wide enough (report[17]).
3. Testing time was not long enough (report[17,23]).

In order to obtain the information enough to satisfy the needs for the practical use, these report are not satisfied. In 1957, F.C. Child[24] reported the platinum creep tests in which over a thousand creep were performed. This is also an important report, but following are absent in his results.

1. The test temperature was only from 673K through 1173K. It is too low comparing with the recent platinum use in the glass melting industry.
2. He only measured the creep rupture time, not steady-state creep rate.

After the report, there were some reports for the practical use of *Oxide Dispersion Strengthening Alloys* (O.D.S. alloys)[25]. But as long as the author knows, there are no other reports of pure platinum except for the three ones already explained. As mentioned previously, there is few report of high temperature creep of the pure platinum.

3.2.2 Grain size dependence of the steady-state creep rate

The steady-state creep rate, where the strain rate ($\dot{\varepsilon}$) is almost constant, is described usually by

$$\frac{\dot{\varepsilon}}{D} = A\left(\frac{Gb}{kT}\right)\left(\frac{\sigma}{G}\right)^{n}\left(\frac{b}{d}\right)^{p}, \tag{3.1}$$

where A, n, p are constants[1], G is the shear modulus, b is the Burgers vector, k is the Boltzman constant, T is the thermodynamic temperature, σ is the applied stress, d is the grain size, D is the diffusion coefficient expressed by $D = D_0 \exp(-Q/kT)$ using the pre-exponential factor D_0 and activation energy of the creep Q. In equation (3.1), Q is defined activation energy of the creep because the activation energy of the creep is almost equal to the activation energy of the self-diffusion in the steady-state creep stage, *i.e.*, the dislocation climb is controlled by the feed of lattice vacancies[18].

Unfortunately, the equation (3.1) is not always derived theoretically but well explains the experiments in all creep region. Theoretical approach has been trying on the basis of vacancy movement and dislocation climbing or gliding and a part of the effect had done successfully, *i.e.*, at very high temperatures (just below the melting point) with low stresses, vacancy movement directly control the deformation. The case corresponding to $n = 1$, $p = 2$ in equation (3.1) is expressed by

$$\frac{\dot{\varepsilon}}{D} = A_1\left(\frac{Gb}{kT}\right)\left(\frac{\sigma}{G}\right)^{1}\left(\frac{b}{d}\right)^{2}. \tag{3.2}$$

[1] In which the n is called **stress exponent**.

When the experimental results are expressed by the equation (3.2), it is called Nabarro-Herring creep named after the persons who introduced the theory[26,27] or diffusion creep based on the phenomenon which controls the creep deformation. In the field, the steady-state creep rate is in inverse proportion to the square of the grain size and its fact is experimentally confirmed[28]. Hereafter we shall donate the grain-size dependence **negative dependence**, *i.e.* the smaller the grain size the larger the steady-state creep rate and the opposite case **positive dependence**, *i.e.* the larger the grain size the lager the steady-state creep rate.

In Nabarro-Herring creep, the steady-state creep rate is proportional to the applied stress. On the other hand, the temperature becomes lower and the applied stress becomes higher, the dislocation climb with the vacancies controls the creep deformation. In this field, the equation (3.1) is replaced by

$$\frac{\dot{\varepsilon}}{D} = A_1 \left(\frac{Gb}{kT}\right) \left(\frac{\sigma}{G}\right)^n . \tag{3.3}$$

In the equation (3.3), the stress exponent n is often 5 in pure metal and 3 in solid solution alloys. Unfortunately, the equation (3.3) hasn't been perfectly introduced yet theoretically[29,30].

There isn't the grain size factor d in the equation (3.3), *i.e.*, **no grain size dependence** of the steady-state creep rate is believed with the large grains, now. The grain size dependence of the steady-state creep rate changes exactly with the critical grain size at about 0.1mm. Under 0.1mm grains, the smaller the grain size the larger the creep rate (**negative dependence**) and no grain size dependence over 0.1mm. The historical process of this general belief is as follows.

In 1962, Sherby[31]collected and analyzed the creep results reported previously, and proposed the steady-state creep rate to be proportional to the square root of the grain diameter. However, the data he collected together were obtained for various metals tested at various conditions and may not be compared to each other, so that his proposal is hardly conclusive. Research with single material, *i.e.*, copper, was performed by Feltham and Meakin[32]. The grain diameter in the research was less than about 0.1mm. The paper reported the positive dependence. And they proposed the critical stress of the grain size dependence depending on the temperature.

E. R. Parker[33] also reported the grain size dependence of copper from 0.025mm through 0.14mm and concluded that the steady-state creep rate depended on the grain morphology, *i.e.*, **positive dependence** when the grains had isotropic morphology, **negative dependence** when the grains had anisotropy morphology. He insisted that the grain boundaries would be in different environment (opposite condition) between the grains which were obtained by the isochronal annealing from the same reduction and minimum temperature annealing from the different reductions.

There was not a common sense or general belief about the grain size dependence of the steady-state creep rate at that time because of the opposite experimental results.

Finally, the experiment by C. R. Barrett, J. L. Lytton and O. D. Sherby[34] was performed and the present general belief was concluded, *i.e.*, the **negative grain-size dependence** for grain diameter below 0.1mm and **no dependence** above 0.1mm. They discussed the reason for the disagreement between the previous and their results. They prepare the specimens with three methods, *i.e.*, (a) *Variable strain Technique*, (b) *Variable Annealing Time Technique* and (c) *Variable Annealing Temperature Technique* are employed for the

Parker's conclusion and annealing effect in hydrogen atmosphere was tested for Felthma's conclusion. After these experiment, they refuted as follows.

1. The grain size dependence was independent of the specimen preparation.
2. There was no critical stress which was mentioned by Feltham *et al.* In the Feltham and Meakin experiment, grain-growth might occur during creep.
3. In Feltham's experiment, the purity and the possible contamination of specimens from the atmosphere might affect the result.

The reason why Barrett *et al.* obtained the different experimental results from other previous study are as follows.

1. Solute hydrogen might affect the results.
2. The difference of the purity of the specimens.

In order to support their results from the theoretical point, they explained with the effect of the grain boundaries.

1. *Grain Boundaries as Barriers.*
2. *Grain Boundaries as Dislocation or Vacancy Sources.*

   Above two effect might work theoretically, but experimental facts didn't support, so that the effect is little and negligible.

3. *Grain Boundary Shearing*
   Dislocations should behave differently in the presence of high-angle boundaries than in the presence of low-angle subboundaries, *i.e.*, grain boundaries may became relatively ineffective barriers to dislocations at high temperatures. Consider the case where material near grain boundaries (within about one subgrain diameter, d_{sg}) deforms at a higher rate than material within the interior of the grain (away from the grain boundaries). If the subgrain size is considerably smaller than the grain size, d, then the over-all strain rate, $\dot{\varepsilon}_s$, is given approximately by

$$\dot{\varepsilon}_s = \frac{\alpha d_{sg}}{d}\dot{\varepsilon}_{gb} + \left(1 - \frac{\alpha d_{sg}}{d}\right)\dot{\varepsilon}_c, \tag{3.4}$$

   where $\dot{\varepsilon}_{gb}$ is the average strain rate near the grain boundaries and $\dot{\varepsilon}_c$ is the average strain rate in the grain interior. The constant α is a factor depending on the physical model used to describe the additive processes of grain and grain boundary deformation. From the equation (3.4), $\dot{\varepsilon}_s$ is given by

$$\dot{\varepsilon}_s = \dot{\varepsilon}_c + (\dot{\varepsilon}_{gb} - \dot{\varepsilon}_c)\frac{\alpha d_{sg}}{d}. \tag{3.5}$$

   This expression suggests $\dot{\varepsilon}_s \propto d^{-1}$. Analysis of the slope of the obtained data indicates that $\dot{\varepsilon}_{gb} \approx 5\dot{\varepsilon}_c$, if α is assumed equal to 3, *i.e.*, grain boundaries contribute the deformation[2].

[2] In the original paper, some $\cdot$ of $\dot{\varepsilon}_*$ were missing as misprints.

The results obtained by Barrett *et al.* were the experimental results, so that their suggestion of the grain size dependence in copper is true. However, I think it is dangerous to extend their conclusion to other f.c.c metals and alloys unconditionally. Following are lacked or doubtful points in the experiment by Barrett *et al.*

1. **A few experimental conditions**
   As Barrett *et al.* obtained from 0.03mm through 0.77mm grain size specimens to examine the **grain size dependence** with various technique, the creep tests were performed only three temperature and stress conditions, *i.e.*, (a) 697K, 35MPa (b) 742K, 21MPa and (c) 899K, 21MPa. I think three conditions are few and the conditions themselves were higher stress and lower temperatures compared with the conventional creep tests conditions.

2. **Influence of the impurities except for hydrogen ?**
   They examined the effect of hydrogen, but they only mentioned " The difference of the impurities" for other impurities.

As long as the present author searched for the power-law creep of pure metals after the report of Barrett *et al.*, there is only a report by J. D. Parker and B. Wilshire[35] in aluminum. In their report, they supported the results of Barrett *et al.*, *i.e.* there is no grain size dependence in large grain size region even if comparing the single crystal with polycrystal. So that the results of Barrett *et al.*, *i.e.*, **negative dependence** in small grains (below 0.1mm) and **no grain size dependence** in large grains (over 0.1mm), are the general belief of the grain size dependence of the steady-state creep rate of the pure metals.

3.3 Experimental results

First, I'll show the summary of the present result of the pure platinum creep.

1. Followings are equal or similar phenomena obtained previously in other metals.
   (a) In this experimental conditions, stress exponent n of the steady-state creep rate is 5 with a few exceptions. The result implies that the dislocation climb controls the steady-state creep rate.
   (b) Rupture mode is the void-coalescence in grain boundaries at low temperatures with fine grains. The rupture mode is similar to those of the other metals[36,37].

2. Followings are newly found phenomena in platinum.
   (a) Strain-burst was observed in some limited experimental conditions for a specific ingot.
   (b) Rupture mode changes to the necking or shearing-off at high temperatures for the specimens with coarse grains. The phenomenon is different from others where fine grains are often obtained by dynamic recrystallization[36,37].

3. Following is the firstly found phenomenon to amend the common sense.

(a) Strong grain size dependence of the steady-state creep rate is observed in wide range of stresses and temperatures.

Details of the strain-burst and grain size dependence of the steady-state creep rate of the platinum are explained and discussed.

3.3.1 Creep curves and microstructures

Specimens In this section, all specimens were loaded after the pre-annealing, *i.e.*, annealing prior to the creep test, at the same temperatures of the creep tests. The pre-annealing condition is different from that of section 3.3.2. UPP-2, 4, 5 and 6 in Table 2.1 and 2.3 were applied in this section.

Initial grains Each specimen was annealed for an hour at each temperature before creep test. The microstructure is similar for all specimens before loading in spite of the different annealing temperatures. The grains are isotropic and the average size is about 0.2mm as shown in Fig. 3.1. Hence the difference in the annealing temperature before the test is considered to have no effect on the results.

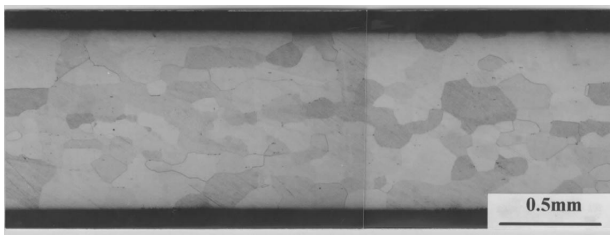

Figure 3.1: Initial microstructure of UPP-4 annealed for an hour at 1673K.

Creep curves Figure 3.2 shows creep curves tested at 1673K and at various applied stress[38]. These curves were obtained from the specimens taken from ingot UPP-4 in Table 2.3.

The creep curve at 3.0MPa (Fig. (a)), shows a typical three-stage creep, *i.e.*, the primary, steady and acceleration stage. As the applied stress is decreased to 2.5MPa, a sudden increase in the strain (a strain burst) appears after the elongation of about 1%, and the incubation time before the strain burst increases with decreasing the applied stress as shown in Fig. 3.2 (b), (c) and (d). Eleven specimens from ingot UPP-4 were tested at 1673K to confirm the appearance of the strain burst. All specimens showed the strain burst when tested at a stress from 1.5MPa to 2.5MPa, and no burst was observed at other stresses. The appearance of the burst depends on the applied stress. Figure 3.3 shows the same curve as shown in Fig. 3.2 (c) with the vertical axis being magnified. The inserted figure shows that the specimen elongates slowly during the incubation period. At 1.0MPa, the specimen creeps but no strain burst occurs.

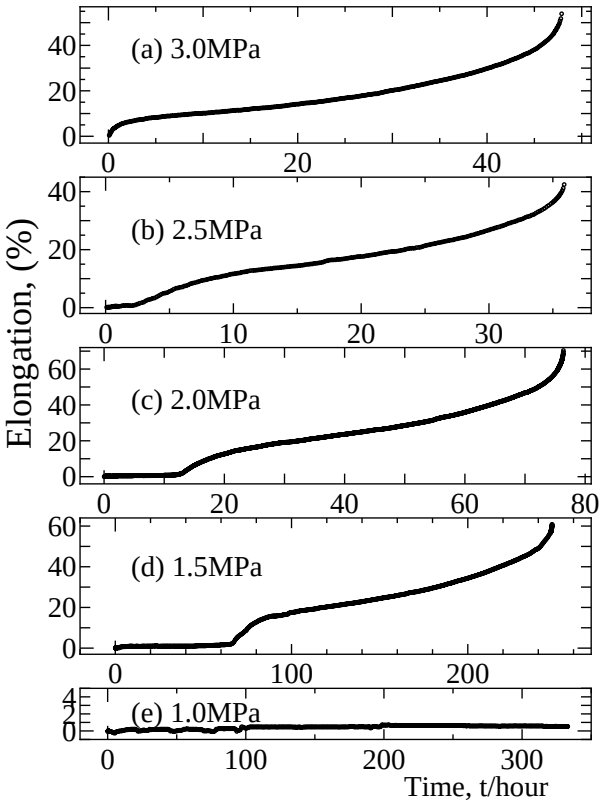

Figure 3.2: Creep curves at 1673K from ingot UPP-4.

Microstructures after the creep tests Figure 3.4 (a) and (b) are typical microstructures of crept specimens taken from ingot UPP-4. They show the cross-section parallel to the tensile axis and normal to the wide surface. In the specimen crept at 1473K and 4.5MPa (Fig. 3.4 (a)), the grain size is similar to the initial size (see Fig. 3.1). There are many voids on boundaries normal or nearly normal to the tensile axis. The rupture takes place by the void coalescence, *i.e.*, the intergranular creep fracture. The majority of the specimens crept at and below 1573K have microstructures similar to that shown in Fig. 3.4 (a).

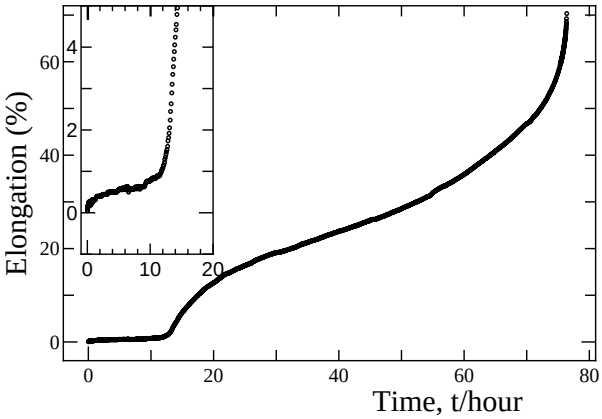

Figure 3.3: A creep curve at 1673K and 2.0MPa.

When the specimen was crept at 1673K, the microstructure is completely different from those after crept at and below 1573K. There are a few large grains whose grain boundaries are normal to the wide surface and no void exists at the boundaries. Obviously the recrystallization of the initial microstructure took place. Although not shown in a figure, a specimen tested at 1673K and 1.0MPa (Fig. 3.2 (e)), was partially recrystallized but not completely recrystallized. The initial microstructure has been completely recrystallized in specimens which show the strain-burst. The specimen tested at 1673K and 3.0MPa (Fig. 3.2 (a)), was also completely recrystallized. The recrystallization occurred immediately after the loading and the incubation period could not be recorded.

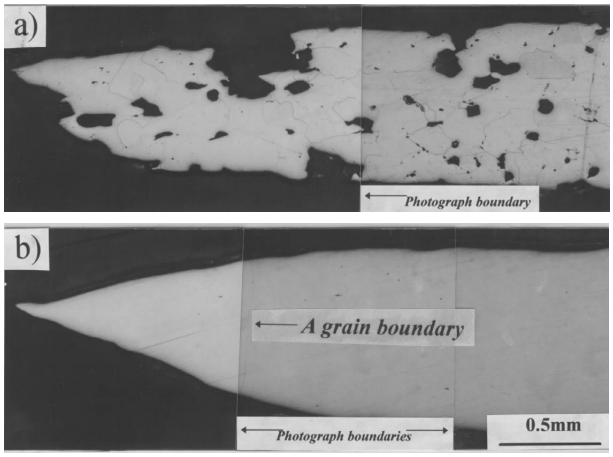

Figure 3.4: Microstructures of the crept specimens from ingot UPP-4.

Surface morphology after the creep test Figure 3.5 shows examples of morphology of the wide surface of the specimens from ingot UPP-4. In the specimen crept at 1673K and 2.5MPa, the surface relieves are observed (Fig. 3.5 (a)). They are slip bands. There are also the image of the initial microstructure overlapping the slip bands. The image is erased by chemical polishing the surface, and the microstructure resulted is quite similar to that shown in Fig. 3.4 (b). These observations imply that the initial grain boundaries were revealed by thermal etching and the instantaneous deformation upon the application of the load, and then the recrystallization took place and the slip bands were formed in the new grains. Figure 3.5 (b) shows the microstructure of the specimen crept at 1473K and 4.0MPa. Slip lines are hardly observed and the grain boundaries are revealed by thermal etching and deformation. The microstructure was reserved when the surface was chemically polished. Cross section of microstructures is similar to Fig. 3.4 (a). There is little grain growth or no recrystallization at this temperature and stress.

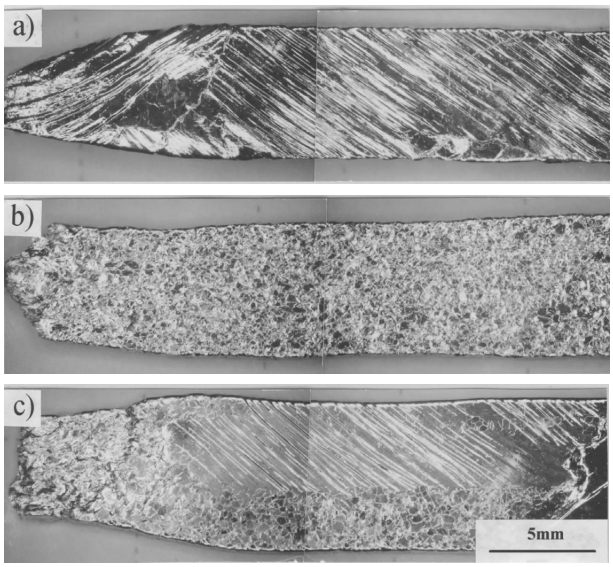

Figure 3.5: Wide surface of the crept specimens from ingot UPP-4.

Figure 3.5 (c) is for the specimen tested at 1573K and 3.0MPa. The surface has the two characteristics for the 1673K and 1473K creep. At some parts of the specimen slip lines are observed, and at other parts initial grain boundaries are observed. The recrystallization was not completed. No strain burst was observed in specimens shown in Fig. 3.5 (b) or (c). It is obvious that the strain burst is observed only when the specimen is completely recrystallized. There is no strain burst on the creep curve when the partial recrystallization took place. The occurrence of the strain burst and recrystallization depends more strongly on the test temperature than the stress. The critical temperature for the burst and recrystallization is around 1573K.

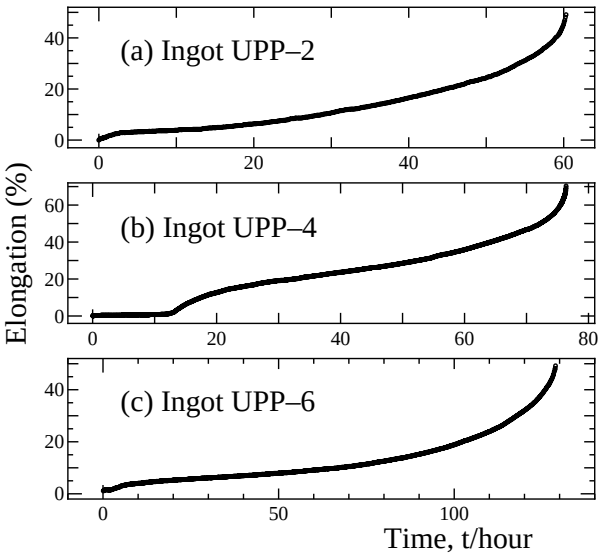

Figure 3.6: Creep curves for different ingot.

Creep curves from the specimens taken from other ingots Figure 3.6 shows creep curves at 1673K and 2.0MPa for specimens taken from ingots UPP-2 (a), UPP-4 (b) and UPP-6 (c). UPP-4 gives the same curve as shown in Fig. 3.2 (c), and is shown again for comparison. Although all the specimens show the three-stage creep curve, UPP-2 and UPP-6 show no strain burst. These specimens are not recrystallized. The relation between the burst and complete recrystallization is confirmed. Figure 3.7 shows a creep curve for ingot UPP-5 tested at 1773K and 1.0MPa. A strain burst is observed. Micrograph has revealed that the specimen was completely recrystallized. Thus, the critical temperature is between 1673K and 1773K for UPP-5. The critical temperature may be increased by the hot-forging of the ingot, since UPP-4 and UPP-5 were cut into two pieces from the same ingot. The critical temperature has not been determined for specimens from ingots other than UPP-4 and UPP-5. It should be higher than 1673K. Since all the ingots are of similar purity, slight difference in the concentration of minute impurities is considered to affect the critical temperature. 凸凹 in the Fig. 3.7 during the incubation time is the noise in measuring system.

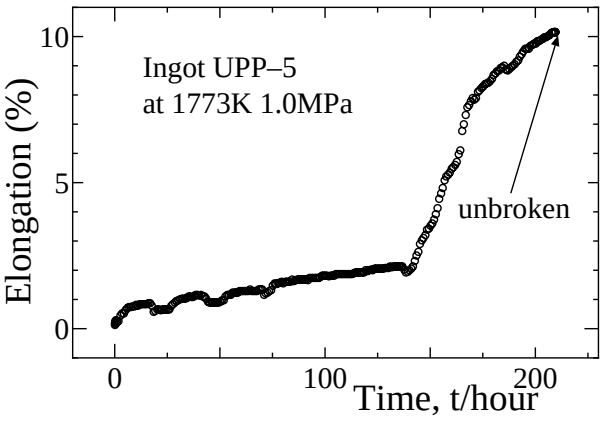

Figure 3.7: A creep curve at 1773K and 1.0MPa from ingot UPP-5.

Observation by interrupting creep

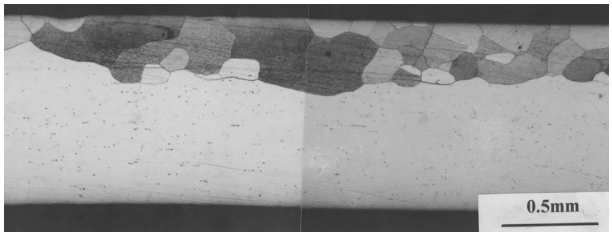

Figure 3.8: Microstructure of a specimen after creep interruption.

Figure 3.8 shows the microstructure of the specimen from ingot UPP-4. This specimen was crept for 5minute at 1673K and 2.5MPa. Then the load was removed and the specimen was kept for 5 hours at the same temperature with a stress of 0.5MPa due to holders. As shown in Fig. 3.2, the elongation of this specimen is still in the incubation stage. The grains are partially recrystallized. The results show that the main source of the stress causing the recrystallization was given by the initial short period loading (mostly the instantaneous strain) and that the accumulation of strain by creep is not always necessary for the present recrystallization to occur.

Figure 3.9 is another interrupted creep curve to observe the surface morphology and the surface is also shown in Fig. 3.10. This observation was performed for the specimen taken from UPP-4 after pre-annealed at 1673K for an hour. To make observation easy between the initial grains and the slip lines, the surface was etched by aqua regia and scratched lines beforehand. After the preparation, the specimen was crept at 1673K with 1.5MPa, respectively. The test condition is within the condition of the appearance of the strain-burst. After 25 hours passed, the sign of the strain-burst was shown, so that the specimen was taken off from the furnace. The slip bands were observed clearly on the surface (see Fig. 3.10), however, the relationship between the initial grain boundaries and slip bonds was not clear, *i.e.*, it is not clear whether the slip lines across or does not across the initial grain boundaries because it might have just started the strain-burst and the strain was small. So that the specimen was back into the furnace and loaded again with the same conditions. More 80 hours passed, the surface was observed again. There are the image of the initial microstructure and scratched lines overlapping the slip bands, *i.e.*, the initial fine grains were only traces and have turned to coarse grains. The observation is the same with the other surface observation in Fig. 3.5 (page 22).

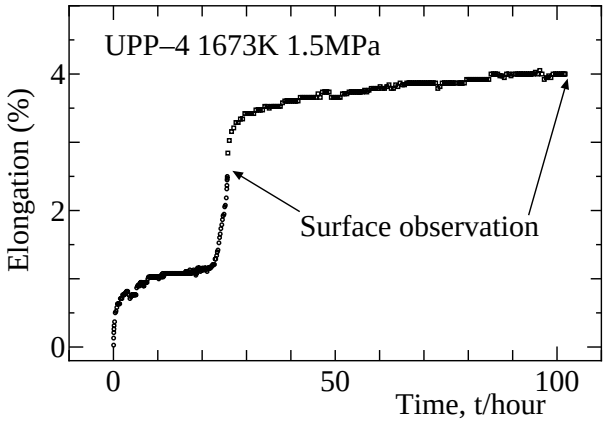

Figure 3.9: A creep curve after creep interruption.

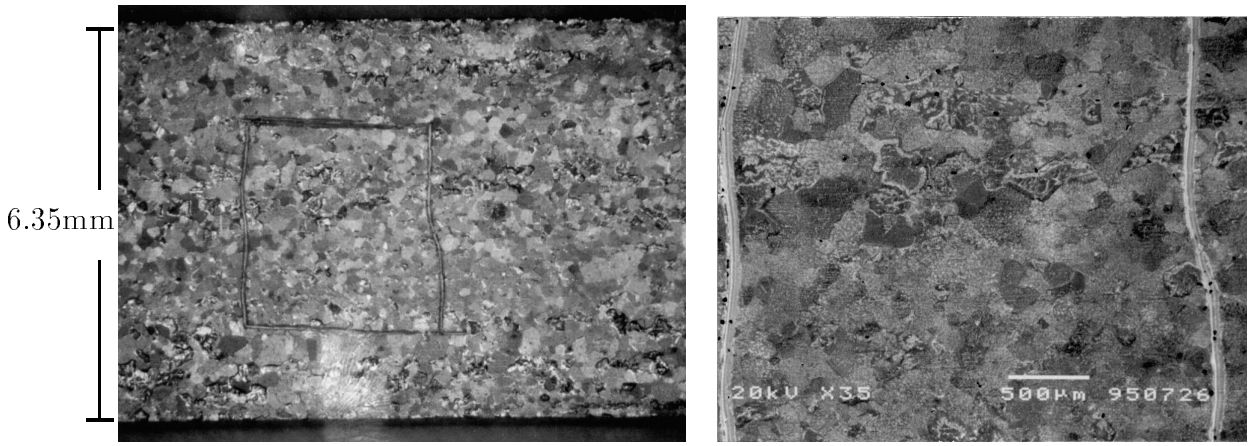

Initial surface

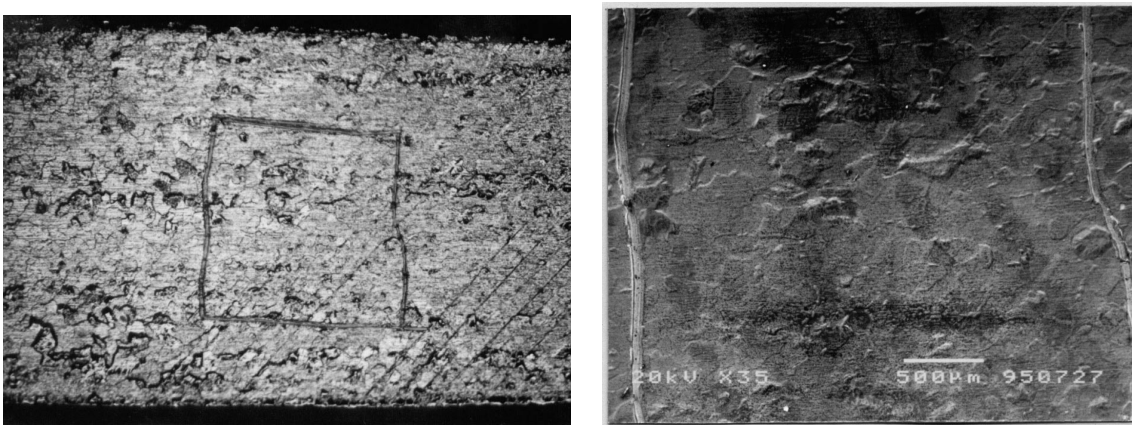

After 25 hours

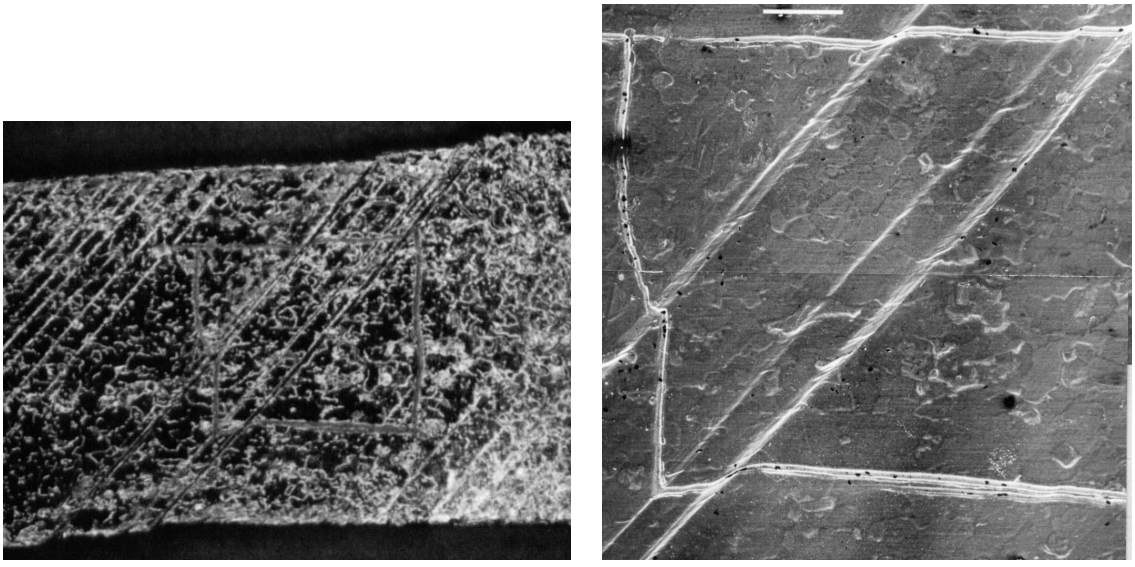

After 100 hours

Figure 3.10: Wide surface after creep interruption from ingot UPP-4.

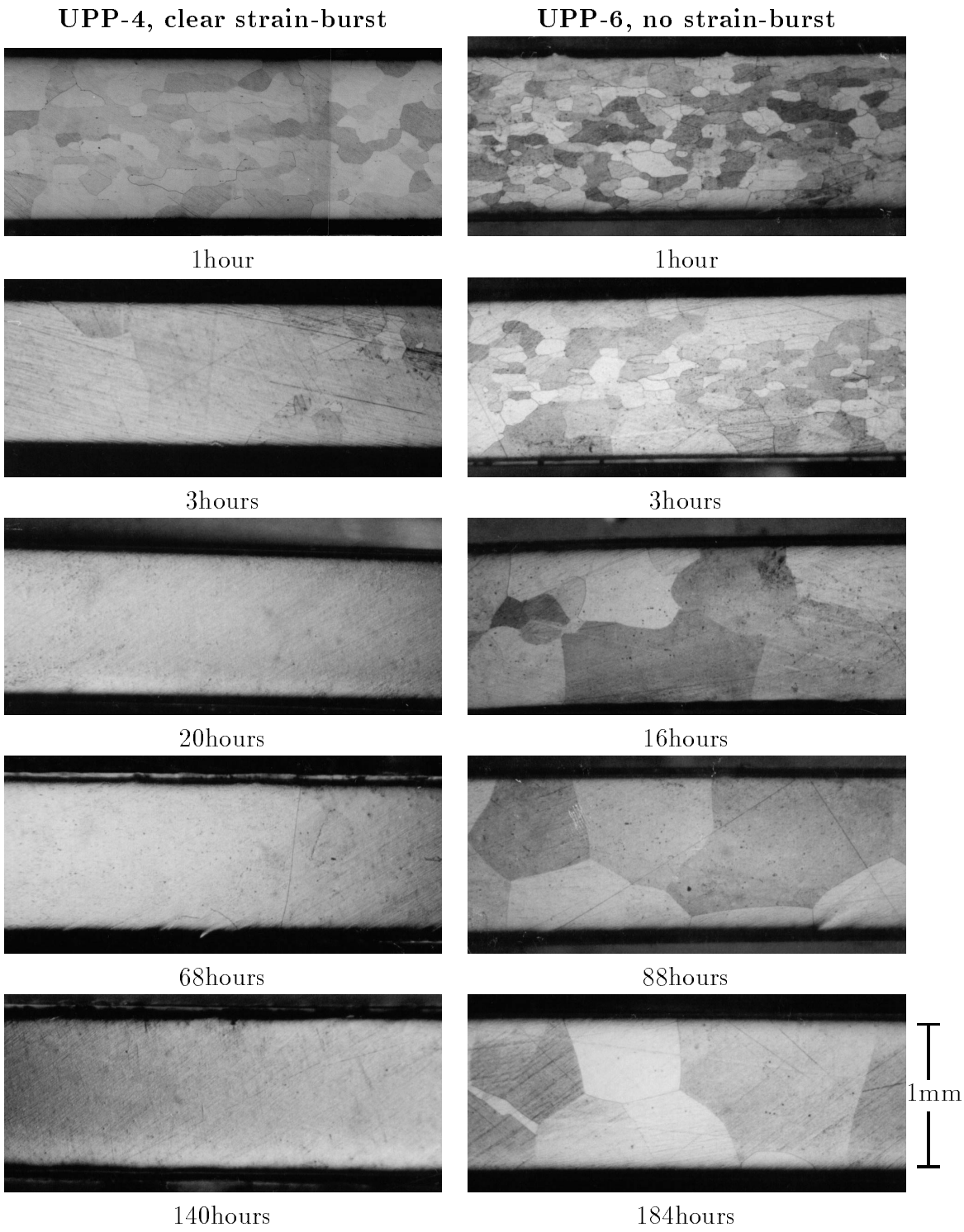

Figure 3.11: Microstructures after isothermal annealing at 1673K.

Microstructures after isothermal annealing Strain-burst has explained with the microstructures after the creep tests. From the interrupting observation in Fig. 3.8, a part of the grains recrystallized to the coarse grains.

In order to clarify the accumulation of strain by creep which is the origin of the driving force for the usual dynamic recrystallization, static isothermal annealing character was compared between UPP-4[3] and UPP-6[4]. The results were shown in Fig. 3.11. There is no difference for an hour annealing. Although the tendency of the grain growth with the annealing time is similar, the magnitude of the growth is completely different between UPP-4 and Upp-6. After 20 hours, the grain boundaries are scarcely observed in UPP-4[5]. On the other hand, UPP-6 have the similar tendency to grow, but the magnitude is very small. Even if after 188 hours annealing, the grain size is about the half of the specimen thickness and the grain boundaries are observed clearly.

The result implies that the UPP-4, which shows the clear strain-burst, has a tendency to became coarse grains with long time annealing even when the static conditions are applied without stresses. As shown in Fig. 3.5 and 3.4, it is confirmed that the appearance of the strain-burst has strong relationship with the grain growth from the observations after the creep tests. I think the strain-burst appeared when the static grain growth (or recrystallization) took place remarkably. The applied stress of the creep might help the grain growth. According to the present experimental results, the strain-burst is not strictly dynamic recrystallization, which needs the accumulation of strain by creep.

[3] Show clear strain-burst.

[4] No strain-burst was observed in any present experimental conditions

[5] In order to confirm the **few boundaries**, the specimen was etched strongly, so that the polished scratch lines were stood out.

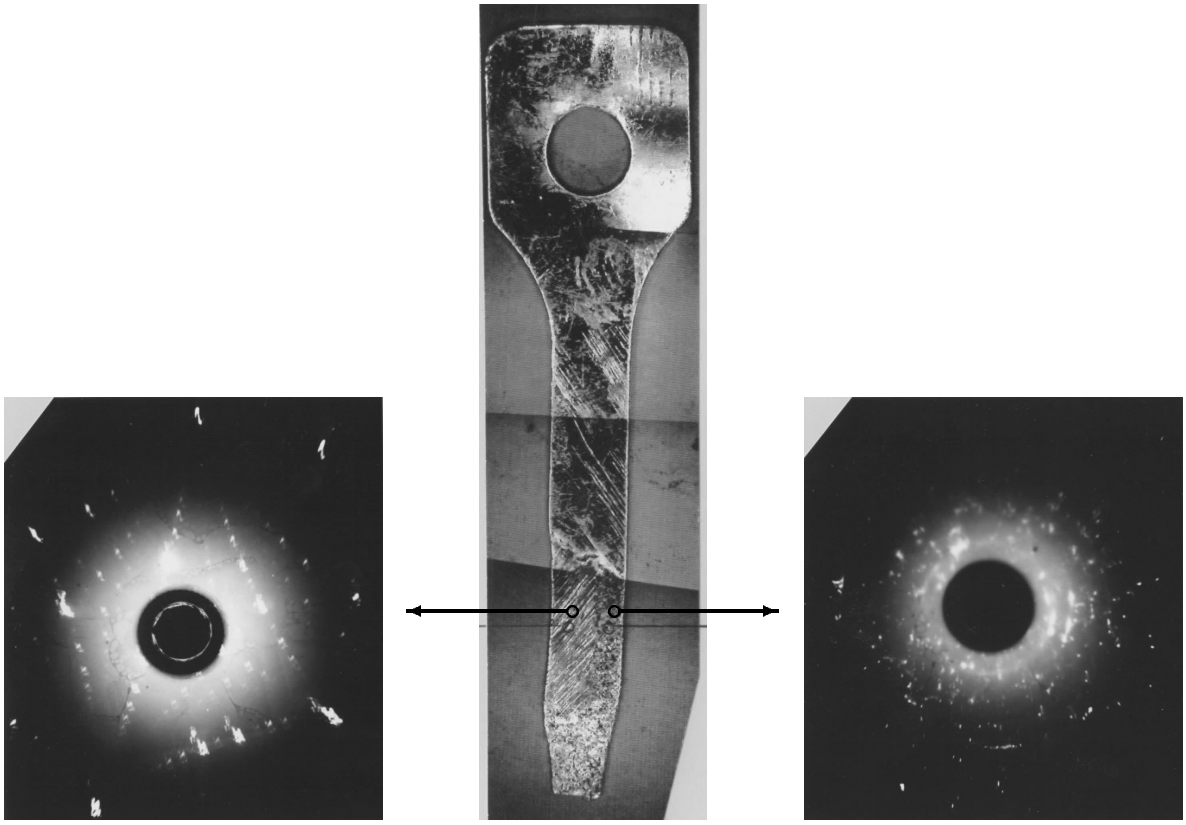

Figure 3.12: Back scattered Laue patterns from a crept specimen.

X-ray diffraction results Microstructures of the surface correspond to those of cross section to each other as shown in Fig. 3.4 and 3.5. In order to confirm that the microstructure observed at the surface is the same as that of inside, X-ray diffraction is taken. Figure 3.12 shows the surface morphology and two back scattered Laue photographs of a specimen from ingot UPP-4 crept at 1573K and 3.0MPa. A single crystal diffraction pattern is obtained from the area with coarse slip bands. Metallography shows this area to be a single crystal. Polycrystalline pattern is observed from the area reserving the initial small grains. Same results were obtained with specimens crept at other temperatures and stresses. The result also shows that the polycrystalline structure is changed to bamboo-type structure with a few large crystals when the specimen is crept above the critical temperature, and the initial polycrystalline structures are reserved below its temperature.

Conclusion in this section High temperature creep behavior has been investigated with high purity platinum (99.999 mass%) at high temperatures from 1373K up to 1773K with various stresses. As the results, following are obtained.

1. In this experimental conditions, typical three stage creep curves, *i.e.*, primary, steady-state and accelerating stages, were obtained. The power-law creep is observed with the stress exponent n of the steady-state creep is around 5. The results imply that the dislocation climb controls the creep deformation. The creep mechanism of the platinum is similar to that of other pure metals.

2. The grain growth (or recrystallization) to almost single crystal during the creep and the strain-burst (a sudden increase in the strain) were observed in the specimens taken from an ingot with good reproductively. The phenomenon is,

   (a) To appear the strain-burst, perfect recrystallization (or grain growth), which means to be an almost single crystal of a specimen, is required. Partial recrystallization is not enough to appear.

   (b) This recrystallization seems to be different from usual strictly defined dynamic recrystallization, which needs the accumulation of strain by the creep deformation. The phenomenon concerns with the strain just after the loading or static grain growth[6].

   (c) The phenomenon occurs in the ingot in which the static grain growth appears remarkably.

   (d) The phenomenon has a tendency to appear at high temperatures and high stresses.

   (e) The phenomenon is influenced by trace impurities, test temperatures, applied stresses and production process *etc.*

3. The creep rupture mode is the void coalescence on the grain boundaries in small grains. This is the similar phenomenon with other metals and alloys.
   The rupture mode changes to the necking or shearing-off by the recrystallization in coarse grains. Usually, in other metals and alloys, the grains became small because of the dynamic recrystallization. On the other hand, the grains in platinum are large and slip bands are observed on the surface of the specimen. The final grain size is completely different from others.

[6] The phenomenon occurred under the stress and the deformation, in a wide meaning it is called a dynamic recrystallization.

3.3.2 Grain size dependence of the steady-state creep rate

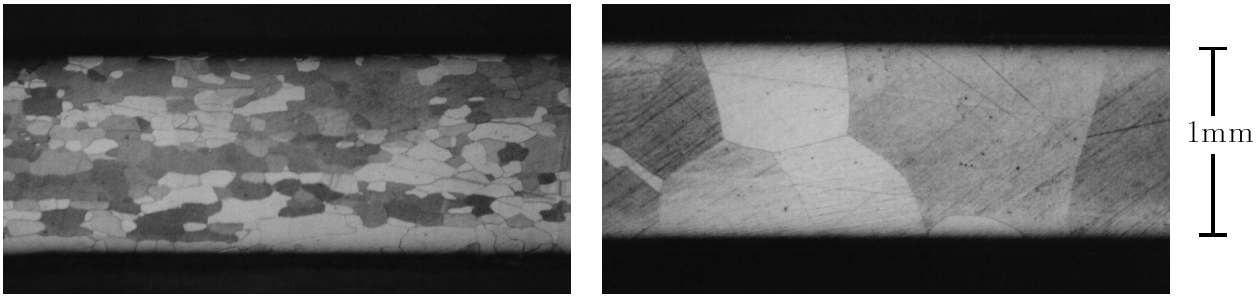

(a) Annealed at 1673K for 1 hour (b) Annealed at 1973K for 1 hour

Figure 3.13: Initial microstructures after pre-annealing.

Creep specimens In order to examine the grain size dependence of the steady-state creep rate of the platinum, all creep specimens were annealed for one hour at several temperatures to obtain various grain size. The final heat-treatment will be referred to the pre-annealing, *i.e.* annealing prior to the creep tests. Please be careful the pre-annealing conditions in this section is different from that in the section 3.3.1. The detailed conditions will be declared with the results. Specimens were taken from the ingot UPP-2, 3, 6, 8, 9 and IND in Table 2.1 and 2.3.

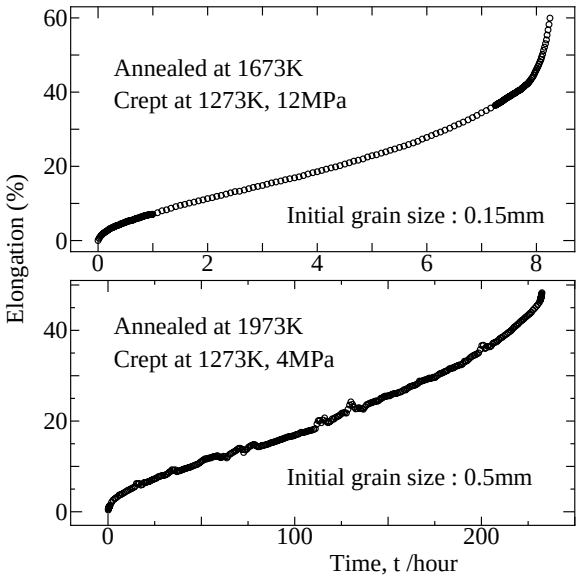

Figure 3.14: Examples of creep curves for specimens with various grain-sizes.

Initial microstructures before the creep test (after the pre-annealing) are shown in Fig. 3.13. At 1673K, homogeneous isotropic grains with 0.15mm average grain size is obtained like Fig. 3.1. For all specimens, the standard deviation of the grain size data in a specimen is close to that among specimens; the grain size dose not vary from ingot to ingot but determined by the pre-annealing temperature only. Usually, the grain size is smaller for the lower pre-annealing temperature, but in the high purity specimens it is independent of the annealing temperature below 1673K. The grain size of the industrial grade specimens depends on the pre-annealing temperatures even below 1673K. It is noted that for the same pre-annealing temperature the industrial grade specimens have larger grain size than the high purity specimens, and the critical temperature for the grain-growth during creep is lower for the industrial grade specimens than the high purity ones. This is opposite to the usual tendency that the purer specimens are easier to recrystallize. This unusual purity dependence of recrystallization will not, however, be discussed further. The grain size and its standard deviation of the specimens applied in the present experiment are summarized in Table 3.1.

Creep curves Example of creep curves of high purity platinum is shown Fig. 3.14. Each specimen was pre-annealed at 1673K[7] and 1973K[8], and crept at 1273K with stresses of 12MPa and 4MPa, respectively. Three-stage creep curves are observed and we determined the steady-state creep rate as described before (see page 8). Because of the difference of the initial grain size and stress, the creep rupture time and ruptured elongation are completely different each other[9]. However, the shape of the obtained creep curves are similar to each other. As sometimes a little different creep curves as shown in Fig. 2.4 were obtained, steady-state creep rate is analyzed from these curves as explained in section 2.2.

Table 3.1: Initial grain-size of the specimens.

Specimen	Annealing temperature	Grain size (mm)	σ_1 (%)	σ_2 (%)	Specimen thickness 1mm	0.5mm	5mm
High-Purity	1673K	0.18	3	2	□	—	■
Platinum	1973K	0.52	5	5	○	—	●
Industrial	1273K	0.21	10	9	◇	△	—
Grade	1473K	0.40	11	17	◇	△	—
Platinum	1973K	0.64	18	14	◎	▽	—

σ_1 : standard deviation within a sample
σ_2 : standard deviation between samples

Steady-state creep rate Figure 3.15 shows the summary of the observed steady-state creep rate against the applied stress. Symbols in the Fig. 3.15 is given in Table 3.1. In each figure, results from specimens with two different grain sizes are compared. Except for the industrial grade specimens pre-annealed at 1473K, the creep rate depends clearly on the grain size; the creep rate is smaller for the specimens with smaller grain size, *i.e.*, **positive dependence** is observed. The stress exponent n of the creep rate is also shown in the figure. it is about 5. However $n = 7.9$ was obtained for the coarse grained specimens tested at 1073K. The stress exponent of about 5 and 7.9 means that the creep in these specimens is controlled by dislocation climb. The data for the industrial grade specimens pre-annealed at 1473K show some scatter. This is due to the various grain sizes as seen from Table 3.1. The standard deviation of the grain size among specimens is large for the industrial grade specimens pre-annealed at 1473K.

Microstructures after the creep tests Microstructures after the creep tests is shown in Fig. 3.16 with the initial ones, which has already shown in Fig. 3.13 for the comparison. Grain growth is hardly observed for the specimen crept at 1473K after pre-annealed at 1673K. And the creep rupture mode is the intergranular one with the void-coalescence in the grain boundaries vertical to the stress axis similar to that of 3.4 (a). The grain growth was taken place during the creep test where the same pre-annealed specimen was crept at 1673K. On the other hand, when the initial grains were coarse, the grain growth

[7] The initial grain size is 0.15mm as shown in Fig. 3.13 (a)
[8] The initial grain size is 0.5mm as shown in Fig. 3.13 (b)
[9] Of course the steady-state creep rate is also different.

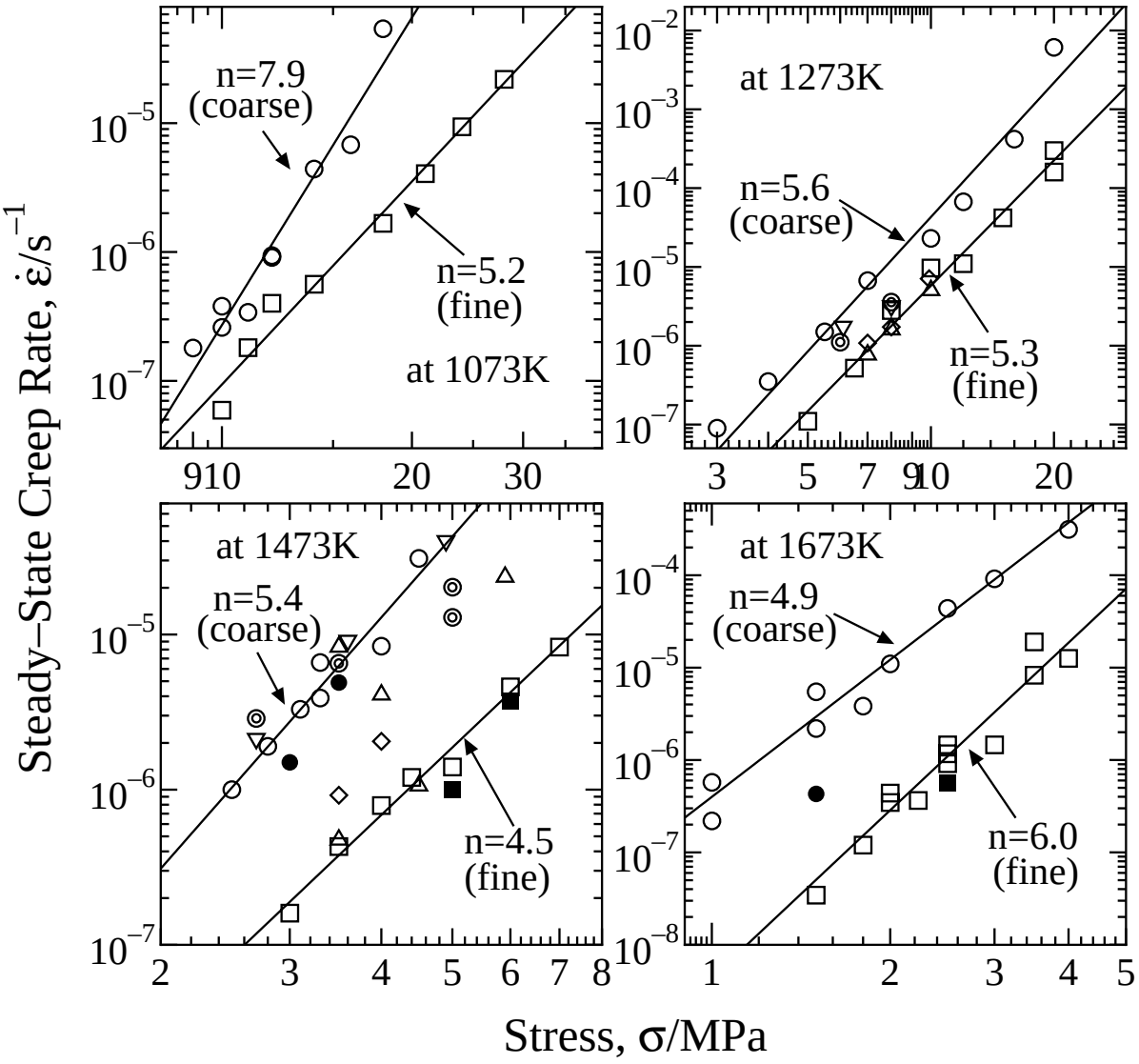

Figure 3.15: Steady-state creep rate of platinum at various temperatures.

occurs independently on the crept temperatures. But no strain-burst[10] was observed in this experiment. Hence it is not clear yet whether the grain-growth during creep is solely due to dynamic recrystallization or static grain-growth.

Creep rupture mode is the void-coalescence in the grain boundaries vertical to the stress axis in fine grains and the necking or shearing-off in coarse grains. No brittle fracture in the grain boundaries was observed like Fig. 1.2 and 1.3[11].

[10] See Fig. 3.2
[11] See page 2.

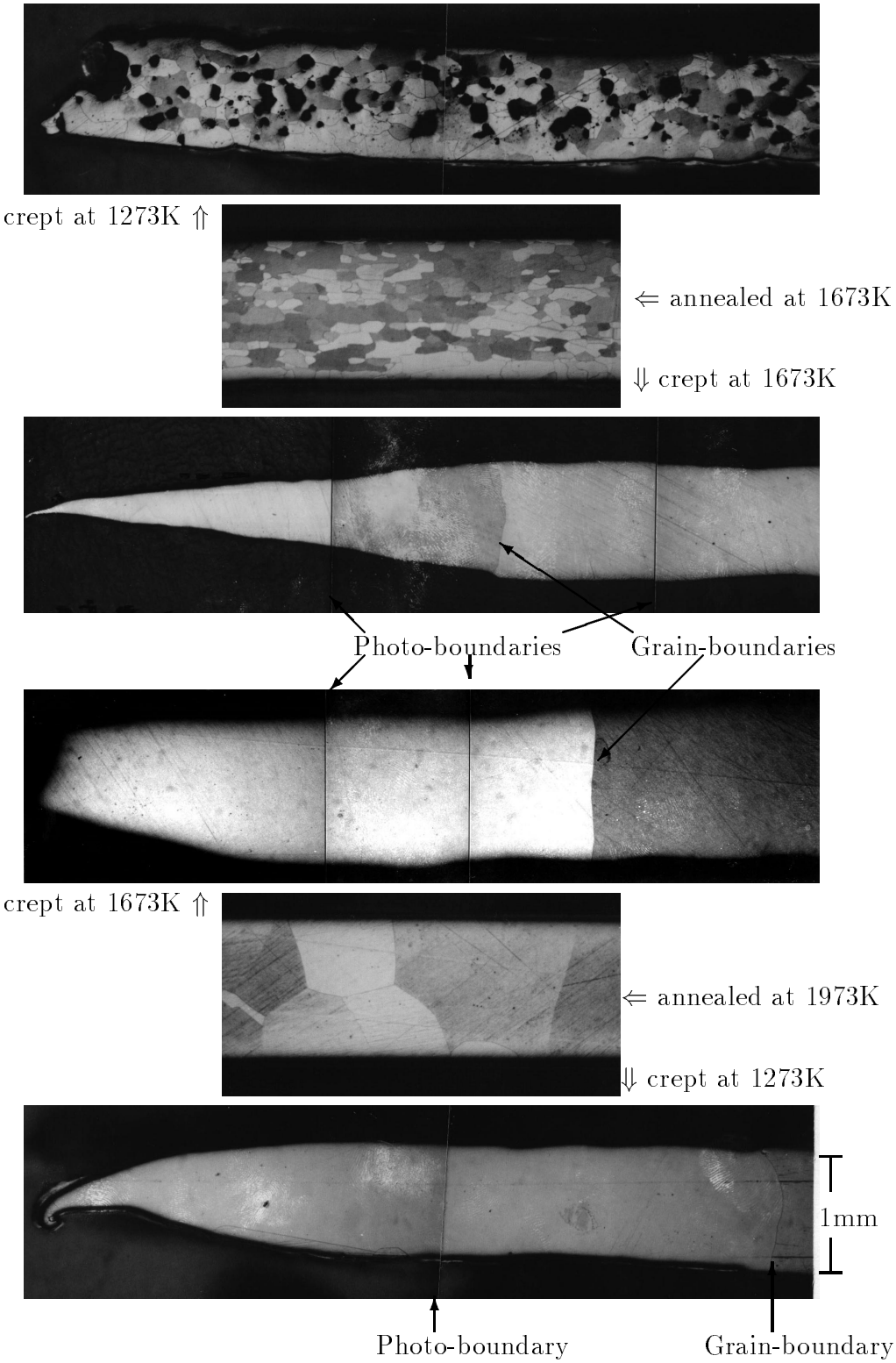

Figure 3.16: Microstructures of high purity platinum before and after the creep test.

Results of 5mm specimens As already mentioned previously as the examples of the practical platinum use in chapter 1, platinum and its alloys are usually used from 0.5mm through 1.5mm thickness in glass melting industry where the high temperature creep takes place[12]. In the present experimental conditions especially specimen thickness[13] is imitated the practical use, *i.e.*, the all present experimental conditions is required to understand the platinum **as a practical material**.

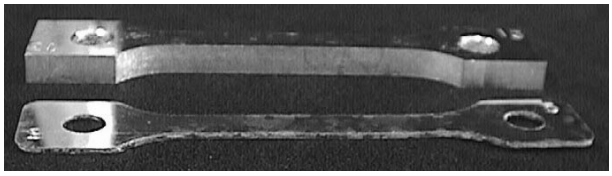

Figure 3.17: A 5mm specimen comparing conventional 1mm specimen.

However, platinum is an f.c.c. metal, so that it is very important to compare the high temperature properties with other f.c.c. metals and alloys. Especially, in order to compare the **positive grain size dependence**, which is newly found phenomenon in the present experiment and requires to amends the general belief, with other f.c.c. metals and alloys such as austenitic stainless steel, aluminum, copper, nickel and so on, 1mm thickness with 1 or 2 grains is a quite different condition from other metals and alloys in experimentally or practically. That is, grain size is too large comparing with the specimen thickness. This suggestion has pointed out in the domestic and international presentations.

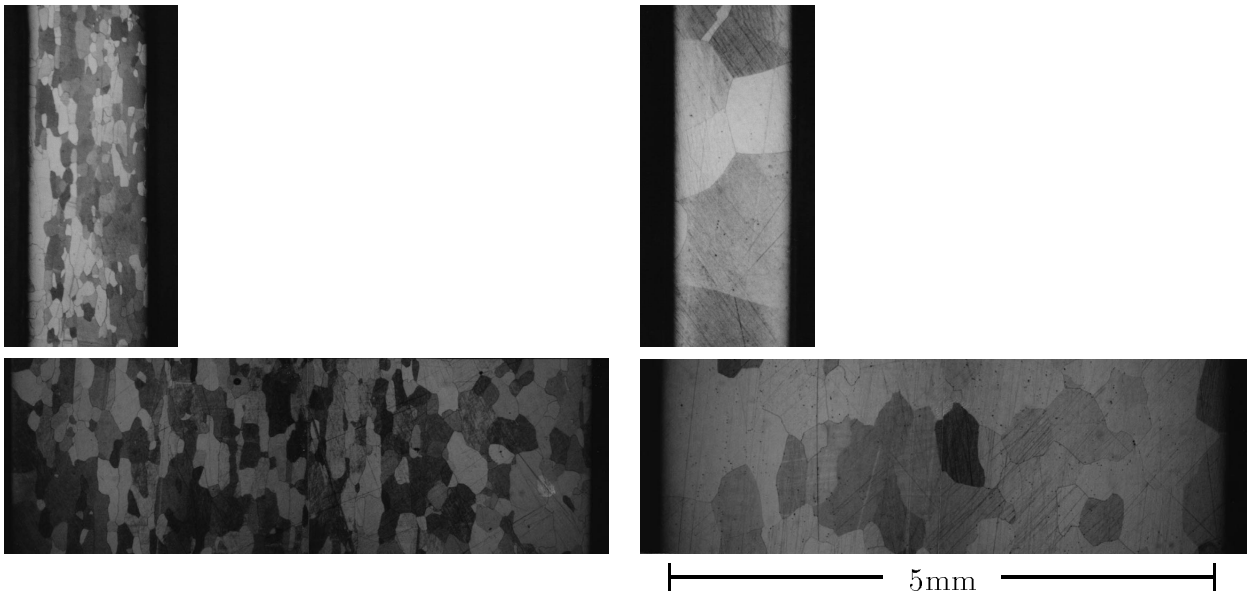

Annealed at 1673K for 1 hour Annealed at 1973K for 3 hours

Figure 3.18: Microstructures of 5mm specimens.

In order to confirm the results and to make it possible to compare with other metals and alloys, 5mm specimens were crept. The microstructures of 5mm specimens are shown in Fig. 3.18. In this figure, conventional 1mm specimen, as shown in Fig. 3.13, is also shown for the comparison. The grain size of the specimen pre-annealed at 1973K for an hour is slightly smaller than that of 1mm specimen due to the final reduction difference, so that 3 hours pre-annealing was applied to obtain the similar grain size. As shown in Fig. 3.18,

[12] Because of the cost of platinum itself.

[13] In this experiment, mainly 1mm thickness specimens were crept at various conditions.

there are more than 10 grains across the specimen thickness. UPP-9 was supplied for the 5mm specimens and a part of it was also supplied for conventional 1mm specimens.

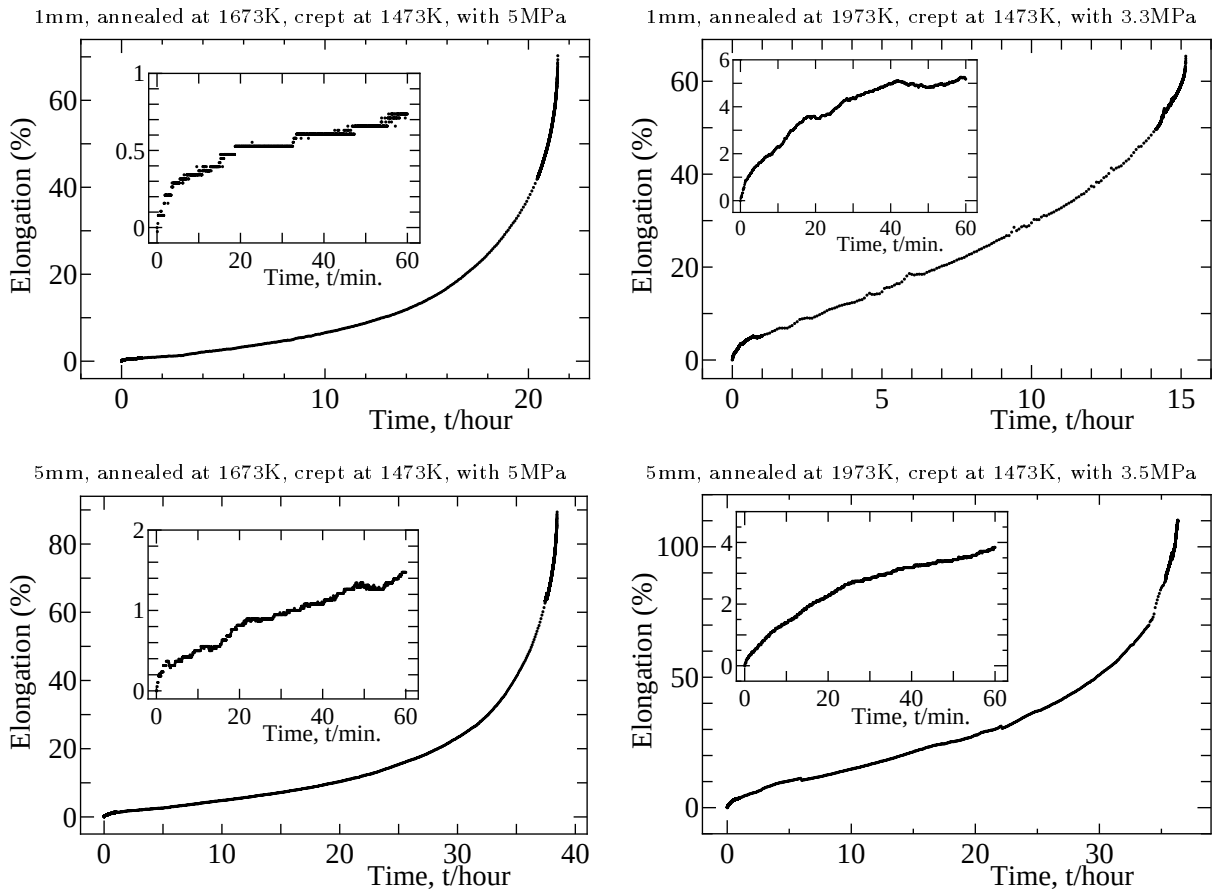

Figure 3.19: Creep curves of 1mm and 5mm thick specimens.

A 5mm specimen is shown in Fig. 3.17 comparing with conventional 1mm specimen. As noticed before, the results of the 5mm specimen have already plotted in Fig. 3.15. The results are ● and ■ in Table 3.1. These results are on the same line with 1mm results except for one point which is obtained from coarse grained specimen crept at 1673K, 1.5MPa. One point is not on the same line. The point is between the coarse grain results and fine grain ones, so that there is no qualitative inconsistency. Please notice that the specimen thickness gives no influence to the **positive dependence** as long as the specimen thickness is from 1mm to 5mm in platinum.

Figure 3.19 shows the comparison of the creep curves between 5mm specimens and 1mm ones in the similar creep conditions. Detailed experimental conditions are shown above each graph. The inserted figure is magnified vertical and horizontal axis for 60 minutes to show the appearance of the steady-state creep. No difference is observed for the shape of the creep curves due to the specimen thickness. Creep rupture time and rupture elongation are longer for 5mm specimens, *i.e.*, the specimen thickness influences the creep rupture time and the rupture elongation. However, the specimen thickness does not affect the steady-state creep rate at all. The reason why the specimen thickness affects the creep rupture time and elongation, is due to our experimental conditions crept with constant load. The reduction of the cross section of the specimen is independent of the specimen thickness but

the time to reach the absolute thickness to rupture depends on the specimen thickness.

3.3.3 Activation energy of the creep

As already mentioned in section 3.2.1, the activation energy of the steady-state creep of the platinum was calculated by Dushman *et al.*[17]. As long as I know, this is the first and last one. Steady-state creep rates were measured in the present experiment with various temperatures and stresses, which make it possible to calculate again.

Figure 3.20 is the rewrite figures in each grain size of Fig. 3.15 in each temperature. In the present experiment as shown in section 3.3.2, platinum shows **positive grain size dependence**, so that the activation energy should be calculated for each grain size.

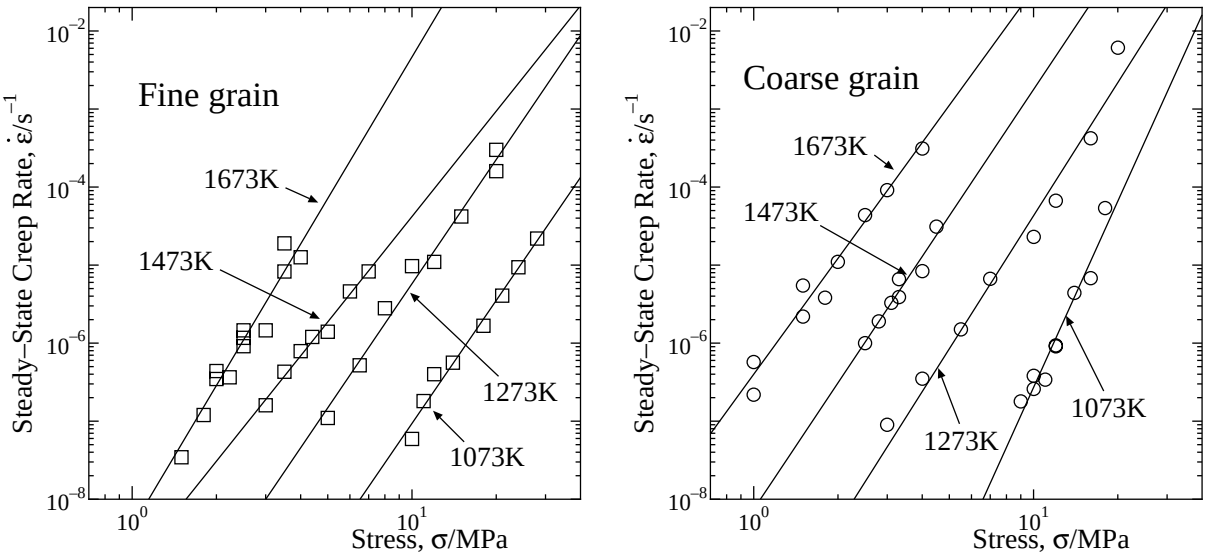

Figure 3.20: Steady-state creep rate at various temperatures.

As shown in Figure 3.15, platinum obeys the power-law creep with the stress exponent $n = 5$ except for the case of the coarse grain results at 1073K. The activation energy of the creep is obtained as follows.

The steady-state creep rate $\dot{\varepsilon}$ is expressed with equation (3.1). The temperature dependence of the elastic moduli was measured from 300K to 1673K to normalize the applied stress in the calculation of the activation energy for creep. The results are shown in Fig. 3.21. Figure 3.20 is a plot for the same grain size results, so that d in equation (3.1) is regarded as a constant. Temperature dependence of the Burgers vector d is similar to the thermal expansion (10^{-6}/K) and is negligibly small. So, the equation (3.1) is transferred to the equation (3.6) for the same applied stress σ where B include the

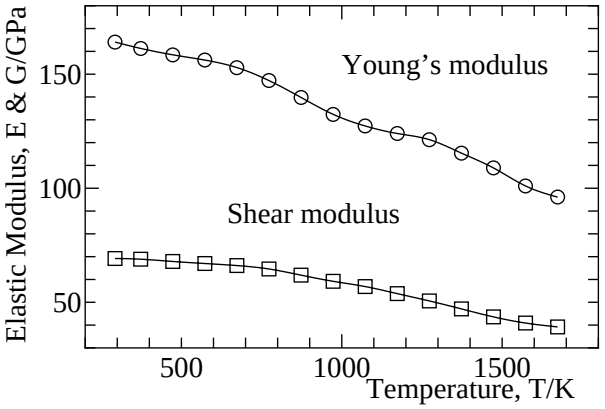

Figure 3.21: Temperature dependence of elastic moduli.

all constant terms.

$$\dot{\varepsilon} = B \exp\left(-\frac{Q}{kT}\right). \tag{3.6}$$

With a logarithmic expression of the both left and right hand terms, the above equation is given by

$$\log \dot{\varepsilon} = \log B - \frac{Q}{kT}. \tag{3.7}$$

When the creep rate is $\dot{\varepsilon}_1$ at a temperature T_1 and it is also $\dot{\varepsilon}_2$ at anther temperature T_2, under the same stress, the above equation gives

$$\log \dot{\varepsilon}_1 = \log B - \frac{Q}{kT_1}, \tag{3.8}$$

$$\log \dot{\varepsilon}_2 = \log B - \frac{Q}{kT_2}. \tag{3.9}$$

The activation energy of the steady-state creep Q is expressed in equation (3.10) by taking equation (3.8) and (3.9).

$$Q = -\frac{k(\log \dot{\varepsilon}_1 - \log \dot{\varepsilon}_2)}{\frac{1}{T_1} - \frac{1}{T_2}}. \tag{3.10}$$

Table 3.2: Activation energy of the steady-state creep rate of pure platinum.

Grain	Stress	T_1 (K)	$\dot{\varepsilon}_1$	T_2 (K)	$\dot{\varepsilon}_2$	Q ($\times 10^5$J/mol)
Coarse	10MPa	1073	2.9×10^{-7}	1273	5.9×10^{-5}	3.02
	5MPa	1273	7.3×10^{-7}	1473	4.0×10^{-5}	3.12
	3MPa	1473	2.7×10^{-6}	1673	1.0×10^{-4}	3.70
Fine	20MPa	1073	3.3×10^{-6}	1273	2.2×10^{-4}	2.38
	10MPa	1073	9.0×10^{-8}	1273	5.4×10^{-6}	2.32
	5MPa	1273	1.3×10^{-7}	1473	1.9×10^{-6}	2.09
	3MPa	1473	1.9×10^{-7}	1673	3.2×10^{-6}	2.89

The calculation results, which are calculated from the stress of 3MPa, 5MPa, 10MPa and 20MPa, are summarized in Table 3.2, except for the coarse grain at 1073K with 20MPa because of the different stress exponent. The result 2.4×10^5J/mol, obtained from the fine grains at 1073K and 1273K, is almost same as that of Dushman *et al.* The reason might be due to the similarity of the experimental conditions between present work and Dushman's. On the other hand, over all average value is to be 2.8×10^5J/mol. The value is larger than that of Dushman *et al.* and same as the activation energy of self-diffusion of the platinum 2.8×10^5J/mol[18].

There seems to be not only dependence of the grain size, however, but also some scatter of the data. It is a purpose of this experiment to calculate the activation energy of the creep, but the creep rates were essentially obtained another purpose, so that the scatter is not be discussed further here.

3.4 Discussion

Pure platinum was crept with various conditions. Similar results and phenomena with other metals or alloys are obtained and summarized as follows.

1. Platinum shows the power-law creep with the stress exponent n of the steady state rate of about 5 with an exception at low temperature. The results imply that the dislocation climb controls the creep deformation in the all present conditions.

2. The creep rupture mode is the void-coalescence in the grain boundaries vertical to the stress axis in fine grains. It is similar to that of other metals and alloys[36,37].

Following phenomena are newly found in platinum.

1. A strain burst (a sudden increase in the strain) has been detected.

2. Creep rupture mode changes to the necking or shearing-off by the recrystallization in the coarse grained specimens. The mode is different from that of others. When the necking or shearing-off occurs, the grain size is usually small by the dynamic recrystallization in other metals and alloys[36,37].

Following phenomenon is a newly found in present creep study and the general belief for the creep may be amended.

1. **Positive grain size dependence** of the steady-state creep rate was observed in this experiment.

The details of the newly found phenomena in platinum creep is discussed in the following sections.

3.4.1 Strain-burst

Strain-burst One of the most significant result in the present investigation is the occurrence of recrystallization during creep and a strain-burst, *i.e.*, a sudden increase in the strain or creep acceleration. Similar phenomena like a strain-burst have not been reported previously in platinum. This is the first report of it[38].

Similar recrystallization and the acceleration of creep were observed in nickel[39,40] and lead[41]. Moreover, when these metals and other metals such as aluminum[42] and iron [5] are tensile-tested at high temperatures, softening or the oscillation of stress in the stress-strain curves are often observed. These softening effects are caused by the dynamic recrystallization. The recrystallization observed in the present experiment appears also to be the dynamic recrystallization. Generally speaking, the dynamic recrystallization often observed in the metals and alloys whose stacking fault energy is moderately low.

> Generally, when crystalline materials are deformed at elevated temperatures, the accumulated dislocations are continuously destroyed by two separate processes. The one is *dynamic recovery* and the other is *dynamic recrystallization*. The more common one, dynamic recovery, leads to the annihilation of *pairs* of dislocations, as well as to the formation of subgrains and regular subboundaries. In high stacking fault energy materials, such as recovery processes completely balance the effects of straining and of work hardening, leading to the establishment of steady-state flow. By contrast, in materials moderate to low stacking fault energy, the dislocation density increases to appreciably higher levels; eventually the local differences in density are high enough to permit the nucleation of recrystallization during deformation. Such dynamic recrystallization leads to the elimination of large number of dislocations by the migration of high angle boundaries[14].

On the other hand, in spite of their relatively high stacking fault energy, the dynamic recrystallization was observed in nickel[39,40], lead[41] and aluminum[42] and the dynamic recrystallization occurs in many f.c.c. metals and alloys. The strain-burst in these metals is caused by the softening with the dynamic recrystallization. Especially, the shape of creep curves, obtained by G. J. Richardson、G. M. Sellars and W. J. McG. Tegart[39] in nickel and R. C. Gifkins[41] in lead, were almost same with those of present experiment, because of the same tensile test condition. The experimental detailed conditions, in which the strain-burst appears in a specific stress range at a temperature, is also similar. As long as just looking at the creep curves comparing previous strain-burst and present ones (see Fig. 3.2), it seems to be the same phenomenon.

But the microstructures were completely different with each other. The recrystallized grains are usually fine in nickel, lead and aluminum, however, the platinum grains grow to almost a single-crystal in the gage of the specimen. There is an report of the detailed observation before and after the dynamic recrystallization in nickel by M. Ohashi, T. Endo and T. Sakai[43]. In their study, when the strain becomes large, the recrystallized grain size is independent of the initial grain size and converge to a certain grain size. The final grains are small size. At least, a grain-growth to almost a single-crystal was not occurred.

From the results of the interrupting creep experiment (in page 24) and isothermal annealing (in page 26), the accumulation of strain by creep, which is the origin of the driving force

[14] Majority of these sentences are quoted from reference (5).

for the usual dynamic recrystallization, is unnecessary for the present recrystallization. The experimental conditions for the occurrence of the strain-burst are as follows.

The specimens taken from the UPP-4 and UPP-5 only shows the strain-burst in the present experiments. The critical temperature to appear the strain-burst is 1673K in UPP-4 and 1773K in UPP-5. These two ingot were taken from the same refined batches, *i.e.* they have the same origin, so that the impurity concentration is almost same as shown in Table 2.3. The production process is different, so that the appearance of the strain-burst is influenced of the production process.

All batches were analyzed by spectroscopic analysis (Table 2.3 in page 13) and UPP-4 and UPP-6 were compared by Inductive Coupled Plasma-mass spectrometry(ICP-mass). As the results, the strain-burst in platinum seems to be appear in a little contaminated ingot. But the purity is lowered to the industrial grade, it hasn't appeared at all. In the study of nickel and lead, the high purity specimens tend to show the strain-burst comparing with the industrial grade ones as same as in the present experiment. In platinum, the phenomenon mentioned above is not exact dynamic recrystallization, which means the origin of the driving forces for the strain-burst is not due to the accumulation of strain by creep. However, the appearance conditions are similar to other metals. The strain-burst appears in relatively high purity specimens only. If the purity is too high or too low, it will not appear.

3.4.2 The grain size dependence of the steady-state creep rate

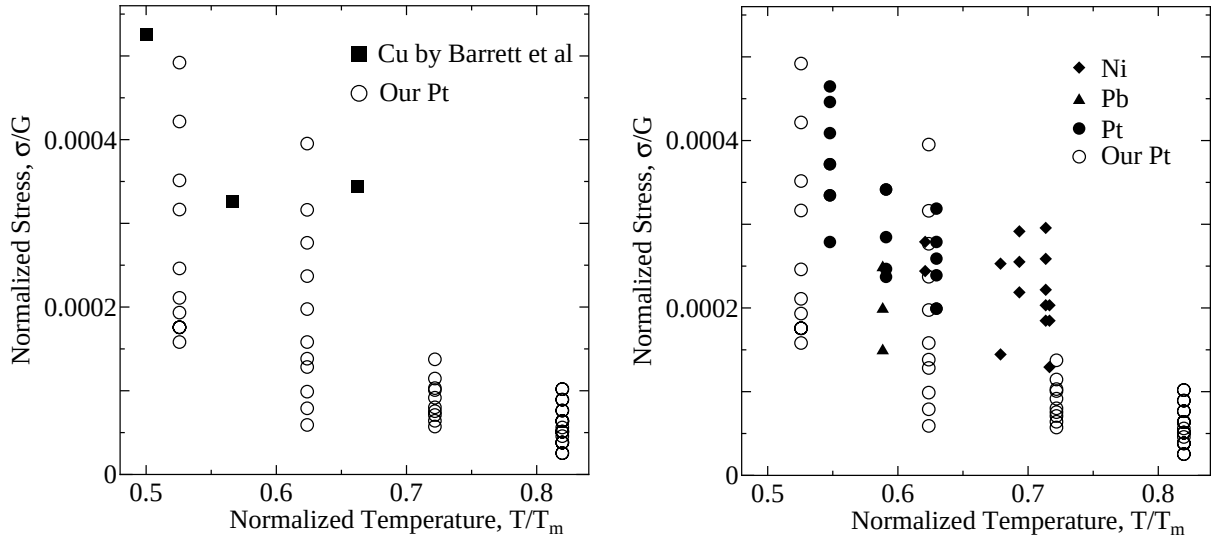

(a) Comparing ours and Barrett's (b) Comparing ours and others

Figure 3.22: Creep test condition in this investigation and other conditions reported previously.

Grain size dependence Another significant result in this experiment is to find the strong grain size dependence of the steady-state creep rate.

To clarify the reason why we have found the grain-size dependence, the experimental conditions in our research are compared with others. Figure 3.22 (a) shows the comparison with the present conditions of platinum ○ and early ones of copper ■ by Barrett *et al.* Similar comparison is also shown in Fig. 3.22 (b) in which the crept conditions of nickel[39], lead[41] and platinum[17] are displayed. Not all the research referred to here were intend to investigate the grain-size effect, but they are shown here to represent the conditions for the creep experiment in general. The experimental conditions shown here are the applied stress normalized with shear modulus in Fig. 3.21 and the test temperature normalized with melting point. Our early experimental conditions were of lower stresses and higher temperatures than conventional creep experiments, and we found the grain-size dependence. We extended the experimental conditions to the higher stress and lower temperature region, hoping to find no grain-size dependence. However, we have still found the dependence. It is unclear at present whether the grain-size dependence is particular for platinum or due to some experimental conditions.

Deformation model In the present experiment, the grain size dependence of the steady-state creep rate is found in the power-law creep region where the dislocation climb controls the strain rate. In order to climb the dislocations, which trap the other dislocations on the slip plane, vacancies should be supplied. In this paragraph, a model is proposed from the viewpoint how the vacancies affect the grain size dependence and when **positive dependence** will be observed.

As there are some models for the polycrystalline deformation[44], we think the relationship between lattice vacancy density and grain size dependence with an assumption that the over-all strain rate $\dot{\varepsilon}$ is additive with the strain rate near the grain boundary $\dot{\varepsilon}_{gb}$ and the strain rate in the grain interior $\dot{\varepsilon}_c$. The relationship of these rates are expressed by

$$\dot{\varepsilon} = \beta\dot{\varepsilon}_{gb} + \dot{\varepsilon}_c, \tag{3.11}$$

where the constant β is a factor depending on the physical model. The strain rate in the grain interior $\dot{\varepsilon}_c$ is also expressed with the factor $\dot{\varepsilon}_{defect}$ depending on the defect[15] and others $\dot{\varepsilon}_0$, as given by

$$\dot{\varepsilon}_c = \gamma\dot{\varepsilon}_0 + \dot{\varepsilon}_{defect}, \tag{3.12}$$

where the constant γ is also a factor depending on the physical model. The strain rate affected by the defect $\dot{\varepsilon}_{defect}$ will be proportional to the point defect density C_v, dislocation density C_{disl} and complex factors and expressed by

$$\dot{\varepsilon}_{defect} \propto C_v + C_{disl} + C_vC_d + \ldots\ldots \tag{3.13}$$

Anyway, the vacancies disappear at the *sink*, *i.e.*, the vacancy density C_v decreases with the number of the *sink* (grain boundaries). So that the equation (3.14) will be given by

$$C_v \propto \frac{1}{sink} \propto d. \tag{3.14}$$

where d is the grain size (diameter).

[15] Point defect and dislocation

When the grain size becomes larger, some vacancies may not migrate to the grain boundaries and they form two-dimensional clusters (such as a small stacking fault) on the (111) plane, which is the usual slip plain of f.c.c. metals and alloys. Moreover, if the strain rate is controlled by the slip depending on the density of the cluster on the (111) slip plain, **positive dependence** is observed. According to the assumptions, platinum shows **positive dependence** depending on the point defect density.

In section 4.2.1 (page 48), The grain size dependence of the steady-state creep rate of **platinum-10%rhodium alloy** was examined, however, no grain size dependence was observed. In the case of the solid solution alloys, it will happen that the solute atom (rhodium) trap some vacancies. So that, no grain size dependence will be appeared and it is reasonable in the case of platinum-10%rhodium alloy.

3.5 Conclusion

Pure platinum was crept at various conditions and following results are obtained.

1. **Strain-burst**
   Platinum shows the strain-burst (a sudden increase in the strain). The phenomenon is concerned with the recrystallization to almost single crystal during the creep. The occurrence of this burst depends on the concentration and kinds of minute impurities, test-temperature, applied stress, and the detailed process of the specimen preparation. This phenomenon occurred under the stress during the deformation and is interpreted as a kind of dynamic recrystallization. However, it is different from exact dynamic recrystallization, in which the origin of the driving force is the accumulation of strain by creep. The present burst may occur based on the static recrystallization and the deformation just after the loading.

2. **Grain size dependence**
   There have been a general belief that **there is no grain size dependence of the steady-state creep rate** in large grained specimens.
   Nevertheless, the strong **positive dependence** was observed. The phenomenon happens in a wide range of temperature and stress, so that this phenomenon is general in platinum.

3. **Activation energy of the creep**
   The activation energy of the steady-state creep rate of platinum is calculated using a same method by Dushman *et al.* reported at 1944[17]. The over all average value is 2.8×10^5J/mol which is larger than the result of Dushman *et al.* and same as the activation energy of the self-diffusion of platinum.

Chapter 4

High Temperature Creep of Platinum-Rhodium Alloys

4.1 Previous work

Previous work There is a conventional method to strengthen the metal with alloying to solid solution metals. The same method is also used in strengthening pure platinum. In glass melting industry, platinum and its alloys are usually used in severe environment such as at high temperatures above 1273K in air. So, it is impossible to use as a glass melting device when the alloying element is oxidized in platinum at high temperatures. Platinum-rhodium alloy is the only one which is useable in glass melting industry[1]. The bushing in Fig. 1.1 shown at the first page of this thesis (see page 1) is also made of a platinum-rhodium alloy.

In 1957, F.C. Child[24] reported the high temperature creep of the platinum-rhodium alloy. In his paper, he declared not only his results but introduced also some old reports by A.S. Darling[45,46] and others[47,48]. As mentioned a part of them in section 3.2.1, these reports concerned with the creep rupture time and ruptured elongation only, not the process or mechanism of the creep deformation.

In 1963, A.A. Bourne and A.S. Darling[49] of *Johnson Matthey* in England set up the new style creep furnace and measured the elongation during the creep deformation up to 1773K. In their study, they reported not only creep rupture time but showed also some examples of the creep curves. They concluded that primary and steady-state stage were only observed at low stresses and their critical stresses were 3.5MPa at 1473K and 1.75MPa at 1773K[2]. They also showed the microstructures of the crept specimens and mentioned the creep rupture mode. As the rupture mode, the intergranular rupture with the voids-coalescence was dominant at low temperature (1473K) and necking or shearing-off was dominant at high temperature (1773K).

Their report is worth to see even if the present time because the test temperature and stress ranges were wide and the details were mentioned on the results comparing with much older reports. The only lack to their report is that they didn't mention the creep deformation mechanism of the platinum-rhodium alloy. Stress dependence of the minimum

[1] In another use, when the temperature is low and/or the oxidization causes little problem, Pt-Ir, Pt-Ni alloys are used. Pt-Pd alloys are also available for jewelry.

[2] In original paper, 500£/inch^2 at 1200°C, 250£/inch^2 at 1500°C.

creep rate of the platinum-rhodium alloy was also reported[50], but there was no discussion on the creep deformation mechanism.

Later, precious metals companies published the stress dependence of the creep rupture time from the view point of the technical document[51], but as long as I know there is no report, in which creep curves were observed and mentioned creep deformation mechanism.

Lack points of the old reports High temperature behavior of the platinum-10%rhodium alloy was made to clear considerably by the report of Bourne *et al.*, but on the other hand, their report is only observed the phenomenon so that further study, such as to clarify the deformation mechanism, is desired. Especially, followings are not mentioned or doubtful points in their reports.

1. Bourne *et al.* were concluded that the primary and steady-state creep were only observed below the critical stresses and temperatures, those are 3.5MPa at 1473K, 1.75MPa at 1773K.

2. Bourne *et al.* were concluded that harmful impurity caused the intergranular creep rupture.

3. Rate control process of the platinum-rhodium deformation has not yet been clear.

The purpose of the study in this chapter In this study, creep tests were performed for the platinum-10% and 20%rhodium alloys to declare the deformation mechanism comparing with the results by Bourne *et al.*. The appearance of the strain-burst and grain-size dependence of the steady-state creep rate, which were observed in pure platinum, was also discussed on the view point of the solid solution alloy of the platinum.

4.2 Experimental results

Specimens The production process of the creep specimen has already shown in Fig. 2.1 (page 5). The thickness of the specimen is 1mm except for the experiment of the grain-size dependence of the steady-state creep rate. The final thickness of the creep specimens, as shown in Fig. 2.3 (see page 8), were obtained by punching out of the specimen sheet. Before the loading, pre-annealing was applied for 1 hour at each temperature of the creep test except for the case shown in section 4.2.1.

Several batches of platinum-rhodium ingots were tested in this study. But distinction of the batches didn't have to need because no difference was observed in the recrystallization and the creep behavior. So that only rhodium concentration is described in this investigation.

4.2.1 Creep of the Platinum-10%Rhodium

Microstructures Figure 4.1 shows the typical microstructures of platinum-10%rhodium alloy before and after the creep tests. The initial grain size depends on the pre-annealing temperature, *i.e.* the higher the pre-annealing temperature, the larger the grain size. The grain size dependence of the pre-annealing temperature is different from that of high purity platinum one. After the pre-annealing, the grains show an isotropic structure. The

intergranular creep rupture with void coalescence is observed at low temperatures (*e.g.* less than 1573K). No grain growth during the creep tests is observed at low temperatures. At high temperature (1673K), the tendency of the appearance of the necking or shearing-off and grain growth during the creep tests is observed. The grain size is similar to the initial one except for the high temperature (1673K).

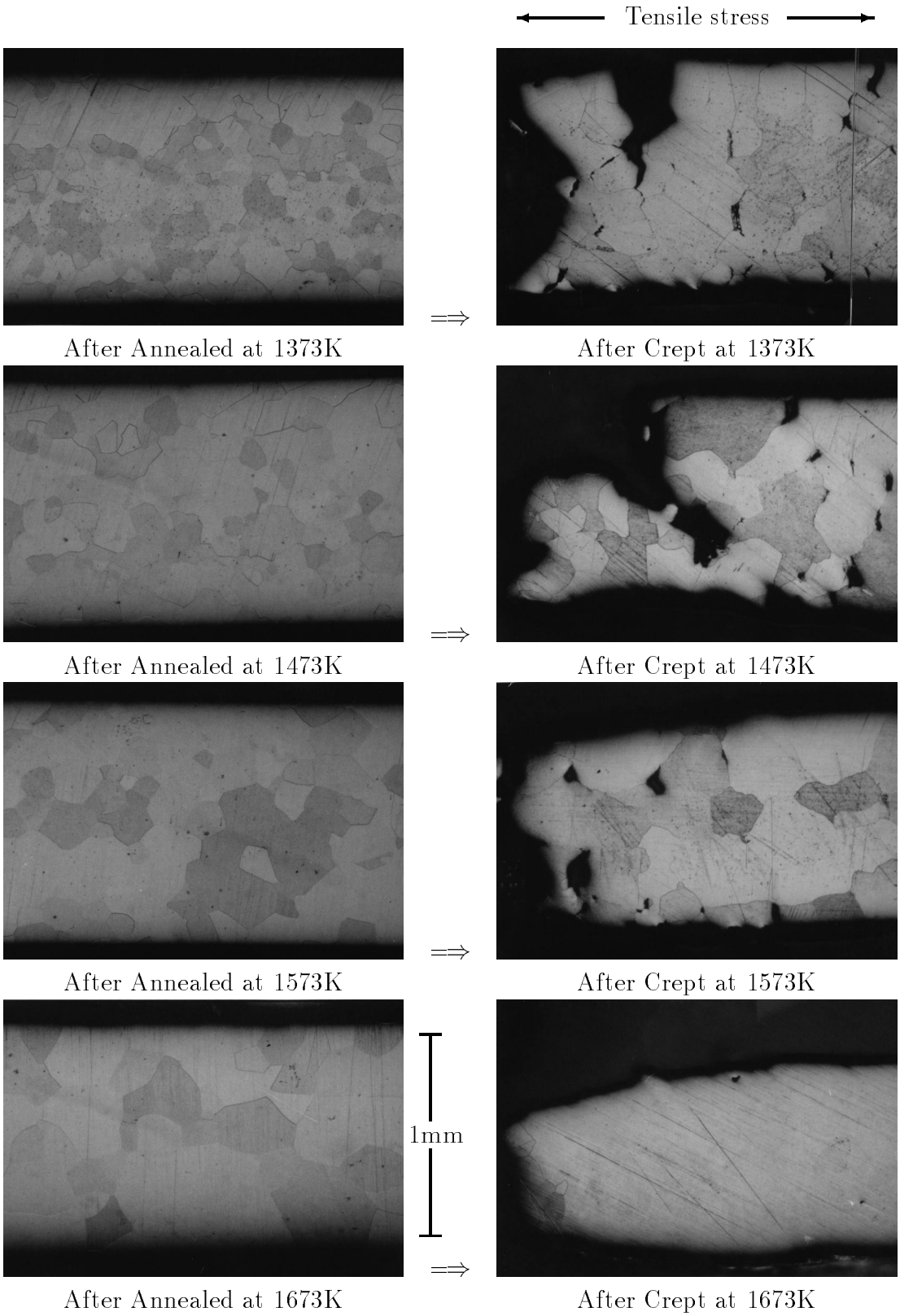

Figure 4.1: Microstructures of platinum-10%rhodium alloy before and after the creep test.

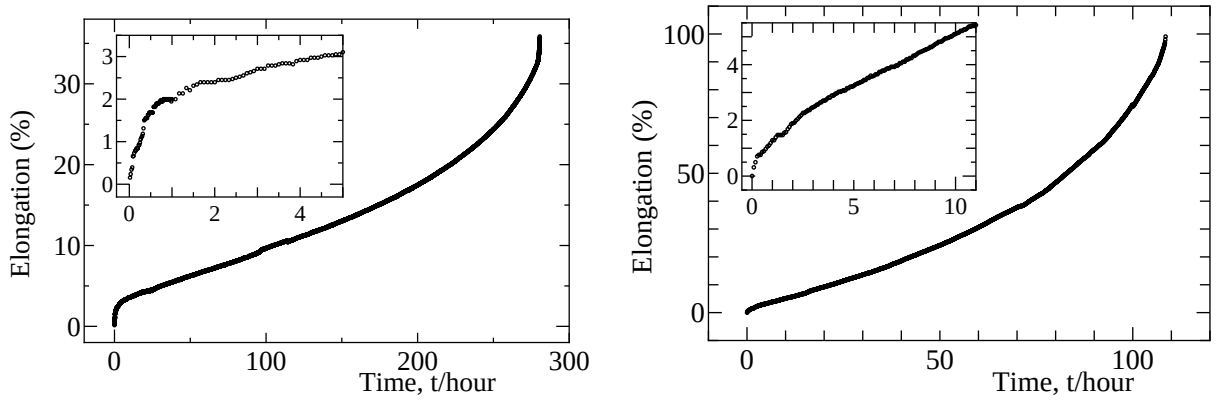

(a)1473K 7MP (b)1673K 5MPa

Figure 4.2: Creep curve examples of platinum-10%rhodium alloy.

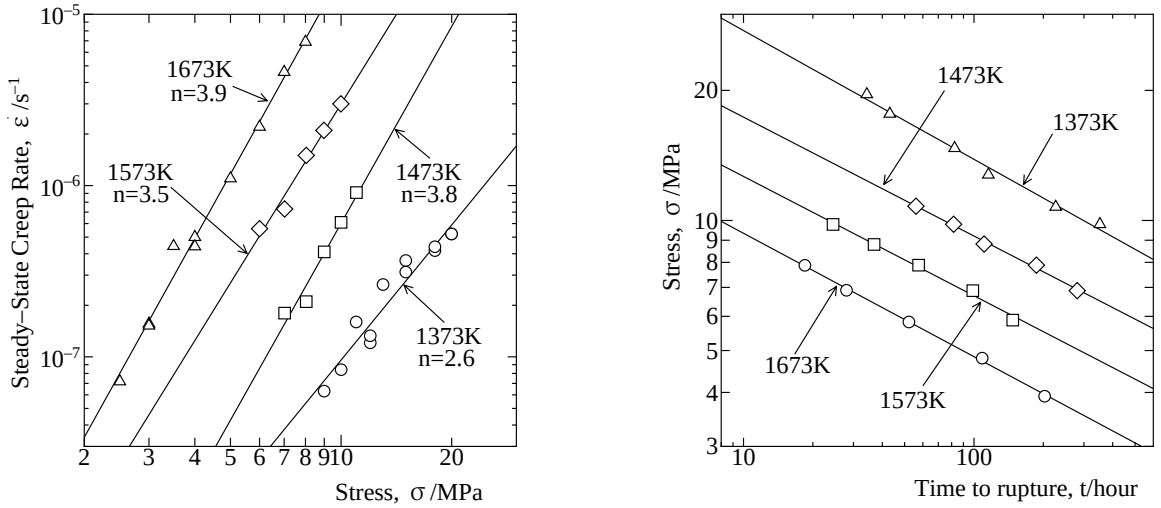

Figure 4.3: Steady-state creep rate and creep rupture time of platinum-10%rhodium alloy.

Creep curves Creep curves are shown in Fig. 4.2, as examples. Creep curve (a) is obtained at 1473K with 7MPa. Typical three stages, *i.e.* primary, steady-state and accelerating stages, are observed. On the other hand, creep curve (b) is an example at high temperatures (1673K). Whole creep curve seems to be expressed by the accelerating stage without primary and accelerating stages like Fig. 2.4 (page 8). But the inserted figures, which is magnified the short period just after the creep started, shows the primary and steady-state stages. The work hardening caused by the creep deformation and the steady-state creep are only appeared in the small deformation area. In these creep conditions, the primary and steady-state stages should not be observed according to the report by Bourne *et al.*[49].

Stress and temperature dependence of the steady-state creep rate and creep rupture time of the platinum-10%rhdium alloy are summarized in Fig. 4.3. The stress exponent n is 3 in all experimental conditions. The results imply that dislocation gliding with the solute (rhodium) drag motion controls the steady-state creep rate.

Grain size dependence of the steady-state creep rate

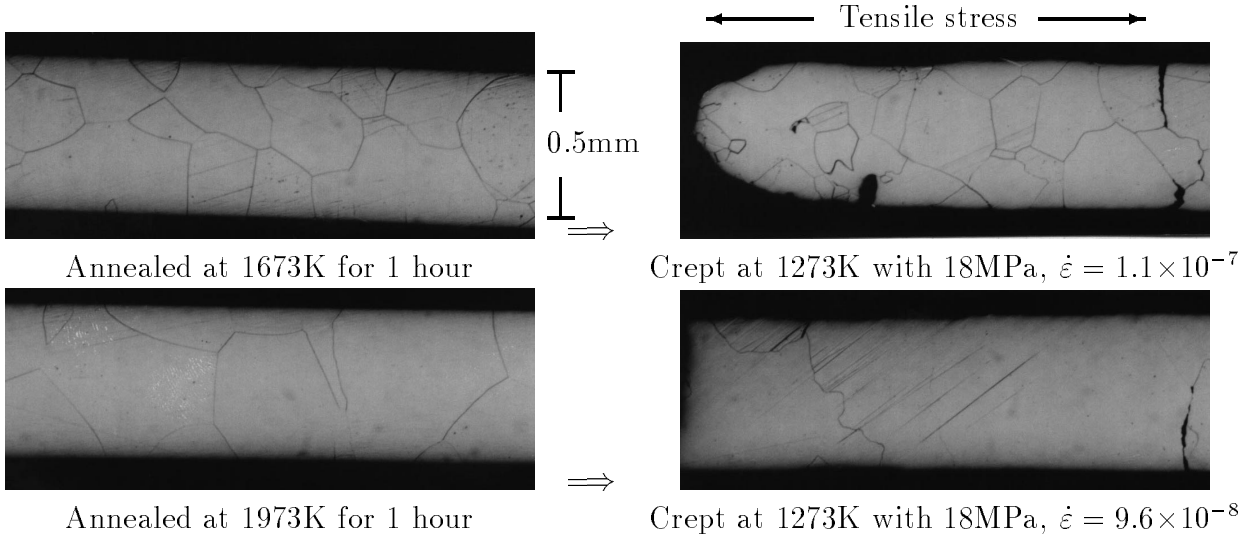

Figure 4.4: Microstructures of different grain size specimen of platinum-10%rhodium alloy before and after the creep test.

Table 4.1: Initial grain-size of the platinum-10%rhodium specimens.

Specimen	Annealing temperature	Grain size (mm)	Symbol 1mm	Symbol 0.5mm
Pt-10%Rh	1473K	0.2	○	-
	1673K	0.35	△	▽
	1973K	0.6	□	◇

In section 3.3.2 (page 30), pure platinum shows the grain size dependence of the steady-state creep rate. And a model is proposed to explain the phenomenon. In order to discuss the suitability of the model, the observation of the dislocations and other defects by the transmission electron microscopy (T.E.M.) is indispensable. However it is almost impossible to prepare the thin films without introducing new dislocation because of the high resistance of the platinum to the chemical polishing.

As this is not a direct way but indirect method, grain size dependence of the steady-state creep rate of the platinum-rhodium alloy is examined from the viewpoint of platinum-rhodium alloy as a solid solution alloy of the pure platinum. The results are summarized in Fig. 4.5. Each symbol distinguishes the specimen preparation in Table 4.1.

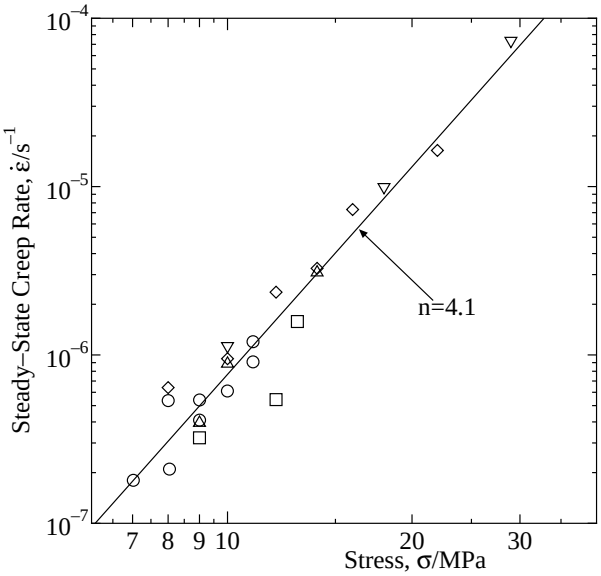

Figure 4.5: Steady-state creep rate of platinum-10%rhodium alloy with various grain size and thickness.

No grain size dependence of the steady-state creep rate of the platinum-10%rhodium alloy is observed in spite of the wide experimental conditions, those are the specimen thickness, pre-annealing conditions and stresses. The stress exponent n is a little large, as a solid solution alloy. However, dislocation gliding with solute drag motion controls the creep deformation.

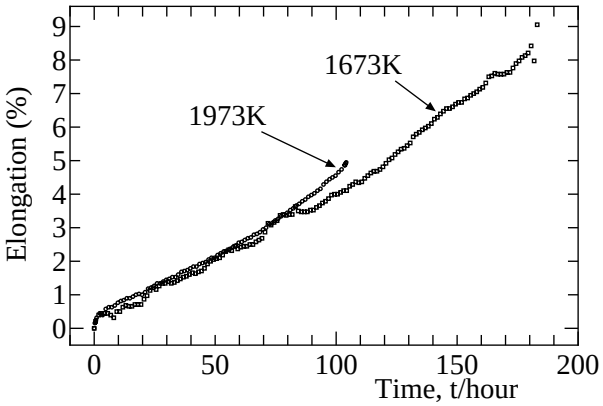

Figure 4.6: Creep curve examples of platinum-10%rhodium alloy at 1273K.

At low temperatures, intergranular creep rupture in grain boundaries with small elongation is observed. But even if in this case, no grain size dependence is observed. Figure 4.6 shows the creep curves, whose microstructures before and after the creep tests were shown in Fig. 4.4. The specimen pre-annealed at 1973K with 0.5mm thickness, which has the almost same grain size with the specimen thickness, shows the intergranular creep rupture with small elongation. The specimen pre-annealed at 1673K has smaller grain size. Both creep curves have three stages and almost overlap to each other. There is no distinguish difference of the steady-state creep rate in spite of the obvious difference of the creep rupture time and elongation. The reason why the creep rupture time and elongation are different in these two specimens, is rupture path formed easily in coarse grain even if the pilling up rate in grain boundaries of the voids is the same.

4.2.2 Creep of the Platinum-20%Rhodium

Microstructures Microstructures before and after the creep tests of the platinum-20% rhodium are shown in Fig. 4.9. The initial grain size depends on the pre-annealing temperatures. This is the same tendency of the platinum-10%rhodium alloy, *i.e.* the higher pre-annealing temperature, the larger grain size. The microstructure after the creep tests is also similar to that of platinum-10%rhodium. It implies that the rupture mechanism is the void coalescence in grain boundaries. At high temperatures, a tendency of grain growth during the creep is observed, but the magnitude of the growth is much smaller than that of platinum-10%rhodium. Although the creep strength $(t_r, \dot{\varepsilon})$ is improved comparing with the platinum-10%rhdium, the creep deformation mechanism and the creep rupture mechanism are the same those of platinum-10%rhodium alloy.

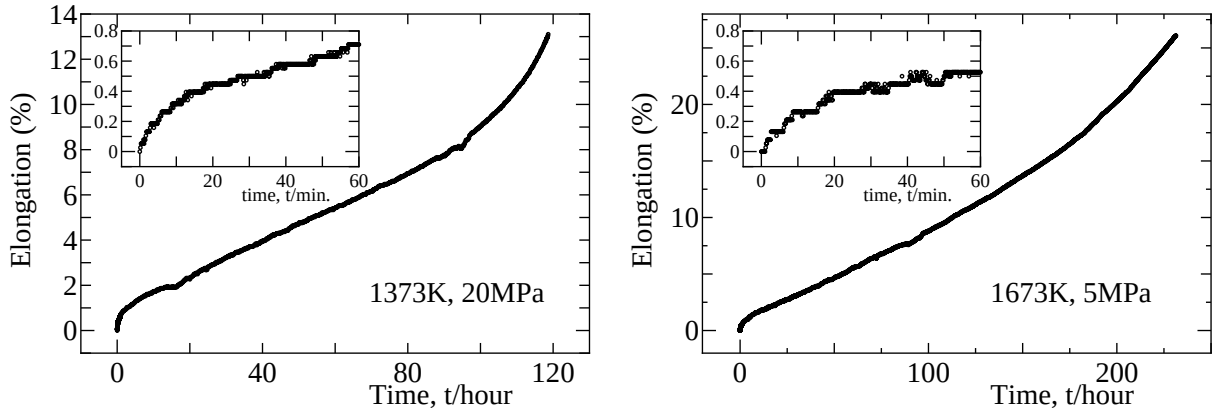

Figure 4.7: Creep curve examples of platinum-20%rhodium alloy.

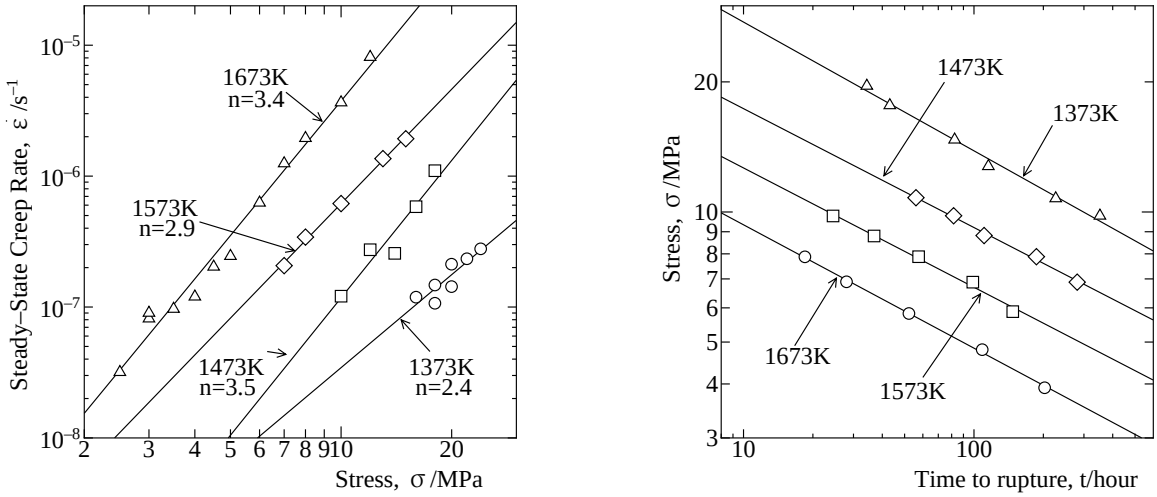

Figure 4.8: Steady-state creep rate and creep rupture time of platinum-20%rhodium alloy.

Creep curves Figure 4.7 shows the examples of creep curves of platinum-20%rhodium alloy. Each curve is the typical creep curve having three stages, *i.e.* primary, steady-state and accelerating stages. The appearance time of the steady-state stage depends on the creep test conditions like pure platinum and platinum-10%rhodium alloy.

Figure 4.8 is the summary of the steady-state creep rate and the creep rupture time of the platinum-20%rhodium alloy. The stress exponent n is 3 in all experimental conditions. The results imply that dislocation gliding with the solute (rhodium) drag motion control the steady-state creep rate. The phenomenon is the same as that of platinum-10%rhodium alloy.

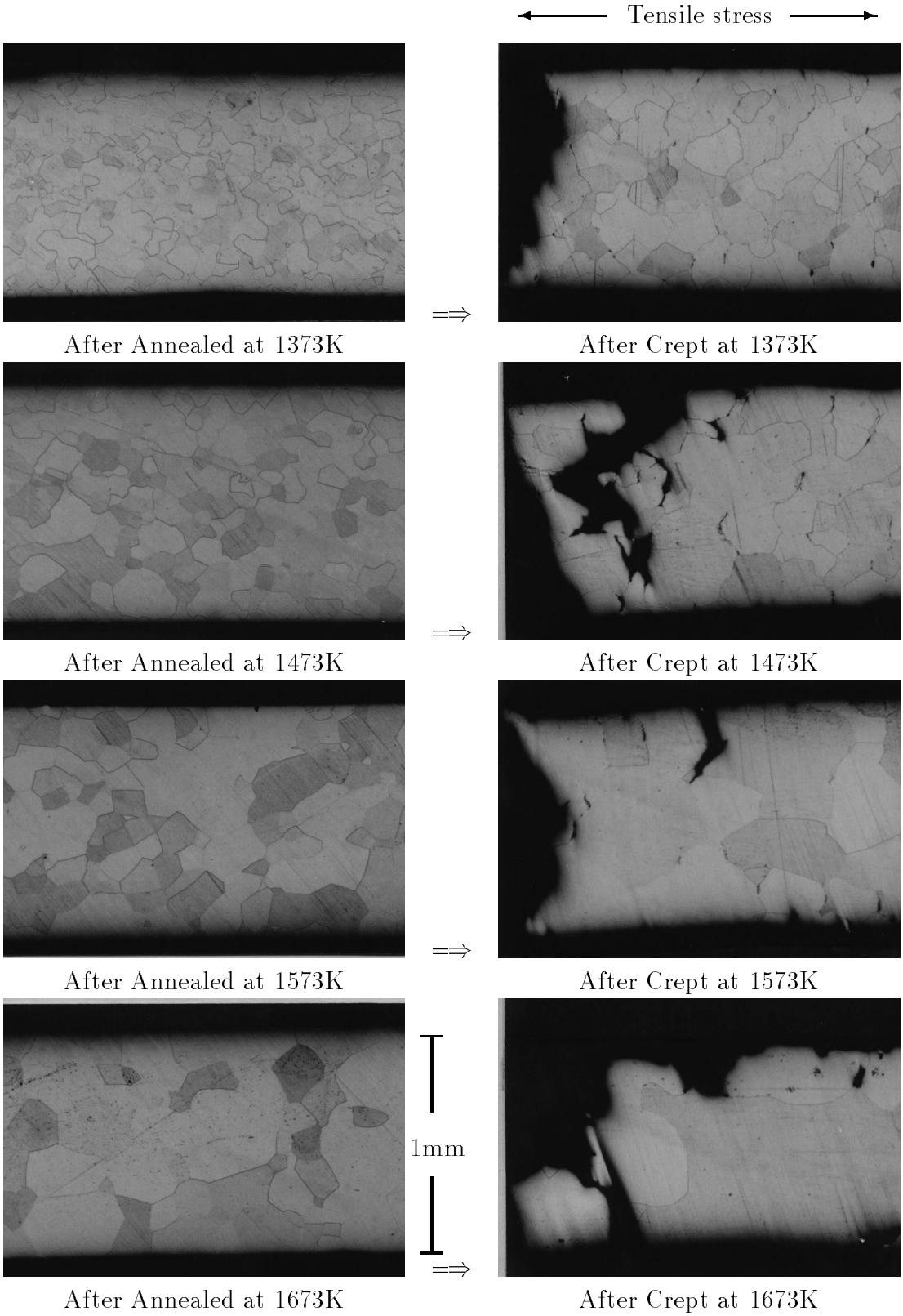

Figure 4.9: Microstructures of platinum-20%rhodium alloy before and after the creep test.

4.3 Discussion

Platinum-10% and 20%rhodium alloys were crept at various conditions. On the bases of the results obtained, the creep phenomena of the platinum-rhodium alloy will be discussed by comparing pure platinum and the results reported previously.

Deformation mechanism The stress exponent n of the platinum-10% and 20%rhodium alloy is about 3 in all experimental conditions. This implies that dislocation gliding with the solute (rhodium) drag motion control the steady-state creep rate. The phenomenon is the same as that of other typical solid solution alloys.

Appearance of the steady-state stage Creep curves were shown in the report by Bourne *et al.*[49]. The similar creep curves are obtained in this experiment when the experimental conditions are same. By the way, Bourne *et al.*[49] measured the elongation at several intervals of hours. Especially, for the elongation measurements, the measurement-interval is too long in spite of its work hardening and the creep rate reduction which occurred just after the loading. So that they missed the primary and steady-state stages and/or they might think it was not important in practical use.

On the other hand, our basic measurement system is similar to Bourne's[49]. But I've employed an automatic method using computer system (see page 10) so that it is possible to measure with the short intervals. Much detailed measurements were performed in this experiment. Even if the whole creep curve is similar between present work and Bourne's, present results contain much numerical data to analyze the creep curves. This is the reason why they concluded that **the primary and steady-state creep were only observed below the critical stresses and temperatures**

Bourne *et al.*[49] concluded that the primary and steady-state stage were only observed at low stresses. They reported that the critical stresses were 3.5MPa at 1473K and 1.75MPa at 1773K and these values are not correct and may be amended. Steady-state stage is observed in whole present experimental conditions.

Intergranular creep rupture Harmful impurities caused the intergranular creep rupture in the report by Bourne *et al.*[49] and the creep rupture mode was not clear at that time. But now, it is the conventional creep rupture mode to rupture with void-coalescence at the grain boundaries especially parallel to the stress axis[36]. Even if the case of the high purity platinum, the similar rupture mode and microstructures are obtained[3]. The present experiment is not the study of the influence of the trace impurities to the creep rupture mode of the platinum-rhodium alloys. But the similar rupture mechanism is observed as a conventional well-known phenomena and conclusion is not always correct.

Grain size dependence of the steady-state creep rate Platinum shows the strong grain size dependence of the steady-state creep rate in this experiment. The similar experiment was performed for platinum-10%rhodium alloy. No tendency of the grain size dependence of the steady-state creep is observed in platinum-10%rhodium alloy. According to the stress exponent n, dislocation gliding with the solute (rhodium) drag motion

[3] *e.g.* see page22 Fig. 3.4(b) and page33 Fig. 3.16.

control the steady-state creep rate. Creep deformation mechanism itself is different between pure platinum and platinum-rhodium alloy. So that no grain size dependence of the steady-state creep rate is observed.

Rhodium contents Creep tests were performed for platinum-10% and 20%rhodium alloys. The stress exponent n is 3 in all experimental conditions for the both alloys. The fact suggests that dislocation gliding with the solute (rhodium) drag motion controls the steady-state creep rate.

In the same experimental conditions[4], the strength of the platinum-20%rhodium alloy is larger than that of platinum-10%rhodium alloy, *i.e.* smaller steady-state creep rate and longer creep rupture time.

Creep rupture mechanism is same in both alloys, *i.e.* voids-coalescence at the grain boundaries especially parallel to the stress axis

These results suggest that the rhodium atom works to, so called, **solute strengthening** only.

4.4 Conclusion

Platinum-10% and 20%rhodium alloys were crept at various conditions and following results are obtained.

1. The stress exponent n of the platinum-10% and 20%rhodium alloy is about 3 in all experimental conditions. The fact suggests that dislocation gliding with the solute (rhodium) drag motion controls the steady-state creep rate. The phenomenon is the same as other typical solid solution alloys.

2. Creep rupture mode is the void-coalescence at the grain boundaries especially parallel to the stress axis. This phenomenon is similar to other solid solution alloys. Harmful impurities caused the intergranular creep rupture in the report by Bourne *et al.*[49] is not always correct.

3. Three stages, *i.e.*, primary, steady-state and accelerating stages, were observed in all creep curves. These experimental results are different from previous report by Bourne *et al.*[49]. Their conclusion should be amended.

4. Strain-burst and grain size dependence of the steady-state creep rate, which are newly found phenomena in pure platinum, were not observed in this experiment on the platinum-rhodium alloys.

[4] at the same stress and the same temperature

Chapter 5

High Temperature Creep of Sm_2O_3 Added Platinum

5.1 Introduction

Introduction Another method of strengthening the metals is to precipitate the second phase in the matrix metal. This method is widely used in metallurgy as well as to produce solid solution alloys. By heat-treatment at a specific temperature above the pre-annealing temperature at which the alloying metals form a solid solution within a solubility for the matrix metal, another phase is formed as precipitated particles and makes, so called, precipitation strengthened alloys. This method have been applied, since the human-being had begun to use alloys for a tool. However, at high temperatures the creep occurs for the alloys and the precipitated particles become larger than initial size (particle growth) by the diffusion with the exposed time at high temperatures. The phenomenon (particle growth) is an immanent problem in precipitation strengthening method.

Recently, mechanical alloying as another method, has been applied to disperse the oxide particles such as Al_2O_3、ZrO_2、Y_2O_3 and so on. This method dose not use the precipitation strengthening[7-9]. The advantage of this method is that the prepared alloys can last the alloys much longer than conventional precipitation strengthened alloys. Because the diffusion between matrix metal and dispersion oxide particle occurs little so that there will be little growth of the particles.

There are some similar strengthened alloys of platinum and its alloys with the dispersed oxide particles in matrix such as ZrO_2[25,52] and Y_2O_3[53] and they have been practically used.

The production process of these platinum alloys are different from mechanical alloying used in nickel based super alloys. In the method of *Johnson Matthey*[25,54] of England, platinum-zirconium solid solution alloy is molten first, and then zirconium is oxygenated to ZrO_2 together with the dispersing. In the method of *Degussa*[52] of Germany, ZrO_2 is dispersed by a coprecipitation method with platinum at the last process of refining. In these method, O.D.S. platinum is manufactured by making use of the specific property of the **never oxygenizable platinum**[1].

[1] Exactly say, platinum-oxide exists, however, it is hard to produce usual conditions and usually platinum metal is much more stable than platinum-oxide. So that, it will be possible to regard the platinum never oxygenated in general.

The purpose in this chapter Samaria (Sm_2O_3) added platinum[2] has been manufactured by the present authors group. The purpose of this chapter is to clarify the following items of the Sm_2O_3 added platinum by creep tests and microstructure observation from the experimental viewpoints.

1. To clarify the similarity and difference between Sm_2O_3 added platinum and other O.D.S. alloys experimentally.

2. Why dose Sm_2O_3 added platinum behave at high temperatures ?

5.2 Experimental results

Specimen The production process of the Sm_2O_3 added platinum has already shown in Fig. 2.1[(10)] (page 5). Generally speaking, O.D.S. alloys with high aspect ratio[3] are obtained by using a hot extrusion and/or a zone annealing *etc.*

In this experiment, any special treatments were not applied but just cold-rolling was applied to obtain the grains with a high aspect ratio. No cross-rolling was applied. So that, anisotropic specimens were manufactured for the high temperature creep tests. The difference between longitude of cold-rolling direction and transverse to the cold-rolling direction is discussed in section 5.2.1. As shown in Fig. 5.1, the two directions are distinguished by L-direction which is longitudinal to the cold-rolling direction, and T-direction which is transverse to the cold-rolling direction. The dimension of the creep specimen is the same as that of pure platinum and platinum-rhodium alloys as shown in Fig. 2.3 of page 8.

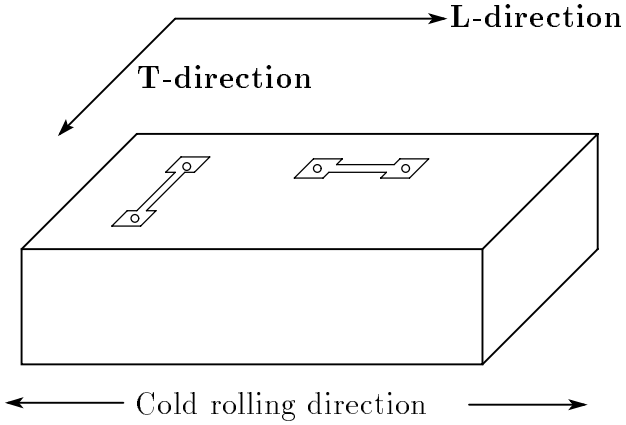

Figure 5.1: L and T directions of the specimen.

5.2.1 High temperature creep of Sm_2O_3 added platinum

Microstructures Initial microstructures are shown in Fig 5.2. The L and T directions are indicated in Fig. 5.1. The high aspect ratio structure is observed for the specimen with

[2] It may be a kind of samaria (Sm_2O_3) dispersion strengthened platinum.

[3] The ratio in length between longitudinal and transverse directions of anisotropic grains.

the longitudinal direction to the cold-rolling. The microstructure is similar to that of other O.D.S. alloys.

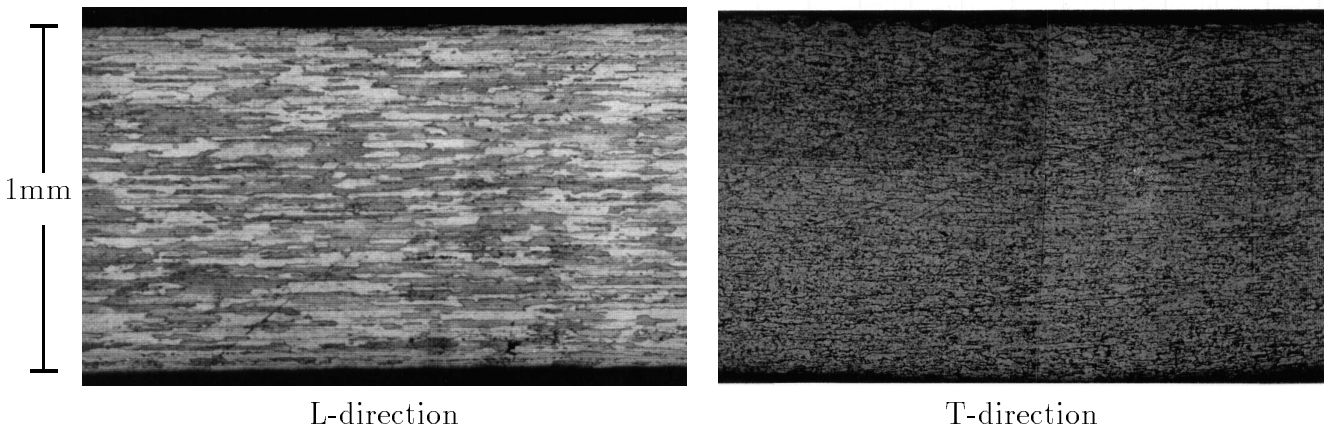

Figure 5.2: Microstructures of L-direction and T-direction of Sm_2O_3 added Platinum.

Figure 5.3 shows the microstructures obtained after the creep test. The cross-sectional microstructures of L and T directions are obtained from the same specimens whose creep curves are shown in Fig. 5.7. The creep rupture mode of them is void-coalescence at the grain boundaries those are parallel to the stress axis. There are fewer rupture paths in L-direction than in T-direction. Although the creep tests were performed with various conditions[4], creep rupture mode was same in all present conditions.

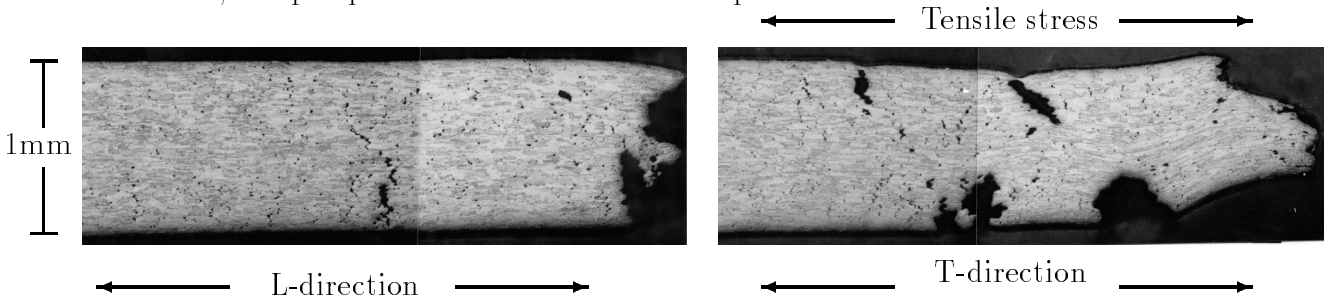

Figure 5.3: Microstructures of the Sm_2O_3 added Platinum after the creep tests.

Creep curves Examples of the creep curve at low temperature (1373K) and at high temperature (1773K) are shown in Fig. 5.4. These curves were obtained from the L-direction specimens. The shape of the creep curves is independent on the test temperatures and applied stresses. Each creep curve has three stages; primary, steady-state and accelerating stages. The difference from pure platinum and platinum-rhodium alloys is very small rupture elongation. The phenomenon is similar to that of other O.D.S. alloys.

[4] See Figure 5.5 and 5.6.

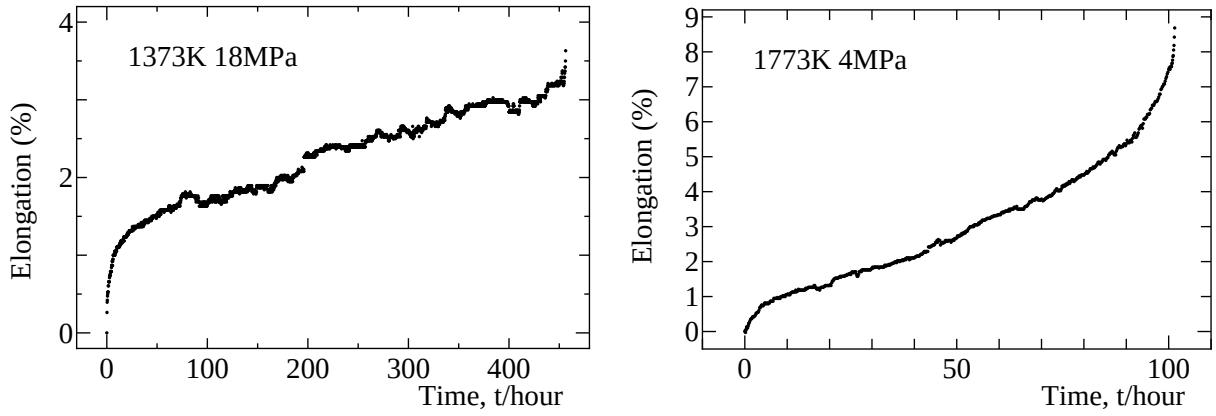

Figure 5.4: Creep curve examples of Sm_2O_3 added Platinum.

Minimum creep rate The minimum creep rate obtained at various temperatures and stresses are summarized in Fig. 5.5. When the strain rate is constant, the creep rate is called **steady-state creep rate**. In the case of pure platinum and platinum-rhodium solid solution alloys, it was clear that the internal structure was kept steady-state when the strain rate was constant[5] even if the internal structure hadn't been observed. However, in the case of complex alloys, the internal microstructure is not always steady such as growth of precipitated particles, the alloying contents change by oxidization and so on, even if the strain rate is constant. So that rate of the stage is called **minimum creep rate** in general. It is the purpose in this chapter to clarify the creep behavior of the Sm_2O_3 added platinum[6], so that we call the rate as **minimum creep rate** in this chapter.

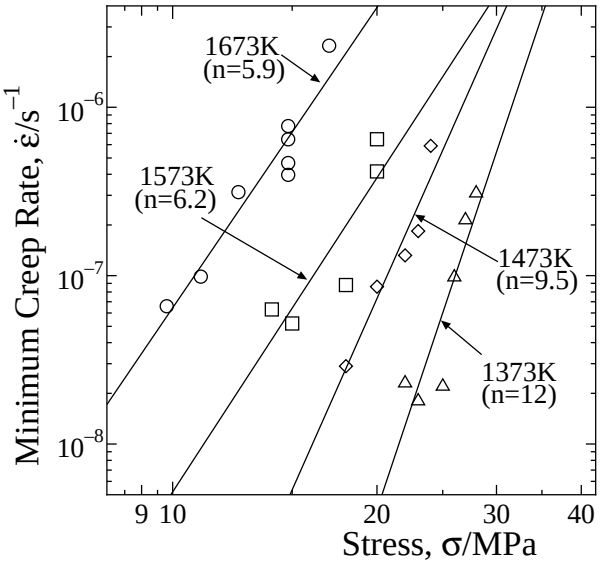

Figure 5.5: Minimum creep rate of Sm_2O_3 added Platinum at various temperatures.

Stress exponent n is also indicated in Fig. 5.5. At low temperatures below 1473K, the stress exponent n is 11. Large value 11 is similar to that of other O.D.S. alloys. As the creep test temperature becomes higher, the stress exponent n becomes to be smaller and finally reaches to the close value 5 of the matrix platinum. The change in the stress exponent suggests that the effect of Sm_2O_3 at high temperatures is different from the effect at low temperatures.

[5] It means that the number of the newly introduced dislocations by the strain (deformation) is equal to that of emitted ones by recovery.

[6] It means that the details of the Sm_2O_3 added platinum are not yet clear.

Stress dependence of creep rupture time Figure 5.6 is the summary of the stress dependence of creep rupture time at various temperatures. The most important information of the creep is the creep rupture time in practically and industrially when the material is used as a heat resistant structural component. It is impossible to predict the creep rupture time accurately even if the creep deformation mechanism and the creep rupture mode are understood. As the prediction of creep rupture time is discussed in section 5.3, it is essentially important to continue the creep test **until the specimens are ruptured** even when some prediction method are applied. As shown in Fig. 5.6, the creep rupture time is proportional to the initial stress in *log-log* plots. The relationship between creep rupture time and initial stress is similar to the results from platinum-rhodium alloys as shown in Fig. 4.3 and 4.8.

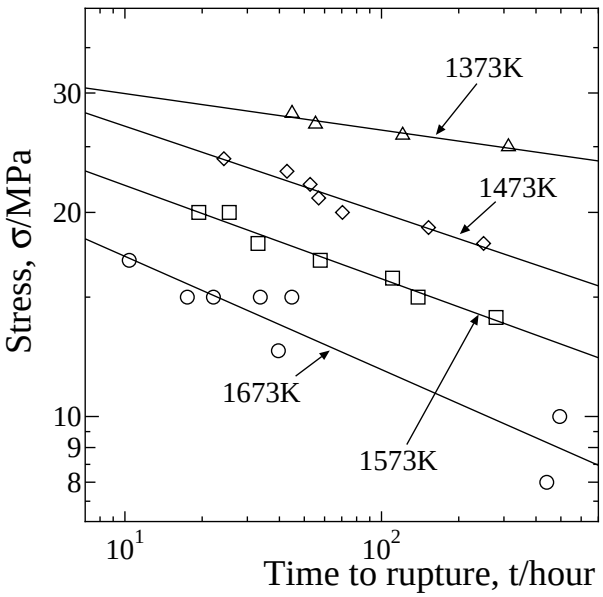

Figure 5.6: Stress v.s. rupture time of Sm_2O_3 added Platinum at various temperatures.

Directional dependence Generally speaking, the creep strength $(\dot{\varepsilon}, t_r)$ in the O.D.S. alloys depends on the production process. When it was manufactured by cold rolling, the strength depends on the cold-rolling direction. The Sm_2O_3 added platinum manufactured in the present experiment also has the anisotropy in microstructures as shown in Fig. 5.2 and 5.3, so that it would be predicted that the strength is different and depends on the directions. Two creep curves are shown in Fig. 5.7 with the same temperature and the same stress conditions for the different directions. The minimum creep rate is smaller in L-direction than in T-direction. The creep rupture time is also much longer in L-direction than in T-direction. L-direction is much stronger than T-direction. The directional dependence is similar to that of other O.D.S. alloys.

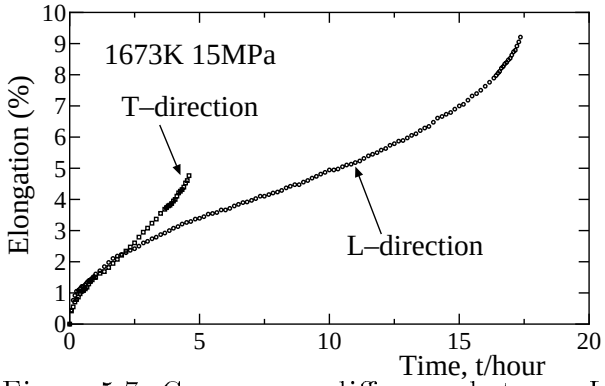

Figure 5.7: Creep curve difference between L and T directions.

Observation of Sm_2O_3 particles The micrographs of Sm_2O_3 particles in platinum matrix are shown in Fig. 5.8[7] and 5.9 taken by the transmission electron microscopy (T.E.M.). It is almost impossible to prepare the thin films for T.E.M. from the crept 1mm specimens without introducing new dislocations because of the high resistance of the platinum to the chemical polishing. However, not suitable but observable thin films for T.E.M. were obtained by the following preparation method, whose process contains the cold-rolling to about 10μm, annealing, chemical polishing by aqua regia and subsequent electro polishing by $HCl + CaCl_2$[56].

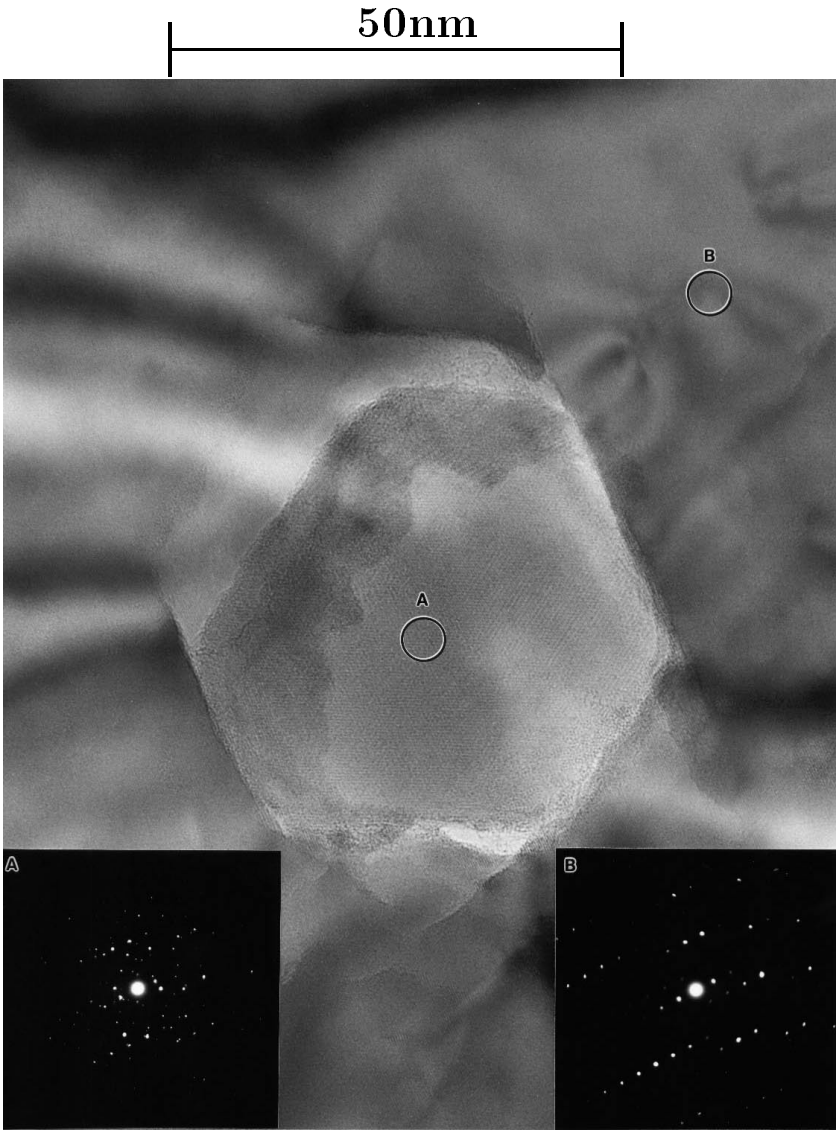

Figure 5.8: A Sm_2O_3 particle in Platinum.

Figure 5.8 is a magnified photograph for Sm_2O_3 particle and the selected area diffraction patterns from A and B areas. Samarium and oxygen were detected from the area A by X-ray analysis of the elements. On the other hand, these elements were not detected from the area B. With the selected area diffraction patterns, the particle was determined to be a monoclinic samaria (Sm_2O_3).

The dimensions and the distribution of the Sm_2O_3 particles were observed and shown in Fig. 5.9. The observed area is very few, so that just the tendency of the dimension and the distribution is observed. However, it will be possible to obtain the overview of them. According to the photograph, the average particle size of the Sm_2O_3 is estimated to be about 50nm. The average distance of the surface of the particles is also able to be obtained from the photograph. However, it will be better to calculate the mutual distance from the volume fraction of the particles which was obtained from the chemical analysis of the samarium. According to the chemical analysis, the volume fraction of the Sm_2O_3 is about 1% and the average distance of the surface of the particle is also calculated to be about 130nm.

[7] This picture was taken by JEM-2010 in *JEOL*.

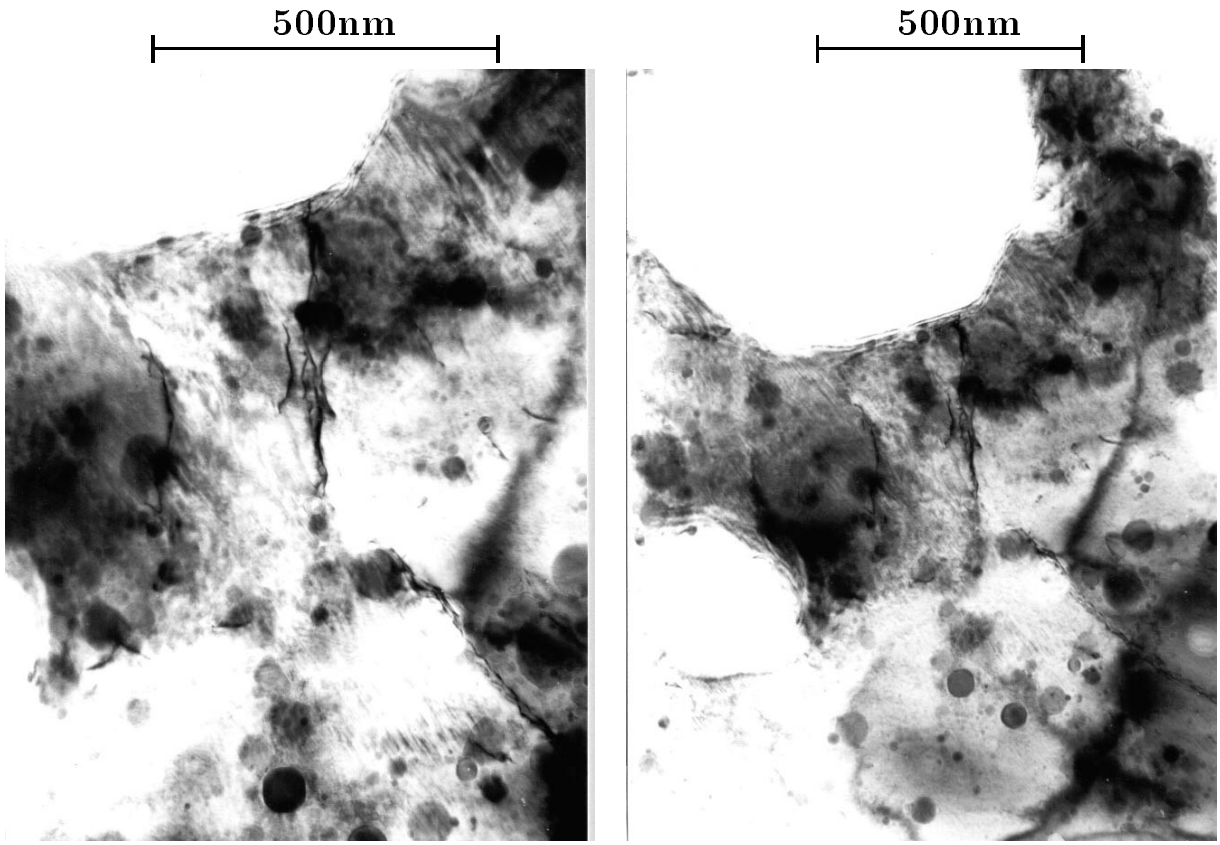

Figure 5.9: Sm_2O_3 particles distribution in Platinum.

5.3 Discussion

Threshold A critical stress, below which the creep deformation scarcely occurs practically, is observed. The critical stress is named as **threshold stress**. The origin of the threshold stress is explained by the *Orowan* process or the *Srolovitz* process[21,57,58]. The magnitude of the *Orowan* stress was estimated for the present Sm_2O_3 added platinum. According to the description by Maruyama and Nakashima[21], the *Orowan* stress σ_{or} is expressed by

$$\sigma_{or} = A_{or}\frac{Gb}{2\pi\lambda}\left[\ln\left(\frac{\tilde{D}}{r_0}\right) + B_0\right], \tag{5.1}$$

where r_0 is the cut-off radius of the dislocation core and its magnitude is usually about b $\sim 3b$. The coefficients of A_{or} and B_0 are given by equations (5.2) for screw dislocation and edge dislocation.

$$\begin{aligned} A_{or} &= \frac{1}{1-\nu}, & B_0 &= 0.6, & &\text{(screw dislocation)}, \\ A_{or} &= 1, & B_0 &= 0.7, & &\text{(edge dislocation)}. \end{aligned} \tag{5.2}$$

$\tilde{D}$ is the harmonic average of $\overline{\lambda}$ and $\bar{\bar{d}}_s$, and given by

$$\frac{1}{\tilde{D}} = \frac{1}{\overline{\lambda}} + \frac{1}{\bar{\bar{d}}_s}. \tag{5.3}$$

By substituting the measured values those are average particle size 50nm and average distance of the surface of the particles 130nm, the *Orowan* stress σ_{or} is calculated to be 1.1×10^8Pa for screw dislocation and 8.5×10^7Pa for edge dislocation assuming $r_0 = 2b$.

However, the calculated *Orowan* stress is not enough to give a confidence, because the basic particle size was determined only by very few observations and the particle size distribution is not considered. When the particle size distribution is not considered, the calculated *Orowan* stress σ_{or} might be far from correct value[58]. So that the *Orowan* stress σ_{or} was estimated again with the conditions that the volume fraction was fixed 1% and the average particle size $\bar{\bar{d}}_s$ was changed from 20nm to 300nm. The results are summarized in Table 5.1. In these calculations, the value of the elastic moduli was used in Fig. 3.21.

Table 5.1: An estimation of Orowan stress.

$\overline{\lambda}$ (nm)	$\bar{\bar{d}}_s$ (nm)	$\tilde{D}$ (nm)	σ_{or} (Pa)		
			dislocation	$r_0 = b$	$r_0 = 3b$
			screw	4.0×10^8	3.0×10^8
55	20	15	edge	7.1×10^8	5.3×10^8
			screw	$\mathbf{2.7\times10^8}$	$\mathbf{2.1\times10^8}$
130	**50**	**36**	**edge**	$\mathbf{3.5\times10^8}$	$\mathbf{2.8\times10^8}$
			screw	1.5×10^8	1.2×10^8
270	100	73	edge	2.0×10^8	8.0×10^7
			screw	8.5×10^7	7.0×10^7
540	200	146	edge	1.1×10^8	9.2×10^7
			screw	6.0×10^7	5.0×10^7
820	300	220	edge	7.8×10^7	6.6×10^7

It is worth to compare the calculated value and measured value. Figure 5.10 is the summary of the steady-state (minimum) creep rate dependence on the applied stress of pure platinum, platinum-rhodium alloys and Sm_2O_3 added platinum in the present experiments. The vertical axis is normalized by the self-diffusion coefficient[8] of the platinum at each temperature in order to compensate the effects of the different temperatures. And the stress is also normalized by using the values in Fig. 3.21.

The line for the minimum *Orowan* stress σ_{or}, which was calculated in Table 5.1 and obtained as 4×10^{-4} for $\bar{\bar{d}}_s = 300$nm, is also illustrated in Fig. 5.10.

[8] As shown in page 36 of section 3.3.3, the self-diffusion coefficient is almost equal to the activation energy of the creep.

The present results compare with another result of Al-1.5vol%Be reported by Y. Ysh, H. Nakasima, H. Kurishita, S. Goto and H. Yoshinaga, in which the clear threshold stress was observed[58]. They clarified that the threshold stress was as same as *Orowan* stress by the accurate calculation with the consideration of particle size distribution. The calculated[9] threshold value[10] is approximately 10^{-4} after the normalizing with Yong's modulus of pure aluminum. And the minimum creep rate is reduced suddenly from $10^{10}\mathrm{m}^{-2}$ to $10^{7}\mathrm{m}^{-2}$. In the present experiment, the *Orowan* stress was estimated without accurate particle size distribution because of the difficulty of the specimen preparation. However, the volume fraction is close to that of the experiment reported by Ysh *et al.*

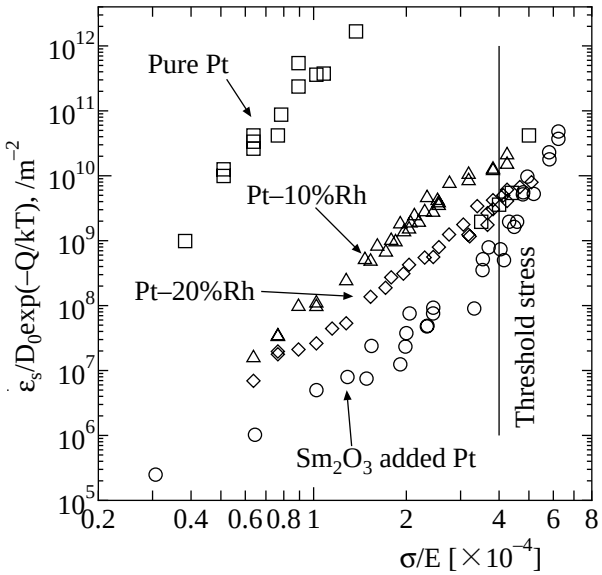

Figure 5.10: Stress dependence of the steady-state (minimum) creep rate compensated by lattice self-diffusion coefficient.

It will be possible to compare the present result with the results reported by Ysh *et al.* after normalizing the stress by elastic modulus and temperature by self-diffusion coefficient even if the metal itself and the absolute value of the test temperatures and applied stresses are completely different.

The present experiments were performed under the condition in which the applied stresses up to one order lower than that of calculated *Orowan* stress. The stress range is similar to that of Ysh's and the strain rate is also similar when both of them are normalized. If the threshold stress were exist in Sm_2O_3 added platinum, it would be observed within the present experimental results. No threshold stress was found in the present experimental conditions.

As shown in Fig. 5.10 and 5.13 (page 66), Sm_2O_3 added platinum shows much improved characteristics in both minimum creep rate and creep rupture time. So that, the Sm_2O_3 particles improve the creep strength, but the improvement is not due to the direct interaction between the particles and dislocations such as the *Orowan* process or the *Srolovitz* process.

Table 5.2: Tensil strength and Vickers hardness.

Metal or Alloy	Tensile Strength (MPa)	Vickers Hardness (Hv)
Pure Pt	150	45
Sm_2O_3 added Pt	200	65
Pt-10%Rh	320	90
Pt-20%Rh	400	110

[9] It is equal to the measured value.
[10] It is equal to the *Orowan* stress.

Another process of dislocations passing through the particles is also suggested such as cross-slip[55,57]. In this case, the threshold stress is much smaller than *Orowan* stress, so that the threshold stress never observed experimentally, that is the particles affect no strengthening. Table 5.2 shows the mechanical properties of pure platinum, platinum-rhodium alloys and Sm_2O_3 added platinum. These specimens were examined in the present experiment. Tensile strength and Vickers hardness were measured at room temperature after full-annealing[51]. The strength of the platinum-rhodium alloys is improved a lot than pure platinum and the improvement depends on the rhodium contents. On the other hand, the strength of Sm_2O_3 added platinum is improved a little, although the high temperature creep properties $(\dot{\varepsilon}, t_r)$ is improved a lot as shown in Fig. 5.10 and 5.13. The result suggests that the dispersed particles affect little on the hardening of the specimen[11].

A model of the rupture As already mentioned, the improvement of the high temperature property of Sm_2O_3 added platinum is not owed to the direct interaction between dispersed particles and dislocations. Now consider the reason why the high temperature creep properties $(\dot{\varepsilon}, t_r)$ was improved in spite of the fact that the hardness at room temperature is improved little.

As already shown in the experimental results, the creep strength $(\dot{\varepsilon}, t_r)$ is completely different for the specimens with L- and T-direction. The fact suggests that the creep strength strongly depends on the shape of the grains and its geometrical arrangement.

M. Cans, B. deBestral and G. Eggeler[59] have proposed a model based on their theory. The voids formed at the triple point of grain boundaries grow and coalesce to make a rupture path across the specimen thickness. The probability to form the voids is smaller in the specimens whose grains have high aspect ratio. Consequently, these specimens show longer creep life. The idea is illustrated in Fig. 5.11 and 5.12. These pictures are also regarded the pictures of the cross-sectional microstructures shown in Fig. 5.3. The actual cross-section is almost same as these illustration, so that the rupture mode of the Sm_2O_3 added platinum is equal to the model reported by M. Cans *et al.*

There is no qualitative inconsistency or problems of the model because the voids by stress tends to be formed at the triple point of the grain boundaries and the boundaries transverse to the stress axis in theoretically and experimentally[36].

The improvement of the high temperature creep strength of the Sm_2O_3 added platinum is owed to Sm_2O_3 particles keeping the high aspect ratio and the geometrical arrangement of the grains.

[11] The little improvement of the hardness is an advantage of the plastic working. It enables the complex cold working.

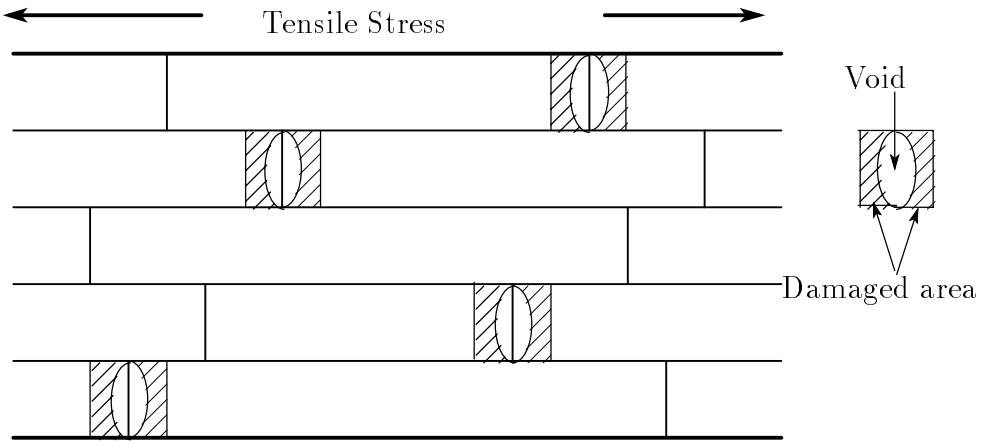

Figure 5.11: L-direction of the specimen.

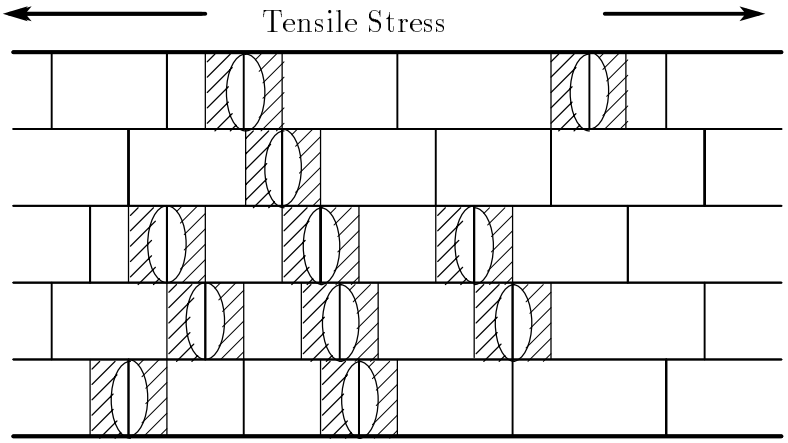

Figure 5.12: T-direction of the specimen.

Creep life Figure 5.13 shows the creep rupture time of the pure platinum, platinum-rhodium alloys and Sm_2O_3 added platinum in the present experiment expressed by the Larson-Miller parameter[60].

In this investigation, the steady-state (minimum) creep rate was mainly discussed in order to know the creep deformation mechanism at high temperatures, although the creep rupture time depends on the stress and temperature. For the practical use of the alloys, the most meaningful and important information for the creep is **when it will brake (or how long it will last)** if the initial conditions (temperature and stress) is given.

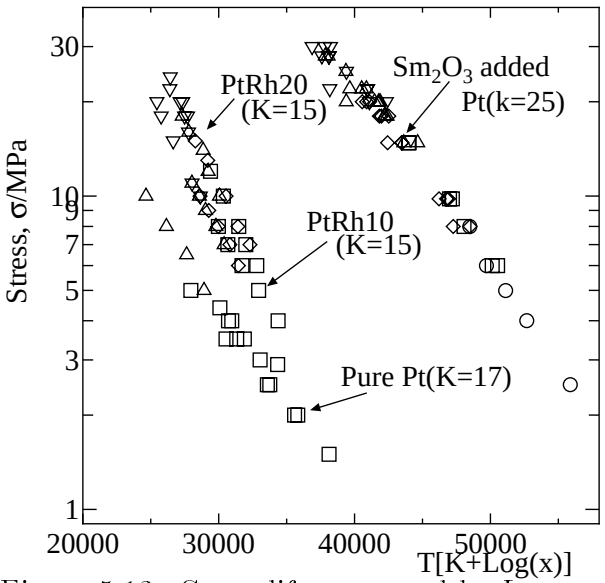

Figure 5.13: Creep life expressed by Larson-Miller parameter

Apart from the basic theory, creep rupture time in the present study is summarized with a prediction method of Larson-Miller parameter, which enables us to predict the long time rupture and/or high temperature rupture time from relatively short time and/or low temperature results. In Larson-Miller parameter method, the relationship of the stress σ, the rupture time x and the temperature T is expressed by

$$\log \sigma = T(K + \log x), \tag{5.4}$$

where the rupture time x must be expressed in hour and the temperature also be expressed in Kelvin. And the parameter K is chosen to be different temperature results being on a line.

When the results predicted by Larson-Miller parameter method is compared with measured results, the predicted results tend to show longer creep rupture time[21]. The results obtained from the short time measurements sometimes have some corners, not on a line in the figure, so that different Ks are applied for each area. The origin to make such behaviors have been studied and in some cases the reasons are the change of the specimen itself such as oxidization, change of the alloy composition, growth of the precipitated particles and so on.

In the case of platinum and its alloys of the present experiment, all points are on a line in the figure, so that the accuracy of the prediction might be higher than that of other alloys. When the creep temperature is very high and the specimen lasts for long time, the cross-sectional reduction by the vaporization is not negligibly small and its effect should be considered[12]. However, no oxidization, no change of the alloy composition and no growth of the dispersed particles will be occurred in the case of platinum and its alloys. As the data obtained are on a line, the creep rupture prediction might be possible with much higher accuracy by using Fig. 5.13.

[12] I think it is a rare case.

5.4 Conclusion

In this investigation, high temperature creep properties of Sm_2O_3 added platinum have been discussed and following conclusions were obtained.

1. The stress exponent n of the minimum creep rate at low temperatures (below 1473K) is around 10. This value is similar one to other O.D.S. alloys. However, the stress exponent n approaches to the matrix value of the pure platinum as the test temperature becomes higher.

2. At high temperatures (above 1573K), the strain control mechanism seems to be different from that of other O.D.S. alloys. No threshold stress was observed in the present experiments. The creep properties were improved especially at the cold-rolled direction, at which the high aspect ratio grains were reserved, *i.e.*, the improvement of the creep properties will be owed by the high aspect ratio grains and the geometrical arrangement of the grains rather than the direct interaction between dispersed particles and dislocations such as *Orowan* process or *Srolovitz* process.

Chapter 6

Conclusion

High temperature creep properties of pure platinum, platinum-rhodium alloys and Sm_2O_3 added platinum were examined. Following phenomena are newly found in experiments.

1. **Pure Platinum**

   (a) A strain-burst (a sudden increase in the strain) has been detected on the creep curves in some specimens. This is the newly found phenomenon in platinum.

   (b) Strong grain-size dependence of the steady-state creep rate is also the newly found phenomenon, which should be looked at again in the conventional common sense for the creep.

2. **Platinum-Rhodium Alloys**

   (a) All creep curves show the three stages, *e.g.*, the primary, steady and accelerating stages. This is a newly found result comparing with the old report in which only accelerating stage was observed at high stress conditions. The old result should be amended.

3. **Sm_2O_3 added Platinum**

   (a) The mechanism to control the creep behaviors seems to be different from that of other O.D.S. alloys at high temperatures (above 1573K). The threshold stress haven't observed in our whole experimental conditions. Sm_2O_3 added Platinum is strengthened not by the direct interaction between oxide particles and dislocations but by its large aspect ratio structure. The creep strength appears to be influenced by the growth of voids located at grain boundaries.

Some parts of the results obtained in this experiment are not clarified yet. So that, more research is desired to clarify them. Especially following items are important.

1. **Strain-burst**
   The strain-burst found in pure platinum is influenced by trace impurities, test temperatures, applied stresses and production process and *etc.* The temperature and stress conditions for its appearance have clarified in this experiment. However, the effect of trace impurities and so on are still unclear. In order to clarify the effect of trace impurities, total technical level up will be required not only to appreciate the creep phenomena but also to make improvements for the refining and the analysis.

2. **Grain size dependence of the steady-state creep rate**
   Positive dependence observed in platinum is an experimental fact and it will not be a specific property of platinum. So that, more thorough research is desired to search for the grain-size dependence in other pure metals such as gold and silver *etc.* whose stacking fault energy is similar to that of platinum.
   The specimens in this experiment for the grain size dependence have only two different grain sizes as 0.15mm and 0.5mm. Although I tried to prepare the differnt grain size specimens by using a different production process, it was not success to get a specimen whose grain size is different from the above two values. More thorough research is desired to search the grain size dependence using various specimens with differnt grain size.

3. **The observation by transmission electron microscopy**
   In order to discuss the high temperature creep phenomena with the movement and relationship of the lattice vacancies, dislocations, precipitations, inclusions and so on, it is indispensable to observe the internal microstructures by T.E.M. It is essentially important to develop the technology to obtain the thin films directly from the crept specimens without introducing new defects. If it would be possible, the observation will not only support the present result but also obtain the new information.

4. **The effect of Sm_2O_3 particles**
   The strengthening mechanism of the Sm_2O_3 added platinum is understood. However, some unclear point is left such as how the Sm_2O_3 particles keep the platinum grains to form their high aspect ratio. The direct observation of the relation between the particles and dislocations, and more accurate measurement of the distribution of the particles and so on, should be studied.

I hope the present results help the development of much strengthened platinum alloys.

Acknowledgment

I am very obliged to Prof. S. Nasu for accepting me as a graduate student in his laboratory and for his encouragements. I would like to express my cordial thanks to Dr. H. Kimura, Professor Emeritus of Tohoku University, for his helpful experimental advice, introducing papers and valuable discussions. I would like to thank Prof. R. Ohsima in Osaka Prefecture University for recommending me to be a graduate student.

I also thank Mr. Y. Tada, vice president, Mr. Y. Tanaka, factory manager and Mr. Y. Muragushi, chief manager, in TANAKA KIKINZOKU KOGYO K.K. for allowing me to be a graduate student.

I am thankful to Dr. S. Morimoto for the use of the computer, especially LaTeX 2_ε use and Miss T. Ukawa for lending books from the library and paper works.

I also thank all the students in Nasu laboratory for having good time together as a student when I'm at school.

I wish to express my grate thanks to Mr.s H. Yamasaki, S. Hitomi, T. Nishimori, Y. Ikematsu and all co-workers in Isehara Works for their help in this experiment.

References

(1) *Edited by* Linda S. Benner, T. Suzuki, K. Meguro and S. Tanaka: "PRECIOUS METALS Science and Technology", International Precious Metals Institute (1991).
Original publication in Japanese in 1985 by TANAKA KIKINZOKU KOGYO K.K.

(2) *T. Hamada: "Long-term Stability Test for Pt Based Thermocouples", Pre-Print of Annual Meeting of The Society of Instrument and Control Engineers, SICE '95 **June** 26-28, Sapporo, (1995) 655-656.

(3) IEC 584-1(1977): Thermocouples Part 1 : Reference table,
IEC 584-2(1982): Thermocouples Part 2 : Tolerances,
published by International Electrotechinical Committee.

(4) *T. Sakai: "Advances in Dynamic Recrystallization and Its Related Phenomena ", Tetsu to Hagane , **Vol.81**, No.1 (1995).

(5) T. Sakai and J. J. Jonas: "Dynamic Recrystallization: Mechanical and Microstructural Consideration", Acta Met. **Vol.32**, No.2 (1984) 189-209.

(6) *K. Tokuno, Y. Tuschida, H. Mabichi and Y. Tokunaga: "Tekko Zairyotyu no koon kyokainshi"V-Wing" ", KINZOKU, **Vol.66**, No.1 (1996) 5-10.

(7) *T. Daikoku and I. Okada: "Y_2O_3 Dispersion Strengthened Ni Base Superalloys", Tetsu to Hagane, No.9 (1989) 157-164.

(8) *K. Mino: "Microstractural Control and High temperature Strength of Oxide Dispersion Strengthed Superalloys", Tetsu to Hagane, No.9 (1989) 166-172.

(9) *T. Tomiyama: "Mekanikaruaroiinguho niyoru chogoukin no kaihatsu to jitsuyoka no doko", KINZOKU, No.2 (1991) 72-76.

(10) *Japanese Patent unexamined publication No. H6-336631 and H8-143915.

(11) *M. Umemoto: "Grain Size Number and Grain Diameter", Feramu, **Vol.2**, No.10 (1997) 731-736.

(12) *T. Hamada and S. Homma: "An Estimation of Uncertainy on temperature measurement Using Platinum Resistance Thermometers", Technical Report of *Japan Electric Meters Inspection Corporation*, **Vol.30**, No.4 (1995) 137-146.

(13) *H. Sakurai, Y. Mizuma, T. Hamada and Y. Suyama: "Reference Functions for JPt100 Thermometers Based on the ITS-90", Transactions of The Society of Instrument and Control Engineers, **Vol.32**, No.8 (1996) 1139-1144.

(14) "Guide to the expression of uncertainty in measurement", International Organization for Standardization (1993).

(15) "The International Temperature Scale of 1990", Metrologia **Vol.27** (1990).
*H. Sakurai, O. Tamura and M. Arai: "Supplementary Information for The International Temperature Scale of 1990", Bulletin of NRLM, **Vol.41**, No.4 (1992) 31-82.

(16) *M. Arai: "Resistance Charactaristics of Platinum in High Temperature Condition", Bulletin of NRLM, **Vol.34**, No.2 (1985) 65-73.

(17) S. Dushman, L.W. Dumbar and H. Huthsteiner: "Creep of Metals", J. Appl. Physics, **Vol.15** (1944) 108-124.

(18) F. Garofalo: "Fundamentals of Creep and Creep-Rupture in Metals", New York, MacMillan, (1965).

(19) S. Takeuchi and A.S. Argon: "Review on Steady-state creep of single-phase crystalline matter at high temperature", Journal of Mat. Sci., **Vol.11** (1976), 1542-1566.

(20) **Edited by* H. Kimura: "Kinzokukyodo no genshiron", Koza・Gendai no kinzokugaku Zairyohen 3, The Japan Institute of Metals (1985).

(21) *K. Maruyama and E. Nakashima: "Koonkyodo no zairyokagaku", Uchidaroukakuho (1997).

(22) *N. Igata: "Zairyokyodogaku", Baifukan (1983).

(23) R.P. Carreker, Jr.: "Plastic Flow of Platinum Wires", J. Appl. Physics, **Vol.21** (1950) 1289-1296.

(24) F.C. Child: "Creep Testing of Platinum Alloy", Platinum Metals Review, **Vol.1**, No.4 (1957) 121-126.

(25) G.L. Selman, J.G. Day and A.A. Bourne: "Dispersion Strengthened Platinum", Platinum Metals Review, **Vol.18** (1974) 46-57.

(26) F.R.N. Nabbarro: "Deformation of Crystals by Motion of Single Ions", Report on a Conference on the Strength of Solids, The Physical Society., London, (1948) 75.

(27) C. Herring: "Diffusional Viscosity of a Polycrystalline Solid", J. Appl. Physics, **Vol.21** (1950) 437.

(28) *Edited by* B. Wilshire and R.W. Evans: "Creep Behaviour of Crystalline Solids", PINERIDGE PRESS Swansea, U.K. (1985).

(29) C.R. Barrett and W.D. Nix: "A model for steady state creep based on the motion of jogged screw dislocations", Acta. Met., **Vol.13** (1965) 1247-1258.

(30) J. Weertman: "Dislocation Climb Theory of Steady-State Creep", *Transactions Symposium*, Transaction of the ASM, Vol.61 (1968) 680-694.

(31) O.D. Sherby: "Factors Affecting the High Temperature Strength of Polycrystalline Solids", Acta. Met., **Vol.10** (1962) 135-147.

(32) P. Feltham and J.D. Meakin: "Creep in Face-Centered Cubic Metals with Special Reference to Copper", Acta. Met., **Vol.7** (1959) 614-627.

(33) E.R. Parker: "Modern Concept of Flow and Fracture", Trans. ASM., **Vol.50** (1958) 52-105.

(34) C.R. Barrett, J.L. Lytton and O.D. Sherby: "Effect of Grain Size and Annealing Treatment on Steady-State Creep of Copper", Transactions of the Metallurgical Society of AIME, **Vol.239** (1967) 170-180.

(35) J.D. Parker and B. Wilshire: "Rate-controlling processes during creep of super-purity aluminum", Philosophical Magazine A, **Vol.41**, No.5 (1980) 665-680.

(36) M.F. Ashby, C. Gandhi and D.M.R. Taplin: "Fracture-Mechanism Map and Their Construction for F.C.C. Metals and Alloys", Acta Met. **Vol.27** (1979) 699-729.

(37) H.J. Frost and M.F. Ashby: "DEFORMATION-MECHANISM MAPS", Pergamon Press (1982).

(38) T. Hamada, S. Hitomi, Y. Ikemastu and S. Nasu: "High-Temperature Creep of Pure Platinum", Materials Transactions JIM, **Vol.37** (1996) 353-358.

(39) G.J. Richardson, C.M. Sellars and W.J. McGTegart: "Recrystallization during Creep of Nickel", Acta Met., **Vol.14** (1966) 1225-1236.

(40) *M. Ohashi, T. Sakai and T. Endo: "Development of Dynamically Recrystallized Bands in Polycrystalline Nickel", J. Japan Inst. Metals, **Vol.56**, No.12 (1992) 1401-1407.

(41) R.C. Gifkins: "Recrystallization of Leed during Creep", Journal of the Institution of Metals, **Vol.87** (1958-59) 225-261.

(42) H. Yamagata: "Dynamic recrystallization of single-crystalline aluminum during compression tests", Scripta Metallurgica et Materialia, **Vol.27** (1992) 727-732.

(43) *M. Ohashi, T. Endo, T. Sakai: "Effect of Initial Grain Size on Dynamic Recrystallization of Pure Nickel", J. Japan Inst. Metals, **Vol.54**, No.4 (1990) 435-441.

(44) N. Hansen: "Polycrystalline Strengthening", Metallugical Transactions A, **Vol. 16A** (1985) 2167-2190.

(45) R.H. Atkinson and D.E. Furman: "Creep Characteristics of some Platinum Metales at 1382°F", *F. Metals*, Vol.3 (1951) 806-808 as ref. 3 in ref[24].

(46) H.E. Stauss: "Time-to-Fracture Tests on Platinum, 10 per cent Iridium-platinum and 10 per cent Rhodium-platinum alloys", *Trans. A.I.M.E.*, Vol. 152 (1953-4) 525-533 as ref. 4 in ref[24].

(47) A.S. Daring: "Rhodium-Platinum Alloys", Platinum Metals Review, **Vol.5**, No.3 (1961) 97-100.

(48) A.S. Daring: "High Temperature Tensile and Creep Properties of Some Platinum Alloys", Platinum Metals Review, **Vol.6**, No.4 (1962) 148-149.

(49) A.A. Bourne and A.S. Darling: "The Tensile Creep Behaviour of Rhodium-Platinum Alloy", Platinum Metals Review, **Vol.7**, No.2 (1963) 42-48.

(50) "Mechanical Properties of Metalic Composites" *edited by* Shojiro Ochiai, Marcel Dekker, Inc. (1994).

(51) "Platinum and its Alloys for Industrial Use": TANAKA KIKINZOKU KOGY K.K. Isehara Works (May 1996).

(52) G. Hammer, D. Kaufmann und M. Clasing: "Harstellung von dispersionsverfestigten Platinwerkstoffen unter Verwendung simultangefällter Pt-$ZrOCl_2$-Pulver", Metallwissenschaft und Technik, **35** (1981) 531-534.

(53) H.A. Jansen and F.A. Thompson: "Use of oxide dispersion strengthened platinum for the production of high-quality glass", Glastech. Ber. **65**, Nr.4 (1992) 99-102.

(54) *Japanese Patent publication No. S52-12125.

(55) *H. Kimura: "Henkei to kyodo no zairyokagaku", AGNE gizyutsu center (to be published in 1998).

(56) C.T.J. Ahlers and R.W. Balluffi: "Electropolishing of Platinum Foils at −35°C for Transmission Ekectron Microscopy", Communications (1966) 910-911.

(57) *E. Nakashima: "Kouon ni okeru ryushi bunsan kyoka", KINZOKU, **Vol.66**, No.9 (1996) 787-792.

(58) *Y. Ysh, H. Nakasima, H. Kurishita, S. Goto and H. Yoshinaga: "Threshold Stress for High-Temperature Creep in Particle Strengthened Al-1.5vlo% Be alloy", J. Japan Inst. Metals, **Vol.52**, No.12 (1988) 1246-1254.

(59) M. Cans, B. deMestral and G. Eggeler: "On the influence of grain morphology on creep rupture times of cavitating materials", Scripta Metallugica et Materialia, **Vol.30** (1994) 107-112.

(60) F.R. Larson and J. Miller: "A Time-Temperature Relationship for Rupture and Creep Stress", Trans. ASME (1952) 765-775.

* Publications in Japanese.

List of Publications

Following papers have been or will be published concerning with the present study.

1. T. Hamada, S. Hitomi, Y. Ikemastu and S. Nasu : "High-Temperature Creep of Pure Platinum", Materials Transactions JIM, **Vol.37** (1996) 353-358.

2. T. Hamada, S. Hitomi, T. Nishimori and S. Nasu : "Grain Size Dependence of Steady-State Creep Rate of Pure Platinum and Its Alloys", Proceedings of the International Conference on Thermomechanical Processing of Steel & Other Materials, July 7-11, 1997 University of Wollongong in Australia **in PRESS**.

3. **Platinum and its Alloys for Industrial Use**, TANAKA KIKINZOKU KOGYO K.K. ISEHARA WORKS, June 1996, (English version).

4. **Platinum and its Alloys for Industrial Use**, TANAKA KIKINZOKU KOGYO K.K. ISEHARA WORKS, May 1996, (Japanese version).

Oral presentations in the international conferences concerning with the present study are as follows.

1. T. Hamada, S. Hitomi, Y. Ikemastu and S. Nasu : "High-Temperature Creep of Pure Platinum",
   International Symposia on Advanced Materials and technology for the 21st Century
   December 13-15, 1995, Hilton Hawaiian Village, Honolulu, Hawaii.

2. T. Hamada, S. Hitomi, T. Nishimori and S. Nasu : "Grain Size Dependence of Steady-State Creep Rate of Pure Platinum and Its Alloys",
   International Conference on Thermomechanical Processing of Steel & Other Materials, July 7-11,1997, University of Wollongong in Australia.

Following papers have been published while the author is a graduate student of OSAKA UNIVERSITY.

1. T. Hamada, S. Hitomi and H. Yamasaki: "Long-term Stability Test of Type R Thermocouples", Transactions of The Society of Instrument and Control Engineers, **Vol.31**, No.4 (1995) 532-534.

2. T. Hamada and S. Homma: "An Estimation of Uncertainty on Temperature Measurement Using Platinum Resistance Thermometers", Technical Report of *Japan Electric Meters Inspection Corporation*, **Vol.30**, No.4, (1995) 137-146.

3. T. Hamada and H. Yamasaki: "Evaluation of Its Reliability on The Fixed Point of Palladium by Using The Crucible and Wire Methods", Transactions of The Society of Instrument and Control Engineers, **Vol.32**, No.6, (1996) 820-825.

4. H. Sakurai, Y. Mizuma, T. Hamada and Y. Suyama: "Reference Functions for JPt100 Thermometers Based on the ITS-90", Transactions of The Society of Instrument and Control Engineers, **Vol.32**, No.8, (1996) 1139-1144.

5. Y. Suyama, M. Miyazato and T. Hamada: "An Evaluation Test on Calibration Accuracy of Type R Thermocouples by Comparison with a Platinum Resistance Thermometer", Transactions of The Society of Instrument and Control Engineers, **Vol.33**, No.4, (1997) 302-304.

6. T. Hamada: "Calibration and Use of the Platinum Resistance Thermometer", *JEMIC* Measurement Circle News, **Vol.26**, No.2〜No.4 series (1997).